



REPUBLIK INDONESIA  
KEMENTERIAN HUKUM DAN HAK ASASI MANUSIA

# SURAT PENCATATAN CIPTAAN

Dalam rangka perlindungan ciptaan di bidang ilmu pengetahuan, seni dan sastra berdasarkan Undang-Undang Nomor 28 Tahun 2014 tentang Hak Cipta, dengan ini menerangkan:

Nomor dan tanggal permohonan : EC00202129241, 22 Juni 2021

## Pencipta

Nama : **Dr. Teddy Purnamirza, ST., M.Eng**  
Alamat : Jl. Tiram No 1, Kelurahan Tangkerang Barat, Kecamatan Marpoan Damai, Pekanbaru, RIAU, 28282  
Kewarganegaraan : Indonesia

## Pemegang Hak Cipta

Nama : **Dr. Teddy Purnamirza, ST., M.Eng**  
Alamat : Jl. Tiram No 1, Kelurahan Tangkerang Barat, Kecamatan Marpoan Damai, Pekanbaru, RIAU, 28282  
Kewarganegaraan : Indonesia  
Jenis Ciptaan : **Buku**  
Judul Ciptaan : **THE NOVEL TECHNIQUE IN SIMPLIFYING THE FABRICATION PROCESS AND IMPROVING THE REFLECTION COEFFICIENT OF THE LINEAR POLARIZED RADIAL LINE SLOT ARRAY (LP-RLSA) ANTENNAS**

Tanggal dan tempat diumumkan untuk pertama kali : 7 Desember 2012, di JAKARTA  
di wilayah Indonesia atau di luar wilayah Indonesia

Jangka waktu perlindungan : Berlaku selama hidup Pencipta dan terus berlangsung selama 70 (tujuh puluh) tahun setelah Pencipta meninggal dunia, terhitung mulai tanggal 1 Januari tahun berikutnya.

Nomor pencatatan : 000256040

adalah benar berdasarkan keterangan yang diberikan oleh Pemohon.

Surat Pencatatan Hak Cipta atau produk Hak terkait ini sesuai dengan Pasal 72 Undang-Undang Nomor 28 Tahun 2014 tentang Hak Cipta.



a.n. MENTERI HUKUM DAN HAK ASASI MANUSIA  
DIREKTUR JENDERAL KEKAYAAN INTELEKTUAL

Dr. Freddy Harris, S.H., LL.M., ACCS.  
NIP. 196611181994031001

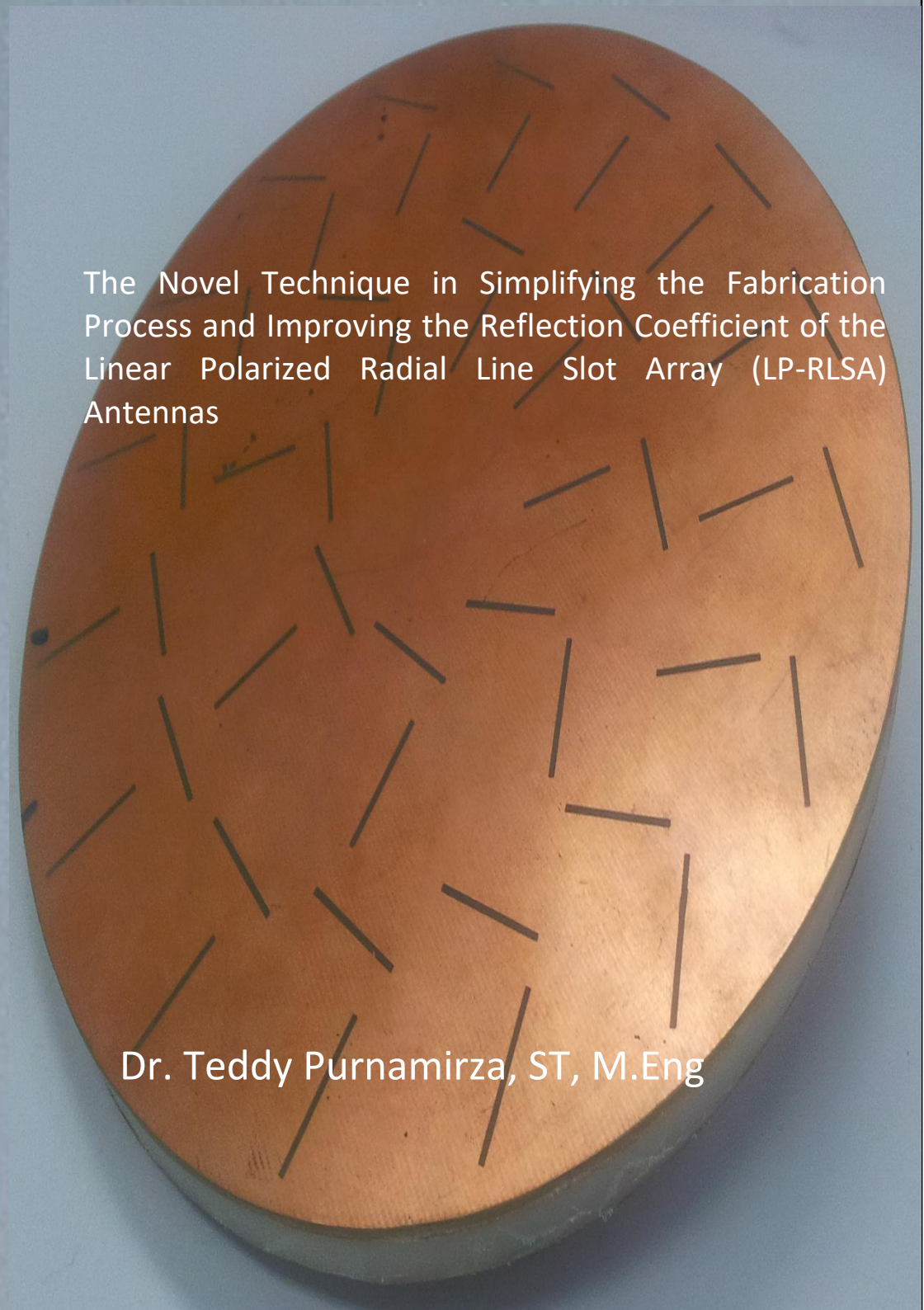
## Disclaimer:

Dalam hal pemohon memberikan keterangan tidak sesuai dengan surat pernyataan, menteri berwenang untuk mencabut surat pencatatan permohonan.

## **Deskripsi**

Buku ini memuat dua teknik yang diusulkan penulis untuk mengatasi permasalahan pada antena RLSA kecil yaitu permasalahan tingginya refleksi. Dua Teknik yang diusulkan adalah teknik FR4 dan teknik extreme beamsquint. Didalam buku ini diuraikan secara rinci bagaimana konsep kerja teknik ini dalam menurunkan nilai refleksi pada antena RLSA, sehingga dua teknik ini mampu mengatasi permasalahan yang terdapat pada perancangan antena RLSA kecil. Buku ini telah memenangkan penghargaan dari Kementerian Agama Republik Indonesia dalam kategori publikasi penelitian di Jurnal bereputasi Internasional dan telah didanai untuk diterbitkan. Buku ini telah didistribusikan ke 210 perpustakaan universitas di berbagai wilayah di Indonesia.



A circular copper antenna with radial slots. The antenna is a flat, circular disc made of copper, showing a reddish-brown patina. It is covered with numerous small, rectangular slots cut into the surface. These slots are arranged in a radial pattern, with each slot oriented parallel to a line extending from the center of the disc towards the outer edge. The slots vary slightly in length and are distributed across the entire surface of the disc. The background is a plain, light blue surface.

The Novel Technique in Simplifying the Fabrication Process and Improving the Reflection Coefficient of the Linear Polarized Radial Line Slot Array (LP-RLSA) Antennas

Dr. Teddy Purnamirza, ST, M.Eng

MILIK KEMENTERIAN AGAMA RI
TIDAK DIPERJUALBELIKAN

THE NOVEL TECHNIQUE IN SIMPLYFING  
THE FABRICATION PROCESS AND IN  
IMPROVING THE REFLECTION  
COEFFICIENT OF THE LINEAR  
POLARIZED RADIAL LINE SLOT ARRAY  
(LP-RLSA) ANTENNAS



Kementerian Agama Republik Indonesia  
Direktorat Jenderal Pendidikan Islam  
Direktorat Pendidikan Tinggi Islam

**The Novel Technique in Simplifying the Fabrication Process and In Improving the Reflection Coefficient of the Linear Polarized Radial Line Slot Array (LP-RLSA) Antennas**

Cetakan Ke-1, Desember 2012

xiv+209 hlm, 16 x 24 cm

ISBN: 978-979-8442-42-1

**Pengarah**

Prof. Dr. Nur Syam, M.Si

**Penanggung Jawab**

Prof. Dr. Dede Rosyada, MA

Prof. Dr. Phil. H. Kamaruddin Amin, MA

**Penulis**

Teddy Purnamirza

**Editor**

Teddy Purnamirza

**Desain Cover & Layout**

Depriwana Rahmi

**Diterbitkan oleh**

Kementerian Agama Republik Indonesia

Direktorat Jenderal Pendidikan Islam

Direktorat Pendidikan Tinggi Islam

Jl. Lapangan Banteng Barat 3-4 Jakarta Pusat

## Statements:

Some of the research results and findings in this book have been previously published in *Journal of Electromagnetic Wave and Application* (JEMWA), 16 April 2012, Volume 26, Issue 4, page 535-548, Taylor & Francis

Available online at:

<http://www.tandfonline.com/doi/abs/10.1163/156939312800030631>

DOI: 10.1163/156939312800030631

# Preface

Radial Line Slot Array (RLSA) antennas have gained many attentions since 1980. Initially, RLSA antennas were developed for satellite signal reception antennas. RLSA antennas have the characteristic of high gain and high efficiency as well as parabolic antennas. Recently, RLSA antennas are also developed for small antenna applications such as Wireless LANs, millimetre waves, and mobile satellites.

Currently, the development of small aperture RLSA antennas faces the problem of a high reflection coefficient that lead to the problem of low efficiency. From the view of antenna theory, this is normal since smaller antennas will have smaller efficiency. This book discusses the research result of two techniques develop to overcome the small aperture RLSA problem. Those techniques are the FR4 technique and the extreme beamsquint technique.

This book consists of seven chapters and each of the chapter consists of:

- Chapter 1 introduces the background of the research and the problem of the research.
- Chapter 2 provides the literature review of RLSA antennas. The literature review consists of the historical development of RLSA antennas, the basic theory of RLSA antennas (including the theory of how RLSA antennas works, the polarization, the orientation of slots, the position of slots, the length of slots, and the slots coupling) and the theory of how the reflection coefficient is generated in RLSA antennas.
- Chapter 3 explains the methodology that used to carry out the research along with a detail research process and its diagram.
- Chapter 4 discusses the first technique developed in this research. The technique name is FR4 technique. The discussion consists of the theoretical analysis of how this technique can minimize the reflection coefficient of RLSA antennas and can simplify the fabrication process of RLSA antennas, several antenna models that designed with and without the FR4 technique, the discussion of the simulation and measurement result, and the conclusion of the chapter.



- Chapter 5 discusses the second technique developed in this research. The named of this technique is the extreme beamsquint technique. The discussion consists of the theoretical analysis of how this technique can minimize the reflection coefficient of RLSA antennas, several antenna models designed with and without the extreme beamsquint technique, the discussion of the simulation and measurement results, and the conclusion of the chapter.
- Chapter 6 concludes all the research discussions as well as proposes several future researches.

The research in this book utilized CST-MWS-2010 software to design and simulate the antenna models. Although CST-MWS-2010 is currently the most powerful electromagnetic simulation software, the complex structure of RLSA antennas is difficult to be drawn manually since it is time consuming and errors are easy to occur. Hence, CST-MWS-2010 needs to be complemented by other software that can command CST-MWS-2010 to draw RLSA antennas automatically. Therefore, in this book, a Visual Basic Application (VBA) based program was developed to complement CST-MWS-2010 software (the detail program code is attached in appendix A). This program is used to

command CST-MWS-2010 to draw the RLSA antenna structure automatically.

## **Acknowledgment**

First of all, I would like to thankful to my God “Allah SubhanaWaTaala” for His mercy and forgiveness.

In preparing this book, I have been helped by many people. In particular, I would like to express my deepest appreciation and thank to the Ministry of Religious, Republic of Indonesia for funding the publication of this book.

I would like to send my fresh love to my wife Depriwana Rahmi, and my three angles, Aliya Nur Fazila, Aqila Nur Fayazza, Ayesha Nur Farhana who have been filling my life with their loves and happiness. Without their support and encouragments, I will not be able to finish this research and this book.

My appreciation, thanks and love to Papa and Mama and all my family members who always give me their supports and loves.

I would like to address my appreciation and thanks to Prof Dr Tharek Abd Rahman from UTM (Malaysia), Prof Peter Hall from University of Birmingham UK, Prof Dr Lau

Buon Kiong from University of Lund Sweden, Late Prof Marek E. Bialkowski from University of Queensland Australia, for their valuable inputs, corrections and comments to this research.

I also would like to address my thanks to my research colleagues, Mr Kseven from Politeknik Kuantan (Malaysia), Mr Imran from Universiti Teknikal Melaka (Malaysia), Mr Hashimu Uledi from Dar Es Salaam University (Tanzania), Mr Teguh from Universitas Diponegoro (Indonesia), Mr Baasyir and Mr Yusuf from Univeristy of Nigeria, Mr Raimi and Mr Amir, for the inputs, the discussions, and the assistants; to Mr Muhammad and Mr Hafizul from UTM Malaysia for the technical assistances.

Last but not at least, I also would like to thanks to my colleagues at Faculty of Science and Technology UIN Suska Indonesia, especially at Departement of electrical engineering, for the valuable corrections during the discussion of improving this book, also of course for their warm friendship; especially for Mr Kunaifi and Mrs Eva for assisting me in preparing my teaching during my leave from Malaysia.

Also to all people that I can not mention their names one by one that have directly or indirectly helped me in completing this book.

I realize that this book is still far from the perfection. Therefore I would be grateful to receive any comments, or suggestions about improvements for further editions.

Pekanbaru, 7 December 2012

Teddy Purnamirza

# Table of Content

<b>Preface</b>	iv
<b>Table of Content</b>	x
<b>Chapter 1 Introductions</b>	15
<b>Chapter 2 Literature Review</b>	21
2.1 The Historical Development of RLSA Antennas	21
2.2 The Basic Theory of RLSA antennas	27
2.2.1 The Structure of RLSA Antennas	27
2.2.2 How RLSA antennas work	29
2.2.3 Linear Polarizations	31
2.2.4 The Orientation of Slots in LP-RLSA Antennas	32
2.2.5 The arrangement of Slot Pairs (Unit Radiator)	34
2.2.6 The Length of Slots	37



2.2.7 Slot Power Coupling	38
2.3 The Theory of Signal Reflections in RLSA Antennas	46
2.3.1 The Signal Reflection Due to Remaining Powers	46
2.3.2 The Signal Reflection Due to the Reflected Signal From Slots	48
<b>Chapter 3 Research Methodology</b>	50
3.1 Research Process	50
3.2 The Flowchart of Research Process in Chapter 4	53
3.3 The Flowchart of Research Process in Chapter 5	55
3.4 Research Methodology	56
<b>Chapter 4 The FR4 Technique</b>	58
4.1 The Theoretical Analysis of the FR4 Technique	59
4.1.1 How the FR4 Technique Can Minimize Reflection Coefficients	59

4.1.2 Why the FR4 Technique can Simplify the Fabrication Process of RLSA Antennas	65
4.2 The Design of Experimental VSA-RLSA Antennas with FR4 Techniques	66
4.2.1 The Designed Antennas for Parametric Study	66
4.2.2 The Prototype of Designed Antennas	70
4.3 The Analysis of Experimental Results of FR4 Technique	72
4.3.1 Parametric Studies to determine appropriate permittivity and thickness	72
4.3.2 The Designed Antenna Utilizing the Appropriate Permittivity and Thickness	80
<b>Chapter 5 The Extreme Beamsquint Technique</b>	87
5.1 Theoretical Analysis	88

5.1.1 The Limitation of Beamsquint Technique	88
5.1.2 How The Extreme Beamsquint Technique Minimize the Reflection Coefficient of VSA- RLSA Antennas	91
5.2 The Structure and the Specification of Experimental Antennas	98
5.3 Results and Discussion	103
<b>Chapter 6 Conclusions and Future Researches</b>	113
6.1 Conclusions	113
6.2 Future Researches	115
<b>References</b>	117
<b>Appendix A The Program Code of VBA Software</b>	126
A.1. The Program Code to Draw RLSA with beamsquint technique	126
A.2. The Program Code to Draw RLSA with beamsquint technique	164

A.3. The VBA Program Code to cut the VBA-RLSA Antenna	190
A.4. The VBA Program Code to Multiply the VBA-RLSA Antenna	202
<b>Indeks</b>	207

# Chapter 1

## Introductions

Radial Line Slot Array (RLSA) antennas have gained many attentions since 1980 [1]. Initially, RLSA antennas were developed for satellite signal reception antennas and have the antenna diameter of not less than 600 mm [2]. Due to the advantages of RLSA antennas such as high gain, RLSA antennas are also developed for smaller antenna applications such as Wireless LANs [3-6], millimetre waves [7], and mobile satellites [8]. Some of these applications utilize the small aperture RLSA (SA-RLSA) antennas with the diameter of less than 300 mm [3-8].

In contrast with the normal size RLSA antennas, the SA-RLSA antennas have lower efficiency [9]. From the view of antenna theory, this is normal since smaller antennas will have smaller efficiency. The lower efficiency is due to insufficient number of slot pairs that the SA-RLSA antennas have. The insufficient number of slot pairs cannot radiate



most of power that come from the feeder, so that there will be a significant amount of remaining power left at the perimeter of SA-RLSA antennas. This remaining power will be reflected back to the antenna feeder and increase the reflection coefficient of SA-RLSA antennas, thus lower the efficiency of SA-RLSA antennas. Normally, the utilization of longer slot length can minimize the remaining power at perimeter of SA-RLSA antennas since the longer slot length can increase the ability of slot in radiating the power [10-11].

For the very small aperture RLSA antennas (VSA-RLSA) which has aperture that smaller than SA-RLSA antennas (diameter of less than 150 mm), the efficiency is lower than the SA-RLSA antennas, hence the design become more difficult. In the VSA-RLSA antennas, the reflection coefficient is not only the contribution of the remaining power at the perimeter like in the SA-RLSA antennas, but also the contribution of reflected signal from the slots. Hence, the utilization of longer slot as explained in previous paragraph is not sufficient to minimize the reflection coefficient of VSA-RLSA antennas. The technique of normal beamsquint in [12-13] -which usually utilized to cancel the reflected signal from the slot in the normal size RLSA and in SA-RLSA, - is no more able to cancel the

reflected signal from the slots, since the number of ring of VSA-RLSA antenna is insufficient.

The other RLSA antenna problem is the fabrication process of RLSA antennas is not simple compared to microstrip antennas. This is due to the need of a special fabrication tools such as a large plotter used to cut the slots on the antenna radiating element [8]. To simplify the fabrication process of RLSA antennas, several researches reported the utilization of the cheap FR4 material with its simple etching process as the material for RLSA antennas [9-13]. However, in those researches, the utilization of several FR4 boards as the antenna cavity reduces the performance of RLSA antennas. This is because the presence of air gap and the poor electrical performance of the FR4 boards.

The research discussed in this book proposes a novel technique to overcome both of the above problems (the poor reflection coefficient and the complex fabrication process). This technique is named FR4 board. In this technique, a FR4 board is added on the top of a VSA-RLSA antenna. The copper material of the FR4 board is utilized as the radiating element of the VSA-RLSA antenna. This can simplify the fabrication process since the slots on the radiating element can be cut by utilizing the simple etching process.

Furthermore, the dielectric part of the FR4 board is able to reduce the reflection coefficient of the VSA-RLSA antenna. Differently from the researches in the references [9-13], the dielectric part of the FR4 board is not utilized as the VSA-RLSA antenna cavity, but as other dielectric material that has a different permittivity. The different permittivity obtains a different phase between the reflected signal within the FR4 dielectric material and the reflected signal within the antenna cavity. Hence, these two signals will not strengthen each other when they meet, thus improve the antenna reflection coefficient.

In addition to the FR4 technique, this book also discusses a new technique to minimize the reflection coefficient of VSA-RLSA antennas. The technique name is the extreme beamsquint technique. This technique utilizes very high beamsquint values (greater than  $70^\circ$ ) to obtain more rings on the radiating element of VSA-RLSA antennas, thus decrease the reflection coefficient and increase the efficiency of VSA-RLSA antennas.

This book consists of seven chapters and each of the chapter consists of:

- Chapter 1 introduces the background of the research and the problem of the research.
- Chapter 2 provides the literature review of RLSA antennas. The literature review consists of the historical

development of RLSA antennas, the basic theory of RLSA antennas (including the theory of how RLSA antennas works, the polarization, the orientation of slots, the position of slots, the length of slots, and the slots coupling) and the theory of how the reflection coefficient is generated in RLSA antennas.

- Chapter 3 explains the methodology that used to carry out the research along with a detail research process and its diagram.
- Chapter 4 discusses the first technique developed in this research. The technique name is FR4 technique. The discussion consists of the theoretical analysis of how this technique can minimize the reflection coefficient of VSA-RLSA antennas and can simplify the fabrication process of VSA-RLSA antennas, several antenna models designed with and without the FR4 technique, the discussion of the simulation and measurement results, and the conclusion of the chapter.
- Chapter 5 discusses the second technique developed in this research. The named of this technique is the extreme beamsquint technique. The discussion consists of the theoretical analysis of how this technique can minimize the reflection coefficient of VSA-RLSA antennas, several antenna models designed with and without the extreme beamsquint technique, the discussion of the simulation

and measurement results, and the conclusion of the chapter.

- Chapter 6 concludes all the research discussions as well as proposes several future researches.



# Chapter 2

## Literature Review

### 2.1 The Historical Development of RLSA Antennas

It is stated in various researches and literatures, that it was Kelly who introduce the concept of RLSA antennas in the 1950s [14]. Although this initial research could produce a pencil beam antenna for any type of polarizations, this antenna still has a complex feeding structure, yielding this antenna costly and difficult to be fabricated.

In 1988, Ando proposed a linearly polarized RLSA (LP-RLSA) antenna at the frequency of 12 GHz. This antenna was designed using a novel technique of slot arrangements. The novel technique aims to produce a uniform aperture distribution. This antenna has double layer cavity and exhibits 15 dB co-polarization levels above cross-polarization levels. Ando also proposed a beam-tilt technique to improve the poor reflection coefficient in LP-

RLSA antennas [1, 15]. In the same year, by applying reflection coefficient suppression and slot coupling technique, Ando successfully designed a LP-RLSA antenna for DBS applications at 12 GHz. This antenna has the efficiency of 76% and the gain of 36 dB [4, 16-17]. Takada introduced a novel technique to improve the reflection coefficient using a reflection cancelling slot technique. This technique successfully improved the reflection coefficient of RLSA antennas from 2 dB to 10 dB [2]. Endo designed an optimum thickness of double layer RLSA antennas in order to realize the mass production of thinner RLSA antennas [17].

In 1990, Ando furthermore introduced a Circularly Polarized RLSA (CP-RLSA) antenna. This antenna utilizes a single layer cavity instead of a double layer cavity. This simpler cavity structure improves the complexity of the RLSA fabrications and can achieve the gain of 35.4 dBi and the efficiency of 65%. Ando used two techniques to improve the antenna performance. The first is the technique of varying slots length and slots spacing used to uniform the aperture illuminations of the antenna. The second is the technique of matching spiral used to reduce the reflection of the residual powers at the antenna perimeters [18-19]. In 1991, Takashi proposed the technique of varying the slots

length and the spacing of RLSA antennas. Utilizing this technique Takahashi proposed several high efficiency single layer RLSA antennas with the diameter of 25 cm to 60 cm. These antennas can achieve the efficiency of 70% to 84% [20]. Furthermore, Takashi produced and marketed a 78% efficiency and 32.6 dB gain single layered RLSA [21-23].

More innovations in RLSA designs are a dual beam RLSA antenna [24], a dual circularly polarized RLSA antenna [25-26], and a multi beams RLSA antenna [27-28].

Australian researchers started to investigate RLSA antennas in 1995. They reported several investigations to design LP-RLSA antennas for DBS receivers. These investigations used the combination of theoretical and experimental approach. The availability of low cost materials and low cost fabrications also become considerations in these researches. In 1997, Davis reported a 60 cm diameter LP-RLSA prototype designed using the reflection cancelling slot technique. This technique can overcome the inherent poor reflection coefficient [4]. Davis successfully tested a RLSA antenna designed utilizing the reflection cancelling slot technique and a beamsquint value of  $20^0$  [6-7]. Furthermore, Davis reported an investigation of LP-RLSA antennas utilizing the beamsquint technique for several squint angles. This technique successfully improved the

reflection coefficient under -25 dB [5]. Davis also integrated the result of references [17-20] to form a beam synthesis algorithm used to calculate the design parameter of LP-RLSA prototypes [29].

In 2002, Malaysian and Australian researchers started to investigate the application of RLSA antennas for wireless LANs. Farah successfully fabricated a low profile RLSA antenna at frequency of 5.5 GHz with a broad radiation pattern of  $60^0$  used for indoor wireless LANs [30]. Furthermore, Imran reported the design and test of RLSA antennas for outdoor point-to-point applications at frequency of 5.8 GHz [31-33]. Islam reported the utilization of low cost FR4 materials to fabricate RLSA antennas at the frequency of 5.8 GHz for wireless LANs. This invention is quite innovative since FR4 materials are a low cost material and easy to be fabricated [13, 34]. Zariatsky investigated the design of RLSA antennas for wireless LAN and successfully fabricated a dual band 2.4/5.2 GHz antenna [35-36].

Malaysian researchers initially researched reconfigurable RLSA antennas. Jamlos replaced the conventional SMA feeder with a microstrip aperture coupled structure and combined it with a RLSA as the radiating element. With this new feeding structure, Jamlos realized the reconfigurable functions of RLSA antennas in term of

beasteering, beamshaping and frequency [9-11]. However, based on the theory of RLSA antennas and author's observations, this antenna is no more an RLSA antennas. This antenna is more as a microstrip antenna that uses FR4 as its dielectric and a design of RLSA as its radiating element.

Due to the advantages of RLSA antennas such as high gain [4, 37], RLSA antennas are also developed for smaller antenna applications such as Wireless LANs [9-12], millimetre waves [38], and mobile satellites [28]. Some of these applications utilize small aperture RLSA (SA-RLSA) antennas with a diameter of less than 300 mm [9-12, 28, 38].

In contrast with normal size RLSA antennas, SA-RLSA antennas have lower efficiency [39]. From the view of antenna theory, this is normal since smaller antennas will have smaller efficiency. This is due to the insufficient number of slot pairs that SA-RLSA antennas have. The insufficient number of slot pairs cannot radiate most of power that come from the antenna feeder, so that there will be a significant amount of remaining power left at the perimeter of SA-RLSA antennas. The antenna perimeter reflects this remaining power back to the antenna feeder and increases the reflection coefficient of SA-RLSA antennas, thus lowering the efficiency of SA-RLSA antennas. The

utilization of a longer slot length can minimize the remaining power since the longer slot length can increase the ability of slots in radiating power [21, 36]. However, the longer slot length will lower antenna gain.

Several researches reported the design of SA-RLSA antennas with a diameter of 75 mm. However, these researches did not designed the antennas correctly so that the designed antennas have some mistakes such as the overlap slots, the cavity of the antennas that consist of several layer stuck using glue, and the utilization of high loss materials such as FR4. These mistakes cause low gains and high reflection coefficients. Therefore, this literature review still concludes that the development of SA-RLSA still needs some additional techniques to minimize its high reflection coefficient. These techniques should be different from available techniques such as the beamsquint technique and the reflection cancelling slot technique since these techniques were designed to minimize the reflection coefficient of normal size RLSA antennas. The normal size RLSA antennas have different characteristics compared to the SA-RLSA antennas such as low number of rings, low number of slots, small diameters and different signal reflection sources, which make the beamsquint technique

and reflection cancelling technique do not appropriate to be implemented in SA-RLSA antennas.

## **2.2 The Basic Theory of RLSA antennas**

The following discussions about the basic theory of RLSA antennas refer to references [4-8, 29, 40-41].

### **2.2.1 The Structure of RLSA Antennas**

Figure 2.1 shows the illustration of the structure of a RLSA antenna. Figure 2.1 shows that the structure of the RLSA antenna consists of a radiating element, a cavity, a background and a feeder. The radiating element usually is a circular plate that made of metals, such as aluminium, copper or brass. The radiating element consists of many slot pairs. One slot pair acts as one antenna element so that all slot pairs form an array antenna. The background is a metal plate just like the radiating element, but the background does not have slots. The cavity is a dielectric material that has a form of a tube. Together with the radiating element and the background, the cavity operates as a circular waveguide that guides the signal from the feeder to propagate in radial direction. The feeder is a part of RLSA antennas used to feed signals from a transmission line into the antenna.

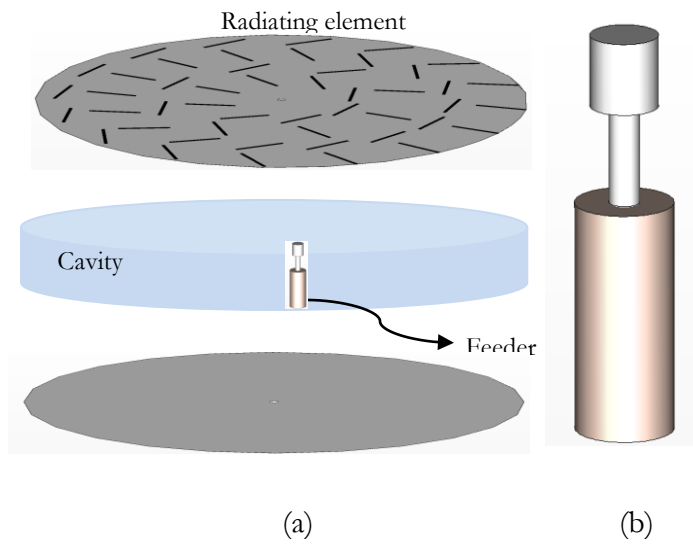


Figure 2.1 (a) The Component of the RLSA Antenna (b)  
The magnificent view of the feeder



### 2.2.2 How RLSA antennas work

The feeder placed in the centre of the antenna cavity feeds the electromagnetic power (indicated by the arrows). The feeder is an ordinary SMA feeder, which is modified by adding a head disc. The head disc has a function to convert the electromagnetic power from a TEM coaxial mode into a TEM cavity mode (a radial mode), so that the electromagnetic power fed by the feeder will propagate in a TEM mode and in radial direction within the antenna cavity, as illustrated by Figure 2.2. A region of radius  $\rho_{\min}$  is left devoid of slots, in order for the radial mode to stabilise within the cavity before encountering the discontinuities related to the presence of the slots.

When the power passes the slot pair, some little amount of power escapes through the slot pair and radiates as illustrated by Figure 2.3. Hence, the slot pair can be considered as one antenna element. Since there are many slot pairs (thousands in normal size RLSA antennas), all the slot pairs will form an array antenna. Therefore, this is the reason why "array" word is included in the name of RLSA (Radial Line Slot *Array*).

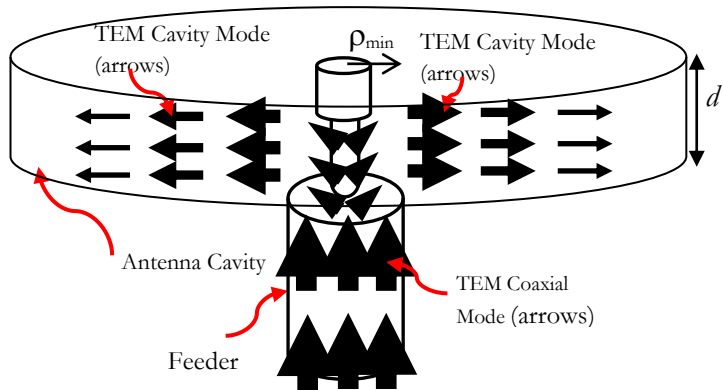


Figure 2.2 The Illustration of TEM Cavity Mode and TEM Coaxial Mode

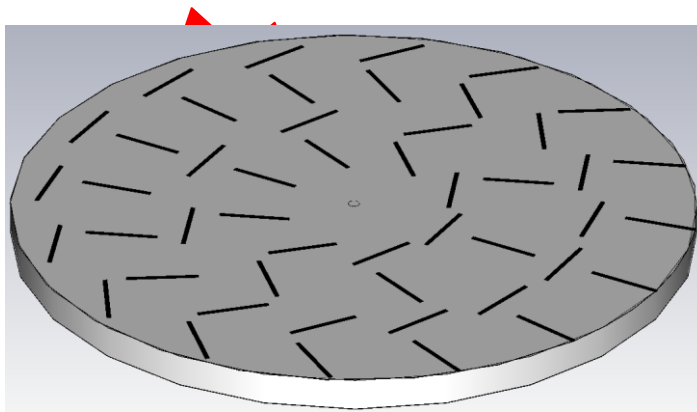


Figure 2.3 The Illustration of the power escaping from the slot pairs

### 2.2.3 Linear Polarizations

A slots pair, which represents one antenna element in RLSA antennas, is located in the top surface of the radiating element of RLSA antennas. A linear polarization in RLSA antennas can be produced by combining two signals from the slot pair. Figure 2.4(a) shows the illustration of a slot pair. The signal from Slot 1 and the signal from Slot 2 have a phase difference of 180 degree or  $\pi$  radians since Slot 1 and Slot 2 have a distance of half wavelength ( $0.5\lambda_g$ ) one to each other. Since the orientation of Slot 1 and Slot 2 is perpendicular one to each other, the signal from Slot 1 (green colour) and Slot 2 (blue colour) are also perpendicular one to each other, as shown in Figure 2.4(b).

Figure 2.4(b) shows that when Signal 1 is increasing in positive values, Signal 2 is decreasing in negative values. Since their position is perpendicular to each other, the resulting wave becomes a line in the Quadrant II. When Signal 1 decreasing toward 0 and Signal 2 increasing toward 0, the resulting signal will be a line in Quadrant II but with the shorter length compared to the line in the previous case. When Signal 1 is decreasing in negative values and Signal 2 is increasing in positive values, then the resulting signal will be a line in Quadrant IV. When Signal 1 is increasing toward 0 and Signal 2 is decreasing toward 0, then the resulting signal

will be a line in Quadrant IV but with shorter length compared to the line in the previous case. Now, we can understand that the resulting signal of Signal 1 and Signal 2 results a signal look like a line that the length changes as a function of time, this is the reason why its name is linear polarizations.

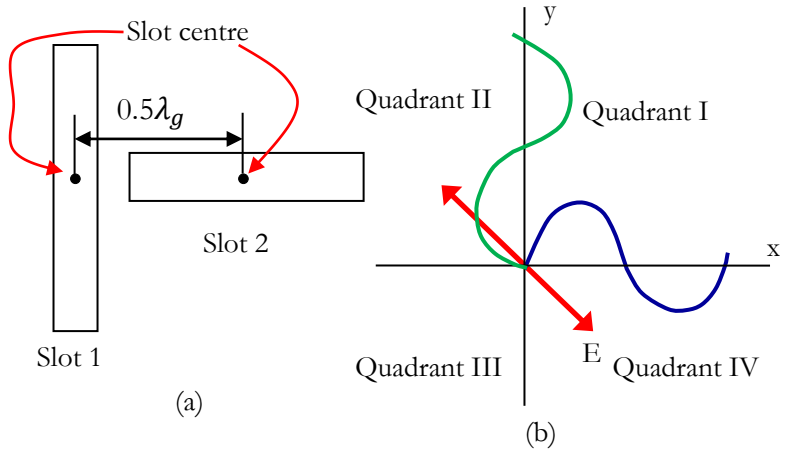


Figure 2.4 The polarization establishment in linearly polarized RLSA

#### 2.2.4 The Orientation of Slots in LP-RLSA Antennas

Slots pairs must be located in correct positions on the radiating surface of RLSA antennas. Slots pairs are located in different and unique positions in order to prevent overlapping between them. Figure 2.5 shows the position of

the slots (indicated by 'A' and 'B') and the squint of the inclination angles of the slots (indicated by ' $\theta_1$  and  $\theta_2$ ').

Equation 2.1 and 2.2 express the squint of the slots obtained by the beamsquint technique.

$$\theta_1 = \frac{\pi}{4} + \frac{1}{2} \left\{ \arctan \left( \frac{\cos(\theta_T)}{\tan(\phi_T)} \right) - (\phi - \phi_T) \right\} \quad (2.1)$$

$$\theta_2 = \frac{3\pi}{4} + \frac{1}{2} \left\{ \arctan \left( \frac{\cos(\theta_T)}{\tan(\phi_T)} \right) - (\phi - \phi_T) \right\} \quad (2.2)$$

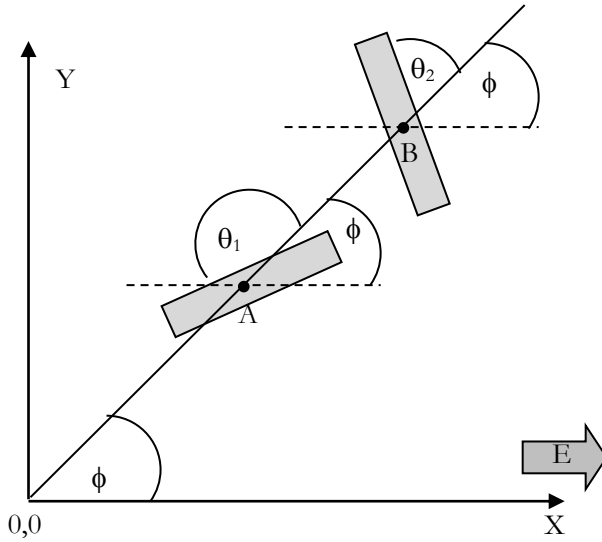


Figure 2.5 The pair of slot geometry

Where

$\theta_i$  is the inclination angle of Slot 1

$\theta_2$  is the inclination angle of Slot 2

$\theta_r$  is the beam squint angle in elevation direction

$\phi$  is the azimuth angle of Slot 1 and Slot 2 positions

$\phi_r$  is the beam squint angle in azimuth direction

### 2.2.5 The arrangement of Slot Pairs (Unit Radiator)

A slots pair that constructs linear polarizations is also called as a unit radiator. The arrangement of unit radiators in the radiating surface of RLSA antennas must be carefully calculated and drawn since a bit deviation and error will rapidly decrease the performance of RLSA antennas. Figure 2.6 shows the geometrical arrangement of a unit radiator.

Based on the Figure 2.6, the distance of a particular unit radiator from the centre point of RLSA antennas is expressed in Equation 2.3.

$$\rho_\rho = \frac{n\lambda_g}{1 - \xi \sin\theta_r \cos(\phi - \phi_r)} \quad (2.3)$$

Where  $\xi = \frac{1}{\sqrt{\epsilon_r}}$

Equation 2.4 expresses the distance between two adjacent unit radiators located in two different rings (the distance in radial direction).

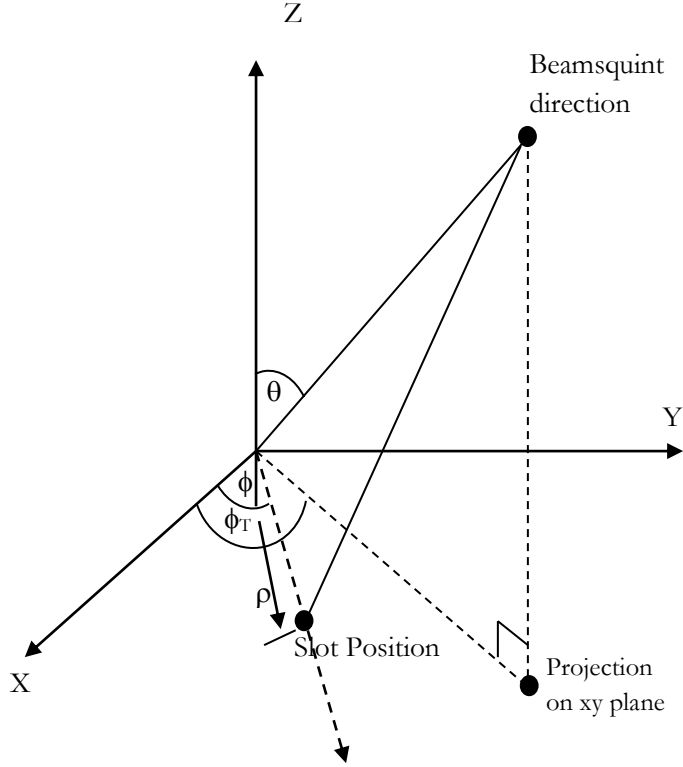


Figure 2.6 The Geometrical arrangement of a unit radiator

$$S_{\rho} = \frac{\lambda_g}{1 - \xi \sin \theta_T \cos(\phi - \phi_T)} \quad (2.4)$$

Equation 2.5 expresses the distance between two adjacent unit radiators in a same ring (the distance in azimuth direction).

$$S_{\phi} = \frac{2\pi\lambda_g}{\sqrt{1-\xi^2 \sin^2 \theta_T}} \frac{q}{p} \quad (2.5)$$

Where

$\lambda_g$  is the length of the wavelength inside the cavity of RLSA antennas

$\epsilon_r$  is the relative permittivity of the cavity of RLSA antennas

$\theta_T$  is the beam squint angle in elevation directions

$\phi$  is the azimuth angle of slot 1 or slot 2

$\phi_T$  is the beamsquint angle in azimuth directions

$n$  is ring numbers (1,2,3....)

$q$  is integer numbers (1,2, 3...) that express the distance of innermost rings from the centre of RLSA antennas

$p$  is the number of unit radiators in innermost rings

Since the distance from the centre of unit radiators to Slot 1 or Slot 2 is ' $\lambda_g/4$ ', based on Equation 2.5, Equation



2.6 and Equation 2.7 express the distance of slots from the centre of antennas.

$$\rho_{\rho1} = \frac{(n - 1 + q - 0.25)\lambda_g}{1 - \xi \sin\theta_T \cos(\phi - \phi_T)} \quad (2.6)$$

$$\rho_{\rho2} = \frac{(n - 1 + q + 0.25)\lambda_g}{1 - \xi \sin\theta_T \cos(\phi - \phi_T)} \quad (2.7)$$

### 2.2.6 The Length of Slots

The length of slots on the radiating surface of RLSA antennas must be varies in order to achieve a uniform aperture illumination. The farther a slot from the centre of antennas, the longer the length of the slot will be. The length of the slot is the function of  $\rho$ , which is the distance of the slot from the centre of antennas, as expressed by following equation:

$$L_{rad} = (4.9876 \times 10^{-3} \rho) \frac{12.5 \times 10^9}{f_0} \quad (2.8)$$

The formula in Equation 2.8 is an approach formula. To get an accurate formula, we need to do some measurement and experiment.

### 2.2.7 Slot Power Coupling

If we assume the weak coupling of the inner cavity field to the radiating slot, and assume that the presence of the slots does not significantly disturb the symmetry of the inner cavity field, we can use a simple incremental power conservation approach to arrive at the slot coupling profile required as a function of the slots radial position,  $\rho$ . Figure 2.7 shows the power flow components considered, consisting of the power component approaching the slot, the power component coupled to the slot, and the component continuing on in the radial guide

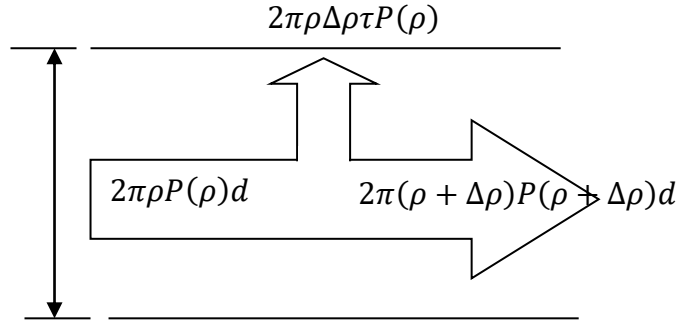


Figure 2.7 Power flow components for slot coupling analysis

In Figure 2.7,  $P(\rho)$  represents the power flow density within the radial cavity at a distance  $\rho$  from the central feeding point, and  $\tau$  represents the proportion of the inner field power in the radial cavity that is radiated by the slot.

From this, we can see that by applying the conservation of power requirement implies that:

$$2\pi(\rho + \Delta\rho)P(\rho + \Delta\rho)d = 2\pi\rho P(\rho)d - 2\pi\rho\Delta\rho\tau P(\rho) \quad (2.9)$$

Where stated in simple terms, the power arriving at point  $\rho + \Delta\rho$  (left hand side of Equation 2.9) is given by the power present at distance  $\rho$  less the power coupled to the slots present at the distance of  $\rho$ .

Upon expanding out the first term on the left hand side of Equation 2.9 and dividing through by the  $2\pi d$  term we obtain:

$$2\pi(\rho + \Delta\rho)P(\rho + \Delta\rho)d = 2\pi\rho P(\rho)d - 2\pi\rho\Delta\rho\tau P(\rho) \quad (2.10)$$

Rearranging gives:

$$\rho \left[ \frac{P(\rho + \Delta\rho) - P(\rho)}{\Delta\rho} \right] + P(\rho + \Delta\rho) = -\rho \frac{\tau}{d} P(\rho) \quad (2.11)$$

Now, if we let  $\Delta\rho \rightarrow 0$ , and allow  $\tau$  to be a function of  $\rho$ , namely,  $\rho = \tau(\rho)$ :

$$\rho \frac{dP(\rho)}{d\rho} + P(\rho) = -\rho \frac{\tau(\rho)}{d} P(\rho) \quad (2.12)$$

$$\frac{d\{\rho P(\rho)\}}{d\rho} = -\rho \frac{\tau(\rho)}{d} P(\rho) \quad (2.13)$$

If we now introduce  $\alpha(\rho) = \frac{\tau(\rho)}{2d}$ , we can write Equation 2.13 as:

$$\begin{aligned} \frac{d\{\rho P(\rho)\}}{d\rho} &= -\rho 2\alpha(\rho) P(\rho) \\ &= -2\alpha(\rho) \rho P(\rho) \end{aligned} \quad (2.14)$$

For the differential equation of Equation 2.14, we can write a solution for  $P(\rho)$  in the form:

$$P(\rho) = \frac{\rho_{min}}{\rho} e^{\left[-2 \int_{\rho_{min}}^{\rho} \alpha(\rho) d\rho\right]} \quad (2.15)$$

Where  $\rho_{min}$  is the radial position of the innermost slots, forming our inner boundary condition.

Now by definition, the aperture power distribution will be given by the product of the coupling factor and the inner field density, namely,  $\alpha(\rho)P(\rho)$ . Thus, from 2.15, we can write this aperture power distribution relationship as:

$$\alpha(\rho)P(\rho) = \alpha(\rho) \frac{\rho_{min}}{\rho} e^{\left[-2 \int_{\rho_{min}}^{\rho} \alpha(\rho) d\rho\right]} \quad (2.16)$$

In order to satisfy the requirement of uniform aperture illumination, we require the product  $\alpha(\rho)P(\rho)$  to evaluate to a constant. Under this requirement, it can be seen that this can be achieved so long as the right hand side of Equation 2.16 evaluates to a constant. This objective can be achieved if we choose  $\alpha(\rho)$  to be of the form:

$$\alpha(\rho) = \frac{\rho}{T - \rho^2} \quad (2.17)$$

where  $T$  is a constant whose value is given later.

With this choice of  $\alpha(\rho)$ , we can see that the right hand side of Equation 2.17 evaluates as follows:

$$\begin{aligned} \alpha(\rho) \frac{\rho_{min}}{\rho} e^{\left[-2 \int_{\rho_{min}}^{\rho} \alpha(\rho) d\rho\right]} &= \\ \frac{\rho}{T - \rho^2} \frac{\rho_{min}}{\rho} e^{\left[\ln|T - \rho^2|\right]_{\rho_{min}}^{\rho}} &= \\ = \frac{\rho_{min}}{T - \rho^2} e^{\left[\ln|T - \rho^2| - \ln|T - \rho_{min}^2|\right]} &= \\ = \frac{\rho_{min}}{T - \rho^2} e^{\left[\ln\left|\frac{T - \rho^2}{T - \rho_{min}^2}\right|\right]} &= \\ = \frac{\rho_{min}}{T - \rho^2} \frac{T - \rho^2}{T - \rho_{min}^2} & \end{aligned}$$

$$\frac{\rho_{min}}{T - \rho_{min}^2} \quad (2.18)$$

It is thus confirmed that by the choice of  $\alpha(\rho)$  given in Equation 2.17, we can obtain a constant aperture illumination profile, as demonstrated in Equation 2.18.

The question still remains as to the value of the constant  $T$ , in Equation 2.17.

In order to arrive at a value for  $T$ , we need to give a consideration to practical limitations that must be placed on the coupling expression of Equation 2.17. under practical consideration, the coupling coefficient,  $\alpha(\rho)$ , cannot be increased arbitrarily, as such circumstances would lead to the rotational symmetry of the inner field becoming excessively perturbed, and the weak coupling assumption used herein would not be as valid. For this reason, it is obvious that there must be some residual amount of power that is dissipated in the cavity boundary termination.

In order to evaluate the power present at various points in the radial cavity, we utilise the findings for  $\alpha(\rho)$  given in Equation 2.17 and the power density function of Equation 2.15, which leads to:

$$P(\rho) = \frac{\rho_{min}}{\rho} e^{[-2 \int_{\rho_{min}}^{\rho} \alpha(\rho) d\rho]}$$

$$\begin{aligned}
&= \frac{\rho_{min}}{\rho} e^{\left[ \ln \left| \frac{T - \rho^2}{T - \rho_{min}^2} \right| \right]} \\
&= \frac{\rho_{min}}{\rho} \frac{T - \rho^2}{T - \rho_{min}^2}
\end{aligned} \tag{2.19}$$

By using Equation 2.19, we can see that the power present within the radial cavity at the distance  $\rho = \rho_{min}$ , just prior to encountering any slots, will be given by:

$$\begin{aligned}
2\pi\rho_{min} \cdot P(\rho_{min}) &= 2\pi\rho_{min} \frac{\rho_{min}}{\rho_{min}} \frac{T - \rho_{min}^2}{T - \rho_{min}^2} \\
&= 2\pi\rho_{min}
\end{aligned} \tag{2.20}$$

The result of Equation 2.20 is not altogether unexpected, given that we took  $\rho_{min}$  as the normalised boundary condition for solving our power density differential equation of Equation 2.21.

Now, use needs to be made of the second boundary condition, namely the power present at  $\rho = \rho_{max}$ . By again utilising Equation 2.19, we can see that the power present within the radial cavity at the distance  $\rho = \rho_{max}$ , just after the last ring of slots has been encountered will be given by:

$$2\pi d\rho_{max} \cdot P(\rho_{max}) = 2\pi\rho_{max} \frac{\rho_{min}}{\rho_{max}} \frac{T - \rho_{max}^2}{T - \rho_{min}^2}$$

$$= 2\pi\rho_{min} \frac{T-\rho_{max}^2}{T-\rho_{max}^2} \quad (2.21)$$

If we now define the proportion of power launched into the radial cavity that is dissipated or wasted at the cavity boundary, as  $t$ , we can write:

$$t = \frac{2\pi d\rho_{max}P(\rho_{max})}{2\pi d\rho_{min}P(\rho_{min})} \quad (2.22)$$

Now substituting from Equation 2.20, Equation 2.21, we can write Equation 2.22 as:

$$t = \frac{2\pi d\rho_{min} \frac{T-\rho_{max}^2}{T-\rho_{min}^2}}{2\pi d\rho_{min}} \quad (2.23)$$

Upon rearranging we find that Equation 2.23 provides us with the required value of the introduced constant,  $T$ , as:

$$T = 2\pi\rho_{min} \frac{\rho_{max}^2 - t.\rho_{min}^2}{1-t} \quad (2.24)$$

Thus we now have by way of Equation 2.14, 2.24 an expression for the required coupling factor,  $\alpha(\rho)$ , expressed as a function of the radial surface location,  $\rho$ , and the desired proportion of the power dissipated or wasted at the cavity perimeter.



Figure 2.8 shows graphically the dependence that  $\alpha(\rho)$  has on the radial distance,  $\rho$ , for a number of different values of the proportion of power dissipated in the cavity termination,  $t$ . as can be expected, as we specify more stringent limits on the amount of power wasted,  $t \rightarrow 0\%$ , the required slot coupling increases exponentially.

We therefore arrive at another compromise situation. The portion of power reaching the cavity boundary,  $t$ , represents power that is not radiated by the slot pattern, and neglecting material losses and return loss, the radiation efficiency,  $\eta_R$ , of the RLSA antenna can be expressed approximately as:

$$\eta_R \leq (1 - t) \quad (2.24)$$

Obviously, the ideal would be to achieve the smallest possible value of  $t$  in order to maximise the antenna's radiation efficiency.

However, as pointed out earlier, as  $t$  decreases, the required slot coupling factor becomes large for slots near the perimeter of the radiating surface.

## **2.3 The Theory of Signal Reflections in RLSA Antennas**

Signal reflections in RLSA antennas stems from two causes. Those are the signal reflection due to the remaining power at the antenna perimeter and the signal reflection due to the reflected signal from the antenna slots. The signal reflection due to the remaining power is significant in small aperture RLSA antennas while the signal reflection due to the reflected signal from the antenna slots is a special case for Linear Polarized RLSA (LP-RLSA). Section 2.3.1 and 2.3.2 explains both of these two signal reflection causes.

### **2.3.1 The Signal Reflection Due to Remaining Powers**

The power ( $P$ ) comes from the feeder, which is located at the antenna centre, and flows toward the antenna perimeter, as illustrated by Figure 2.8(b). When the power passes the slots, some amount of the power radiates through the slots. The power inside the cavity will decrease every time the power passes the slots and will continue to decrease until the power reaches the antenna perimeter. The remaining power ( $P_R$ ) at the antenna perimeter is shown in Figure 2.8 and expressed by Equation (2.25):

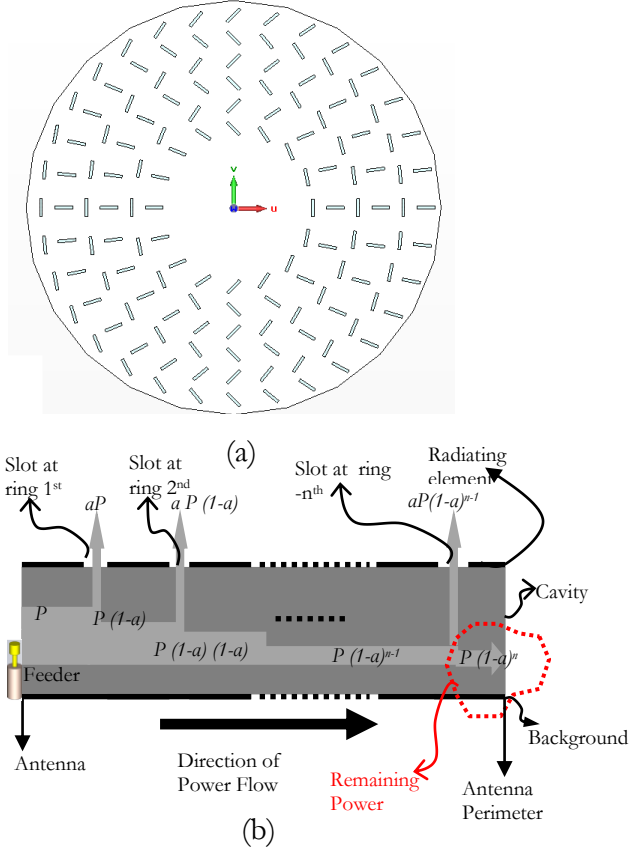


Figure 2.8 (a) The top view of RLSA (b) The cut view of a RLSA antenna and the power flow mechanism inside the RLSA cavity.

$$(P_R) = P (1-a)^n \quad (2.25)$$

Using Equation (2.25), it can be observed that the amount of the remaining power depends on the number of rings ( $n$ ), which also proportional to the number of slots. For small aperture RLSA antennas, which have small number of

slots, the amount of the remaining power at the antenna perimeter will be high. Part of this remaining power will be reflected back to the feeder and result in a high signal reflection, thus increasing the reflection coefficient. For normal size RLSA antennas which have thousand of slots, the remaining power at the antenna perimeter is very small so that its effect to the signal reflection is neglected.

### 2.3.2 The Signal Reflection Due to the Reflected Signal From Slots

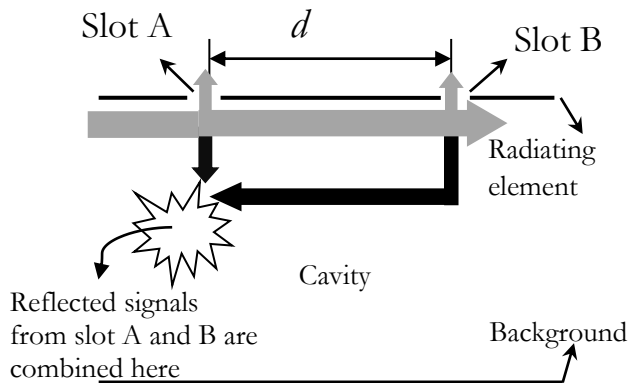


Figure 2.9 The illustration of the reflected signals from the slot

Figure 2.9 shows the front cut view of a RLSA antenna and the signal flow within the cavity of the RLSA antenna. The grey arrows represent the signals that flow

from the centre of the RLSA antenna to the antenna perimeter and the black arrows represent the reflected signal from the slots. Figure 2.29 shows that since the distance between the slots ( $d$ ) is  $\lambda_g/2$ , the signal from slot 'A' will travel for  $\lambda_g/2$  to reach 'B'. At 'B', some of the signal will be reflected back and travel for another  $\lambda_g/2$  to reach 'A'. Therefore, the reflected signal from slot 'A' and slot 'B' will have a different phase of  $\lambda_g/2 + \lambda_g/2 = \lambda_g$  or  $360^\circ$  (or can be said there is no phase different), so that they will strengthen each other and result a high signal reflection .

# Chapter 3

## Research Methodology

### 3.1 Research Process

The research was conducted by firstly analyzing the characteristic of signal reflections and the theory of how the signal reflection generated in RLSA antennas, especially VSA-RLSA antennas. Based on this analysis, two techniques to minimize the reflection coefficient VSA-RLSA antennas were developed. Those are a FR4 technique (discussed in Chapter 4), and an Extreme beamsquint technique (discussed in Chapter 5).

To verify the developed techniques, several antenna models were designed based on the developed techniques. CST-MWS-2010 was used to design and simulate the antenna models. Although CST-MWS-2010 is currently the most powerful electromagnetic simulation software, the complex structure of RLSA antennas is very difficult to be drawn manually since it is time consuming and errors is easy to occur. Hence, CST-MWS-2010 needs to be

complemented by other software that can command CST-MWS-2010 to draw RLSA antennas automatically. Therefore, in this book, a Visual Basic Application (VBA) based program was developed to complement CST-MWS-2010 software (the detail program code is attached in appendix A). This program is used to command CST-MWS-2010 to draw RLSA antenna structures automatically.

For the research in Chapter 4, the hypothesis of the FR4 technique is that the reflection coefficient of RLSA antennas can be minimized by putting the addition layer (FR4 material) on top of the RLSA cavity. The thickness and permittivity of the FR4 material are the parameters that influence the capability of this technique in minimizing the reflection coefficient of RLSA antennas. However, the appropriate values of these two parameters are too complex to be calculated mathematically. Therefore, in this research the appropriate values of these two parameters were determined by conducting a parameterization using CST MWS 2010. An antenna model was designed. By varying the values of the two parameters, the data of the reflection coefficient of the antenna model were gathered. The most appropriate values of these two parameters are the values that give the lowest reflection coefficient.

To verify the simulation and parameterization result, a prototype of the antenna model utilizing the most appropriate values of the two parameters are fabricated and measured. The measurement of the reflection coefficient and the radiation pattern were conducted utilizing the Network Analyzer and the Antenna test chamber. The measurement results were then compared with the simulation results. The agreement between the measurement results and the simulation results is the proof of the validity of the developed technique.

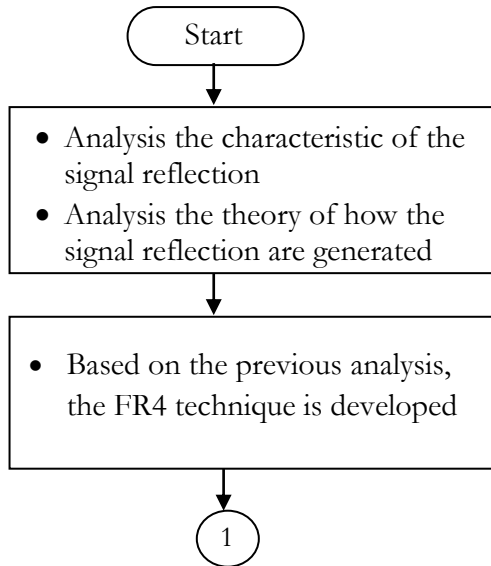
For the research in Chapter 5, the hypothesis of the extreme beamsquint technique is that the reflection coefficient of RLSA antennas can be minimized by utilizing high beamsquint values. Since this hypothesis is developed from a qualitative analysis, the exact values of the beamsquint that can give the lowest reflection coefficient cannot be calculated and formulated in a mathematic equation. Therefore, in this research, the extreme beamsquint technique is proven by simulating various antenna models with the implementation of the beamsquint technique and various antenna models without the implementation of the beamsquint technique. The simulation results such as the reflection coefficient, the

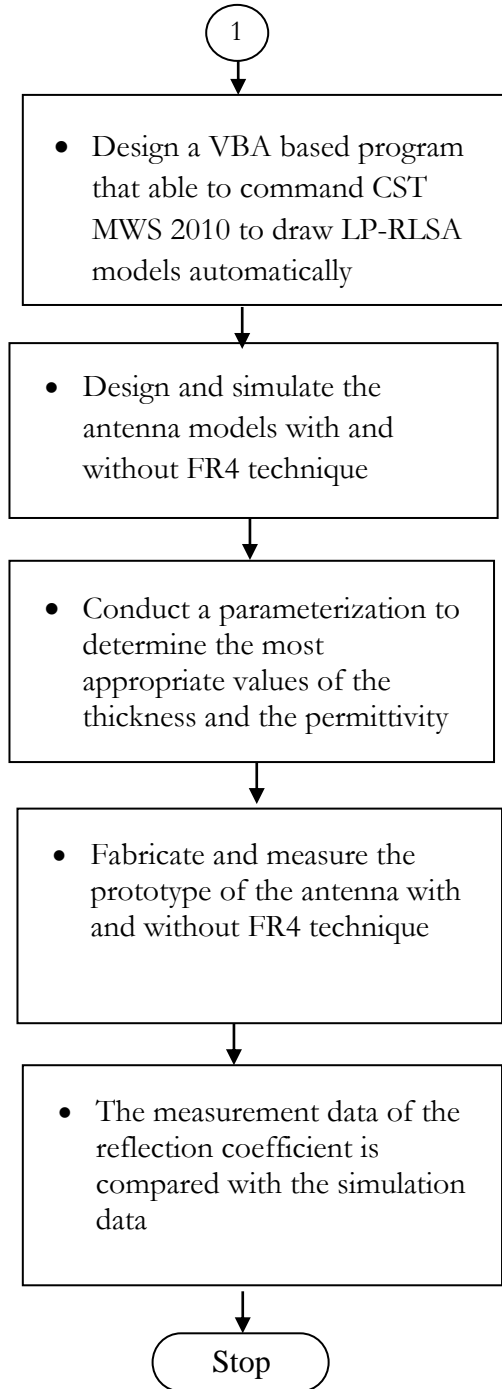


radiation pattern, the directivity of the antenna models were gathered and analyzed.

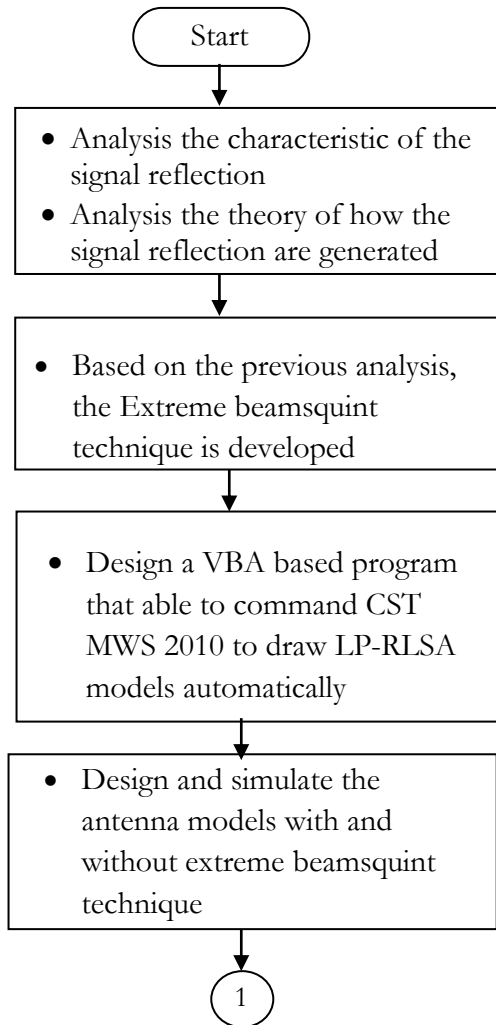
To verify the simulation results, a prototype of the antenna model with beamsquint technique and a prototype of antenna model without beamsquint technique are fabricated and measured. The measurement results were then compared with the simulation results. The agreement between the measurement results and the simulation results is the proof of the validity of the developed technique.

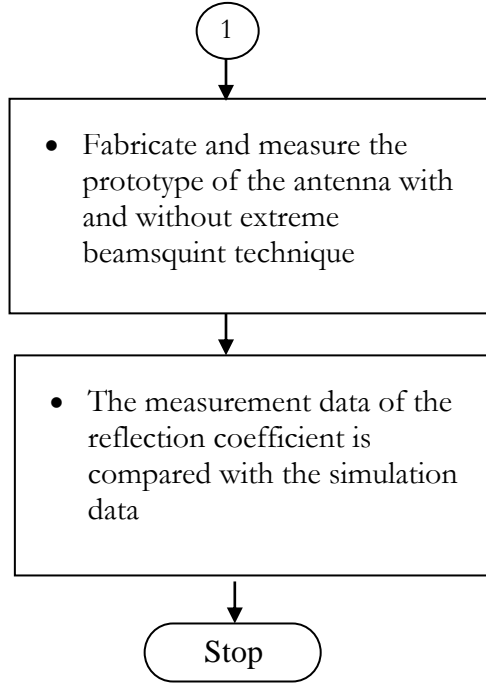
### 3.2 The Flowchart of Research Process in Chapter 4





### 3.3 The Flowchart of Research Process in Chapter 5





### 3.4 Research Methodology

1. The methodology to develop the techniques to overcome the problem of the high reflection coefficient in VSA-RLSA antennas.

The techniques to overcome the high reflection coefficient in VSA-RLSA antennas were developed by analyzing the characteristic of signal reflections in VSA-RLSA antennas and the theory of how the signal reflection generated in VSA-RLSA antennas.

Based on this analysis, this research developed the FR4 technique and the extreme beamsquint technique.

2. The Methodology to gather the data
  - a. Implement the FR4 techniques and the extreme beamsquint technique in designing antenna models and simulate the antenna models
  - b. Fabricate and measure the antenna models
3. The Methodology to verify the developed techniques
  - a. Carry out a comparison between the developed theory, the measurement results and the simulation results.

# Chapter 4

## The FR4 Technique

This chapter discusses a novel technique developed to minimize the reflection coefficient of VSA-RLSA antennas. This technique name is FR4 technique. Besides minimizing the reflection coefficient, this technique also can simplify the fabrication process of VSA-RLSA antennas. Section 4.1 starts the discussion by developing a theory of how the FR4 technique can minimize the reflection coefficient of VSA-RLSA antennas. This section also discusses the parameters that influence the capability of the FR4 board in minimizing the reflection coefficient, such as the thickness and permittivity of the FR4 board. Furthermore, this section explains the reason of why this technique can simplify the fabrication process of VSA-RLSA antennas. In order to verify the validity of the FR4 technique, Section 4.2 discusses the design of several antenna models for various thicknesses and permittivity. The simulation and measurement results of the models such as

the reflection coefficient response, the antenna gain and the beamsquint effect are analysis and discussed in Section 4.3. This section analysis the effect of the thickness and permittivity of FR4 boards to the reflection coefficient and gain of RLSA antennas. The most appropriate value of the FR4 thickness and permittivity are also determined. Finally, Section 4.4 presents the conclusions of this chapter.

## **4.1 The Theoretical Analysis of the FR4 Technique**

### **4.1.1 How the FR4 Technique Can Minimize Reflection Coefficients**

The high reflection coefficient of VSA-RLSA antennas is normally due to the distance of  $\lambda_g/2$  between two neighbouring slots in a same ring as explained in Section 2.3.2.  $\lambda_g$  is the wavelength of signals within the antenna cavity. Figure 4.1 shows that since the distance between slot 'A' and 'B' is  $\lambda_g/2$ , the reflected signals (the grey arrow) from the slot at 'A' and the slot at 'B' will have a same phase at 'C'. Therefore, they will strengthen each other while they are propagating toward the antenna feeder, thus increasing the reflection coefficient.

Figure 4.2 describes the process of how the FR4 board can reduce the reflection coefficient in RLSA antennas. The equation of the two reflected signals at 'C'

reflected from two neighbouring slots ('A' and 'B') can be expressed by Equation 4.1.

$$E_A = X_A \cos(\omega t - k_1 z_1)$$

$$E_B = X_B \cos(\omega t - k_2 z_2) \quad (4.1)$$

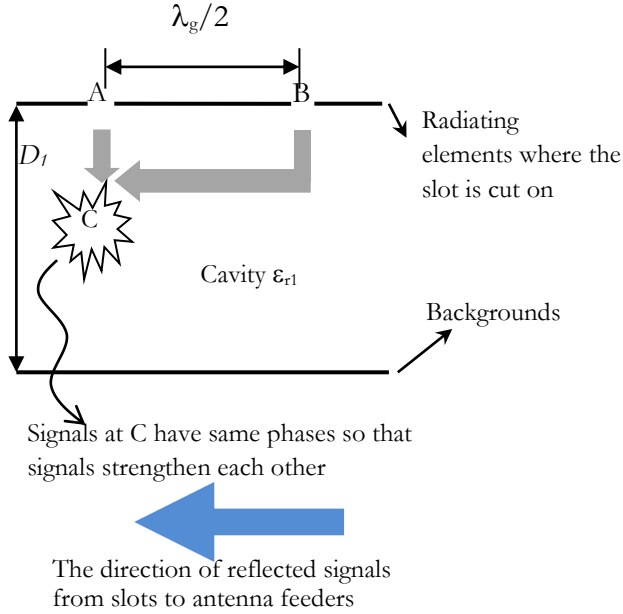


Figure 4.1 The mechanism of generating the reflection coefficient in RLSA antennas

In Equation 4.1, the analysis in this section assumes the magnitude of signal  $E_A$  and the magnitude of signal  $E_B$  (that is  $X_A$  and  $X_B$ ) same in order to simplify the analysis.



The wave vector ( $k_1$ ) and the wave vector ( $k_2$ ) can be written in detail as shown in Equation 4.2:

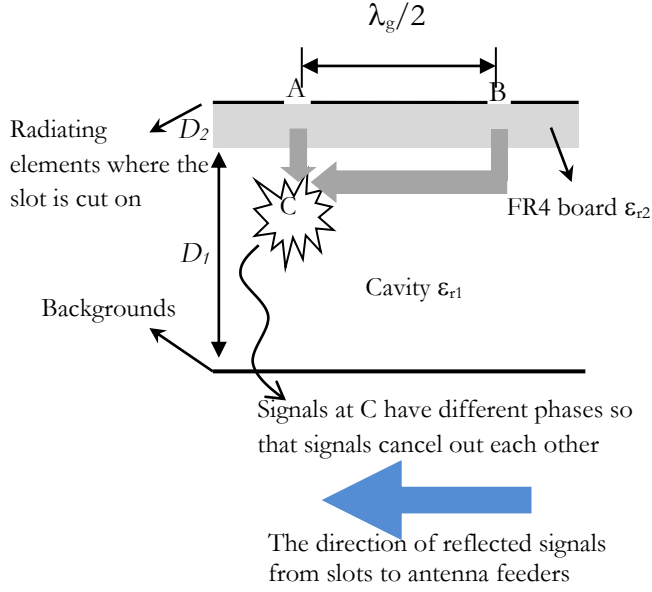


Figure 4.2 The mechanism of reducing the reflection coefficient in RLSA antennas with the FR4 board

$$k_1 = 2\pi/\lambda_{g1} = 2\pi/\left(\lambda_0/\sqrt{\epsilon_{r1}}\right) = \frac{2\pi\sqrt{\epsilon_{r1}}}{\lambda_0}$$

$$k_2 = 2\pi/\lambda_{g2} = 2\pi/\left(\lambda_0/\sqrt{\epsilon_{r2}}\right) = \frac{2\pi\sqrt{\epsilon_{r2}}}{\lambda_0} \quad (4.2)$$

Equation 4.2 is substituted into Equation 4.1 and results Equation 4.3 as below:

$$\begin{aligned}
E_A &= X_A \cos \left( wt - \frac{2\pi\sqrt{\epsilon_{r1}}}{\lambda_0} z_1 \right) \\
E_B &= X_B \cos \left( wt - \frac{2\pi\sqrt{\epsilon_{r2}}}{\lambda_0} z_2 \right)
\end{aligned} \tag{4.3}$$

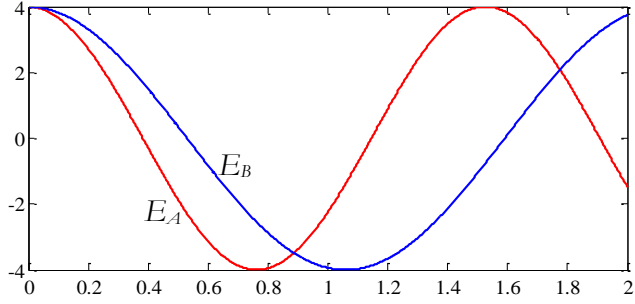
Based on Equation 4.3, signal  $E_A$  and signal  $E_B$  have a same frequency and different phases. The phases difference is determined by the signal position in the cavity ( $z_1$  and  $z_2$ ), the permittivity of the cavity ( $\sqrt{\epsilon_{r1}}$ ), and the permittivity of FR4 board ( $\sqrt{\epsilon_{r2}}$ ). Since the two reflected signals ( $E_A$  and  $E_B$ ) have different phases at C, hence they will cancel out each other while they are propagating toward the feeder, thus decreasing the reflection coefficient of the antenna.

In order to get a minimum reflection coefficient, the total sum of signal  $E_A$  and signal  $E_B$  at all positions along the cavity (all  $z_1$  and  $z_2$  values) and during the operating time (so called  $t_1$  to  $t_2$ ) should be minimum. This condition can be expressed by Equation 4.4 below:

$$\int_{z_1}^{z_2} \int_{t_1}^{t_2} (E_A + E_B) dt dz = \text{minimum}$$

$$\int_{z_1}^{z_2} \int_{t_1}^{t_2} \left( X_A \cos \left( wt - \frac{2\pi\sqrt{\epsilon_{r1}}}{\lambda_0} z_1 \right) + X_B \cos \left( wt - \frac{2\pi\sqrt{\epsilon_{r2}}}{\lambda_0} z_2 \right) \right) dt dz = \text{minimum} \quad (4.4)$$

To achieve the minimum condition in Equation 4.4, the phase difference between signal  $E_A$  and signal  $E_B$  is set to be equal to  $\pi$  radian or  $180^\circ$ . The parameters that can be modified for this purpose are  $\sqrt{\epsilon_{r1}}, \sqrt{\epsilon_{r2}}$   $z_1$  and  $z_2$ . However, the appropriate values for  $\sqrt{\epsilon_{r1}}, \sqrt{\epsilon_{r2}}, z_1$  and  $z_2$  are difficult and too complex to be calculated mathematically. This is because signal  $E_A$  and signal  $E_B$  have a changeable phase difference over various positions ( $z_1$  and  $z_2$ ) in the cavity. As an example, Figure 4.3 shows the plot of signal  $E_A$  and signal  $E_B$  over various positions (for  $X_A=X_B=4$ ,  $f=5.8$  GHz,  $\epsilon_{r1} = 2.33$  and  $\epsilon_{r2} = 4.3$ ). Figure 4.3 shows that signal  $E_A$  and signal  $E_B$  have different phase differences for various positions. The other reason why it is difficult to be calculated mathematically is the signal component  $\sqrt{\epsilon_{r2}}$  of  $E_B$  will gradually change into  $\sqrt{\epsilon_{r1}}$  as signal  $E_B$  exit from the FR4 board and enter into the cavity material (polypropylene) and propagates along this material.



The position (z)

Figure 4.3 The signal  $E_A$  and  $E_B$  along various positions (z).

Other parameter that influences the reflection coefficient is the thickness of the FR4 board ( $D_2$ ). This is because the thickness of the FR4 board determines the volume of the FR4 board, thus determines the amount of signal  $E_B$  that propagates within the FR4 board. However, similarly with  $\sqrt{\epsilon_{r1}}$  and  $\sqrt{\epsilon_{r2}}$ , the most appropriate thickness of the FR4 board that can fulfil the minimum condition in Equation 4.4 is too complex to be calculated mathematically.

Since  $\sqrt{\epsilon_{r1}}$ ,  $\sqrt{\epsilon_{r2}}$  and  $D_2$  are difficult and too complex to be calculated mathematically, the only way to find the appropriate value for them is by conducting a parametric study using an antenna simulation software, which will be discussed in Section 4.3.

#### **4.1.2 Why the FR4 Technique can Simplify the Fabrication Process of RLSA Antennas**

One of the problems of RLSA antennas is the fabrication process of the RLSA antennas are not simple compared to microstrip antennas. This due to the need of a special fabrication tools such as a large plotter that is used to cut slots on the antenna radiating element [8]. To simplify the fabrication process of RLSA antennas, several researches reported the utilization of cheap FR4 materials with its simple etching process as the material for the RLSA antenna [9-13]. However, in those researches, the utilization of several FR4 boards as the antenna cavity reduces the performance of RLSA antennas. This is due to the presence of air gaps, glues and the poor electrical performance of the FR4 board.

In the FR4 technique, a FR4 board is added on the top of a RLSA antenna. The copper material of the FR4 board is utilized as the radiating element of the RLSA antenna. This can simplify the fabrication process since the slots on the radiating element can be cut by utilizing a simple etching process rather than utilizing the large plotter.

## **4.2 The Design of Experimental VSA-RLSA Antennas with FR4 Techniques**

### **4.2.1 The Designed Antennas for Parametric Study**

In order to determine the appropriate permittivity and appropriate thickness of the FR4 board as discussed in Section 4.1.1, a VSA-RLSA antenna with FR4 board was designed and simulated for various permittivities and for various FR4 thicknesses at the frequency of 5.8 GHz. The structure of the VSA-RLSA with FR4 board, a RLSA without FR4 board and their feeder were designed utilizing CST-MWS-2010 simulator and shown in Figure 4.4. To draw the antenna model automatically in CST-MWS-2010, this research developed a Visual Basic Application (VBA) based. Section A.1 of Appendix A shows the program code. To calculate the optimum dimension of the feeder, this research used special software developed by Prof M.E. Bialkowski from University of Queensland.

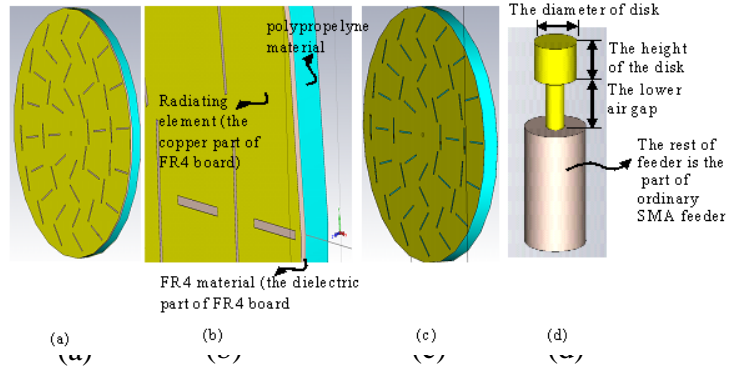


Figure 4.4(a) The structure of the VSA-RLSA antenna with FR4 boards (b) The zoom of Figure 4.4(a) (c) The structure of the VSA-RLSA antenna without FR4 boards. (d) The Antenna feeder

The structure of the VSA-RLSA antenna without a FR4 board consists of a radiating element (made of copper), a cavity (made of polypropylene), a background (made of copper) and a feeder. The structure of the VSA-RLSA antenna with a FR4 board consists of a radiating element (the copper part of the FR4 board), a dielectric material (the material of the FR4 board), a cavity (made of polypropylene), a background (made of copper) and a feeder. Table 4.1 and Table 4.2 list the detail specifications of both antennas and their feeders, respectively.

Table 4.1 The Specification Parameters of the VSA-RLSA Antenna Model

Specification Parameters	Symbol	Value
Centre Frequency	$F$	$5.8\text{ GHz}$
Wavelength inside the cavity	$\lambda_g$	$33.88\text{ mm}$
Slot length	$L$	$0.5\lambda$
Slot width	$W$	$1\text{ mm}$
Spacing between unit radiators in radial directions	$S_\rho$	$\lambda/2\text{ mm}$
Number of rings	$N$	$2\text{ rings}$
Number of slot pairs in first ring	$Z$	$8\text{ pairs}$



Number of slots	$N$	<i>48 slots</i>
Radius of antenna	$R$	<i>85 mm</i>
Cavity material	-	<i>Polypropylene</i>
Cavity thickness	$D_1$	<i>8 mm</i>
Cavity permittivity	$\epsilon_{r1}$	<i>2.47</i>
The thickness of FR4 board	$D_2$	<i>1.6 mm</i>
The permittivity of FR4 board	$\epsilon_{r2}$	<i>4.3</i>

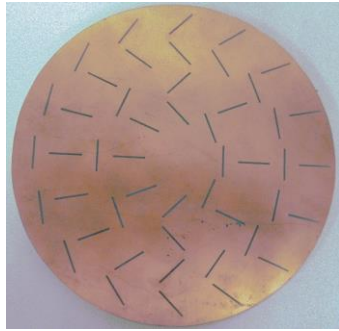
Table 4. 2 The Specification Parameters of Feeder

Specification Parameters	Symbol	Value
Disc Height	$H$	<i>3 mm</i>

Disc Radius	$R_a$	$1.4\text{ mm}$
Lower air gap	$b_1$	$4\text{ mm}$
Upper air gap	$b_2$	$1\text{ mm}$

#### 4.2.2 The Prototype of Designed Antennas

After determining the appropriate permittivity and the appropriate thickness of the FR4 board by parameterizations, their values were utilized as the values to design the fabricated prototype of the VSA-RLSA with FR4 board and the fabricated prototype of the VSA-RLSA without FR4 board. Figure 4.5 shows the prototype structure of the VSA-RLSA with a FR4 board and without a FR4 board and Figure 4.6 shows their feeder. The feeder is an ordinary SMA feeder modified by adding a head disc. The function of the head disc is to convert signals from TEM coaxial modes into TEM cavity modes (radial modes), so that the signal fed by the feeder will propagate in a TEM mode in radial direction within the antenna cavity.



(a)



(b)



(c)



(d)

Figure 4.5 The prototype structure of VSA-RLSA antennas with and without FR4 boards (a) The radiating element (b) The side view of Figure 4.5(a) (c) The cavity (polypropylene) (d) the background



Figure 4.6 the Fabricated Antenna feeder

### **4.3 The Analysis of Experimental Results of FR4 Technique**

#### **4.3.1 Parametric Studies to determine appropriate permittivity and thickness**

The simulation result of the reflection coefficient of a VSA-RLSA antenna for various FR4 board permittivity (the thickness = 1.6 mm) and for various FR4 board thickness (the permittivity = 4.3) are shown in Figure 4.7 and Figure 4.8, respectively. Figure 4.7 shows that the permittivity influences the reflection coefficient response. This is because the permittivity is the parameter that determines signal phases within the FR4 board as explained in Section 4.1.1. Figure 4.8 also shows that the thickness

influences the reflection coefficient response. This is because a different thickness has a different capacity in changing signal phases within a FR4 board as explained in Section 4.1.1.

Figure 4.7 and 4.8 show that the most appropriate permittivity and the most appropriate thickness are 4.3 and 1.6 mm, respectively. This because that these values obtain the reflection coefficient that have a deepest valley at 5.8 GHz. Fortunately, the FR4 board that has the thickness of 1.6 mm and the permittivity of 4.3 is available in markets so that the prototype of this antenna can be fabricated and measured .

Figure 4.9 and Figure 4.10 show the simulation result of the antenna gain for various FR4 board permittivity (thickness=1.6) and various FR4 boards thickness (permittivity=4.3), respectively. In Figure 4.9, it can be observed that varying the FR4 permittivity can obtain the different antenna gain. The antenna for various FR4 board permittivity (3.2 up to 4.4) can achieve a higher gain compared to the gain of the antenna without FR4 board (12.92 dBi). The use of the permittivity of 4.0 obtains the highest gain of 14 dBi. Figure 4.10 shows that various FR4 board thicknesses influence the antennas gain. The antenna with various FR4 board thicknesses (0.2 up to 2.2) can

achieve the gains higher than the gain of the antenna without FR4 board (12.92 dBi). The use of the thickness of 0.8 obtains the highest gain of 14.37 dBi. The gain improvement in the VSA-RLSA antenna with FR4 board is achieved due to the significant improvement of reflection coefficient, which is then improving the efficiency of the antenna.

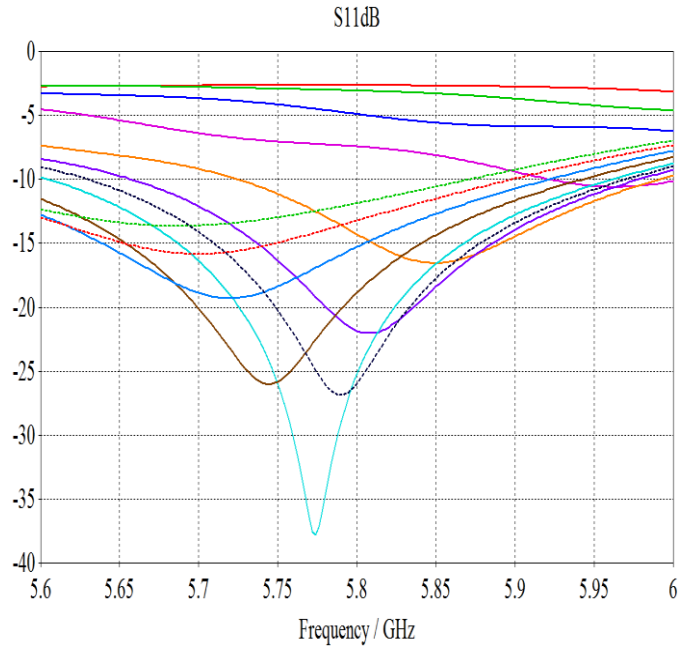


Figure 4.7 The simulation result of the Reflection coefficient for various permittivity of FR4 boards (the thickness =1.6 mm).

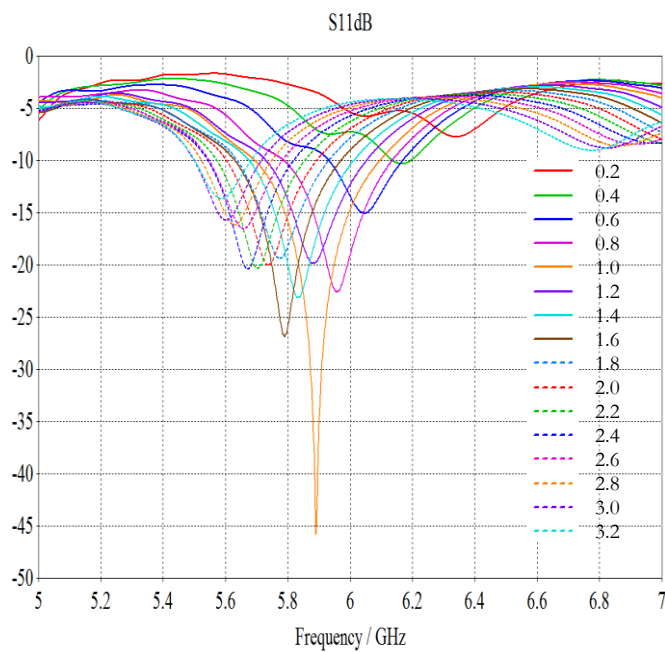


Figure 4.8 The simulation result of the Reflection coefficient for various thickness of FR4 board (the permittivity 4.3)

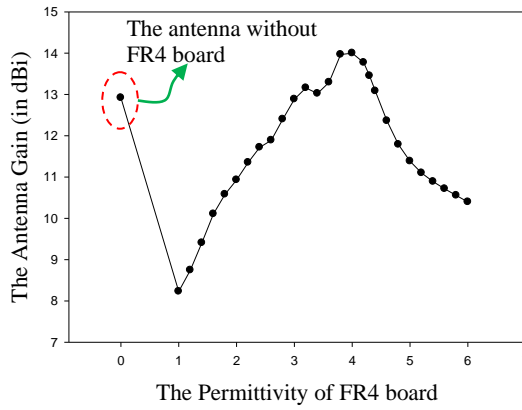


Figure 4.9 The simulation result of the Antenna Gain for various permittivity of the FR4 board (the thickness =1.3 mm)

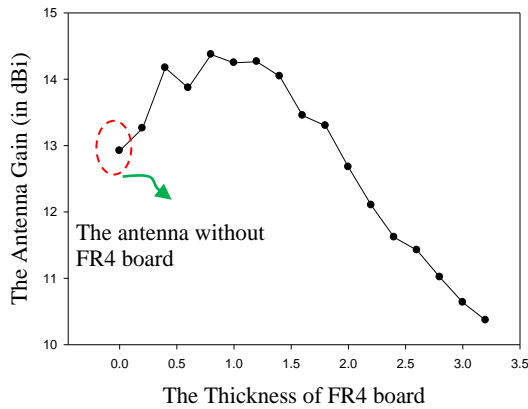


Figure 4.10 The simulation result of the Antenna Gain for various thickness of the FR4 board (the permittivity= 4.3)



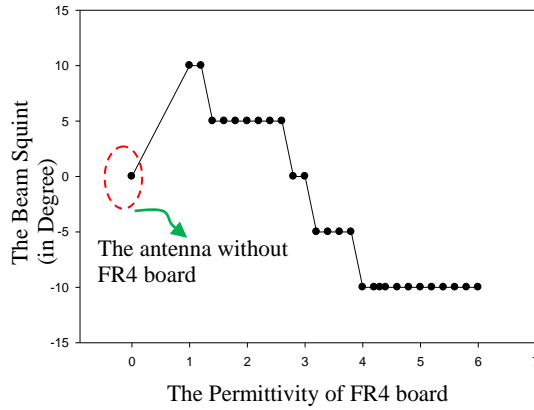


Figure 4.11 The simulation result of the Beamsquint angle for various permittivity of the FR4 board (the thickness = 1.3 mm)

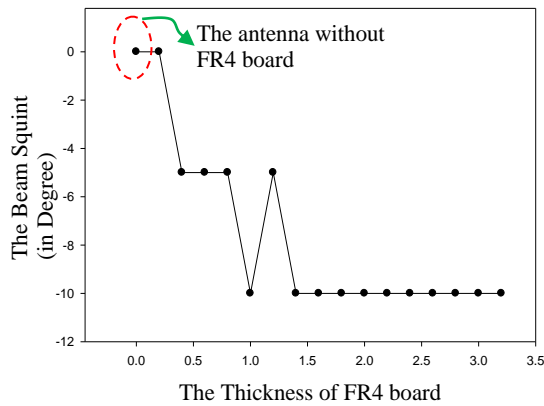


Figure 4.12 The simulation result of the Beamsquint angle for various thickness of FR4 board (the permittivity= 4.3)

The other effect of the FR4 technique is a beamsquint, which is the deviation of the antenna mainbeam

from its boresight direction. The beamsquint for various permittivity of the FR4 board (thickness=1.6) and for various thickness of the FR4 board (permittivity=4.3) are shown in Figure 4.11 and Figure 4.12, respectively. Figure 4.11 and Figure 4.12 show that various permittivity and various thicknesses of the FR4 board impact on the beamsquint ranging from  $10^0$  to  $-10^0$ . This beamsquint effect is because the signal propagates not only within the cavity but also within the FR4 board. Since the slots position and the slots orientation were designed for the cavity permittivity, hence the signal propagates within the FR4 board- which has different permittivity with the cavity- will result the beamsquint effect. However, the beamsquint effect does not disturb the antenna performance since the gain of the antenna utilizing the FR4 permittivity of 4.3 and the FR4 thickness of 1.6 is still higher than the gain of the antenna without the FR4.

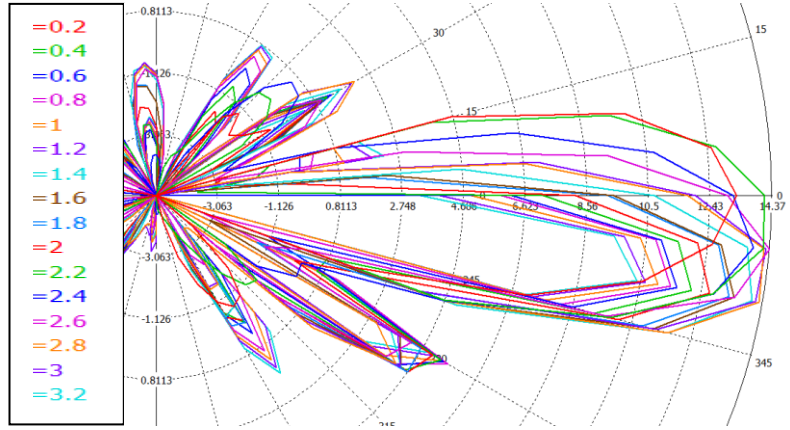


Figure 4.13 The radiation pattern of the VSA-RLSA for various thickness of FR4

Figure 4.13 and Figure 4.14 show the effect of varying the thickness and permittivity of FR4 to the antenna radiation pattern. These figures show that the thickness of FR4 influences the shape and boresight direction of the radiation pattern. The reason is because that the signal propagates not only within the cavity but also within the FR4 board. Since the slots position and slots orientation of RLSA antennas were designed for the cavity permittivity, hence the signal propagates within the FR4 board-which has different permittivity with the cavity-will obtain various different radiation patterns.

However, the effect of the FR4 board to the radiation pattern does not disturb the antenna performance

since the gain of the antenna that utilizing the appropriate FR4 board permittivity of 4.3 and the appropriate FR4 board thickness of 1.6 is still higher than the gain of the antenna without FR4 board.

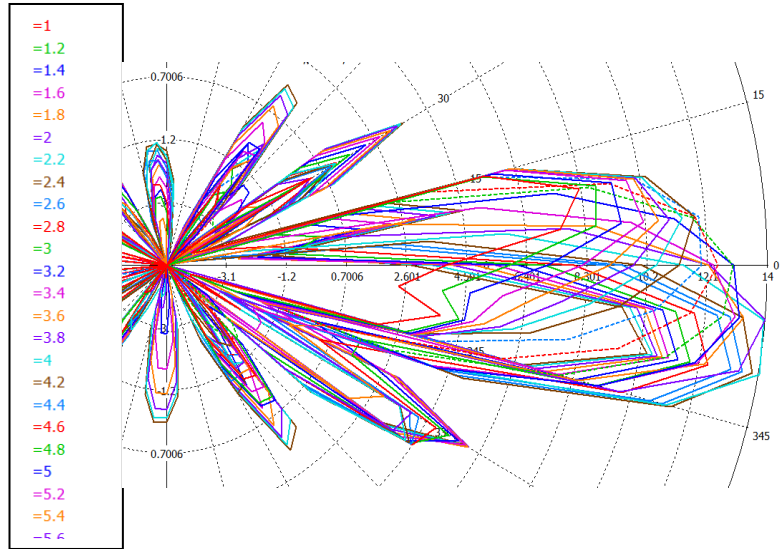


Figure 4.14 The radiation pattern of the VSA-RLSA for various permittivity of FR4

#### 4.3.2 The Designed Antenna Utilizing the Appropriate Permittivity and Thickness

Figure 4.15 shows the characteristic of the reflection coefficient of the VSA-RLSA with FR4 board and the VSA-

RLSA without FR4 board. Both of these antennas utilized all parameters listed in Section 4.2. The thickness and permittivity of the FR4 board are 1.6 mm and 4.3. The reason of utilizing these values are: firstly, these values are the most appropriate values to get the best reflection coefficient at 5.8 GHz as discussed previously at Section 4.3.1. Secondly, the FR4 material that has these specifications is available in markets. The deviation of the measurement result from the simulation result is due to the material imperfection of cheap FR4 boards, and the slight lack of accuracy in fabricating the antenna prototype.

In Figure 4.15, the simulation and measurement results show that the VSA-RLSA with FR4 board is able to improve the reflection coefficient response significantly. That is from about -3 dB become -25 dB at the frequency of about 5.8 GHz. From Figure 4.16, it can be observed that the VSA-RLSA with FR4 board has both inductive and reactive impedances over the test frequency (5.6–6 GHz) since some of the impedance curves lay above and below the equator of the Smith Chart. The resonant frequencies of the VSA-RLSA with FR4 board are 5.792 and 5.871 GHz for the simulation result and the measurement results, respectively. These resonant frequencies are also the frequencies that have the smallest reflection coefficient since they are the closest points to the centre of the Smith Chart.

From Figure 4.15, Figure 4.16 and Figure 4.17, it can also be observed that the reflection coefficient of the VSA-RLSA without FR4 board for both the simulation and measurement results are high as predicted by the RLSA theory. The reflection coefficient lies on around 1–3 dB along the test frequency. The impedance plot shows that the impedance of the VSA-RLSA without FR4 board is inductive since it lies above the equator of the Smith chart. Its position is also far from the centre of the Smith chart, which confirms the high reflection coefficient.

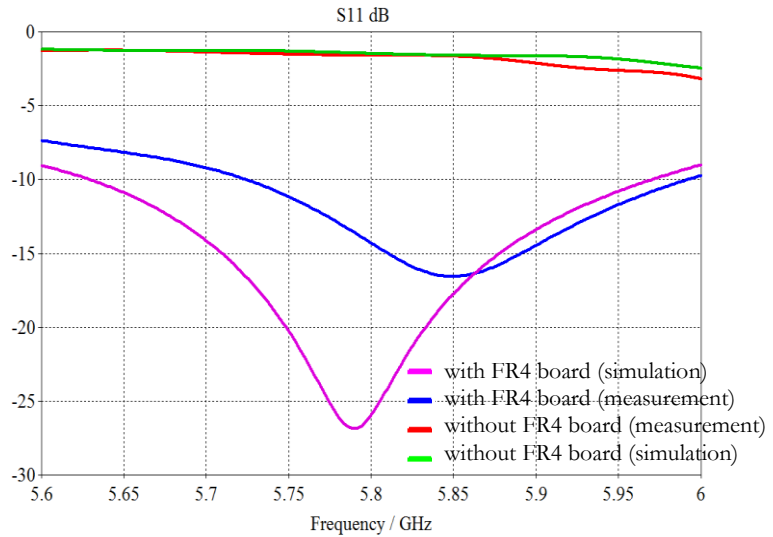


Figure 4.15 The Reflection coefficient of the VSA-RLSA with and without FR4 board both for the simulation result and the measurement result.

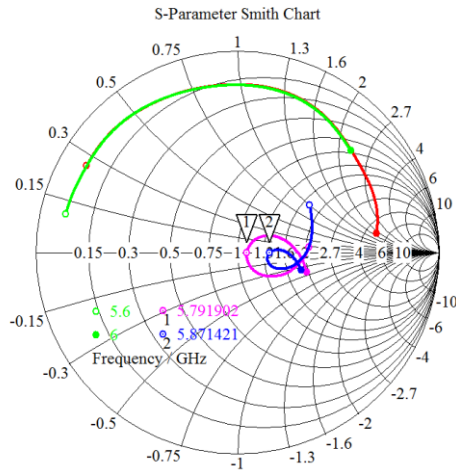


Figure 4.16 The Impedance of VSA-RLSA with and without FR4 board (The simulation and measurement result)

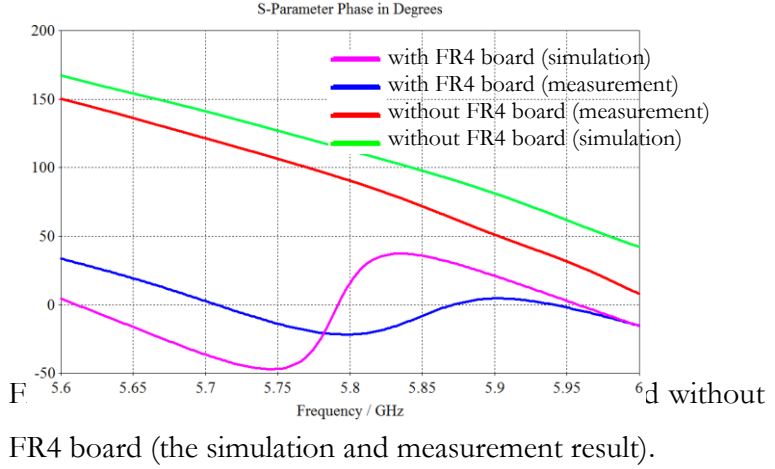


Figure 4.18 shows the polarization radiation pattern of the VSA-RLSA antenna. It can be observed from Figure 4.18 that the radiation pattern of the left polarization and the radiation pattern of the right polarization coincides one to each other. The gain of each polarization is half of the gain of the VSA-RLSA antenna. This means that the signal radiated by the antenna is equally divided into the left polarization and the right polarization. This result confirms the perfect linear polarization of the antenna.

Figure 4.19 shows the radiation pattern of the VSA-RLSA with FR4 board and the radiation pattern of the VSA-RLSA antenna without FR4 board both for the measurement and for the simulation. In Figure 4.19, the simulation result and measurement result show that the



VSA-RLSA with FR4 board has the better gain of about 2.45 dB compared to the VSA-RLSA without FR4 board. It is the improvement of the reflection coefficient, which obtains the gain improvement in the VSA-RLSA with FR4 board, which then improve the efficiency of the antenna. Figure 4.19 also shows that the VSA-RLSA with FR4 board has the beamsquint effect of about  $10^\circ$  that deviate from the boresight direction ( $90^\circ$ ).

Finally, the above result and the above analysis of the reflection coefficient and gain of the VSA-RLSA antenna verify and prove the concept and the theory explained in Section 4.1.

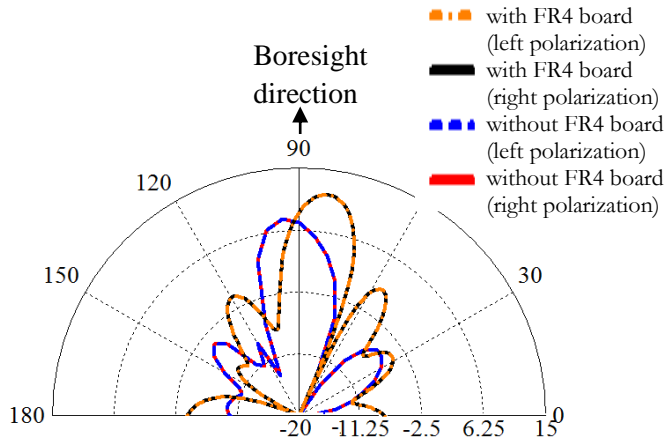


Figure 4.18 The polarization of the radiation pattern in term of gain (dBi) of a VSA-RLSA antenna (the simulation result)

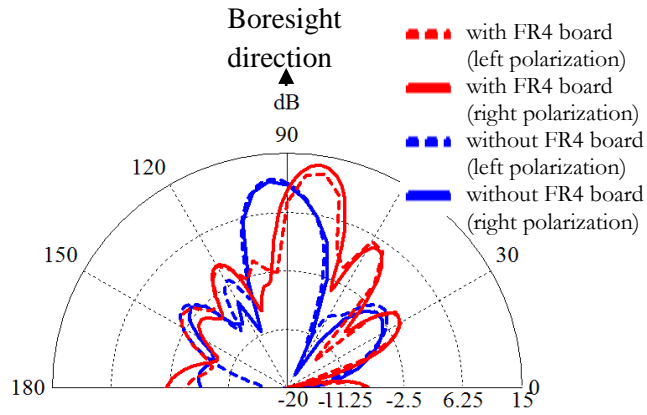


Figure 4.19 The Radiation Pattern (in term of gain in dBi) of the VSA-RLSA with and without a FR4 board (the simulation and measurement result).

# **Chapter 5**

## **The Extreme Beamsquint Technique**

This chapter discusses a novel technique developed to minimize the reflection coefficient of Very Small Aperture RLSA (VSA-RLSA) antennas. This research uses the term of VSA since the diameter of the RLSA antennas in this chapter is less than 150 mm, which is smaller than SA-RLSA antennas (the diameter less than 300 mm). The technique name is the extreme beamsquint technique. This technique utilizes very high beamsquint values (greater than  $70^\circ$ ) to obtain more rings on the radiating element of VSA-RLSA antennas, thus decrease the reflection coefficient and increase the efficiency of VSA-RLSA antennas. Section 5.1 starts the discussion of this chapter by developing a theoretical analysis on the limitation of normal beamsquint techniques and the operational function of how the extreme beamsquint technique can minimize reflection coefficients. Section 5.2 discusses the design of several VSA-RLSA

antennas for various beamsquint values with a diameter of 150 mm at a frequency of 5.8 GHz. The design uses the extreme beamsquint technique and the normal beamsquint technique to observe how the extreme beamsquint technique can minimize the reflection coefficient of VSA-RLSA antennas. Section 5.3 analyzes and discusses the simulation and measurement results of the designed antennas such as the reflection coefficient response, the antenna gain and the efficiency. Finally, Section 5.4 presents the conclusions of this chapter.

## **5.1 Theoretical Analysis**

This section will explain the developed theoretical analysis of how the normal beamsquint is no more able to minimize the reflection coefficient once the number of rings is insufficient, which is the limitation of the normal beamsquint technique. Furthermore, this section will discuss the analysis of how the extreme beamsquint technique can minimize the reflection coefficient of VSA-RLSA antennas.

### **5.1.1 The Limitation of Beamsquint Technique**

Section 2.3.2 has explained that the reflected signal from the RLSA slots is due to a distance of  $\lambda_g/2$  between two neighbouring slots. In RLSA antennas, the normal beamsquint technique can overcome the effect of this kind

of reflected signals [1, 5]. The ability of the beamsquint technique in minimizing the reflected signal depends on one condition that is the number of rings must be sufficient. As an example, Figure 5.1 and 5.2 show the reflected signals of a three rings RLSA antenna and the reflected signals of a two rings RLSA antenna, respectively. Since every ring consists of two slots, hence, there are six reflected signals for the three rings RLSA antenna and four reflected signals for the two rings RLSA antenna. This research assumes that the amplitude of all reflected signals is same in order to simplify the analysis in this section. Figure 5.1 shows that the reflected signals cover all the graph space, hence all reflected signals cancel out each other and their combination is a small amplitude signal. In contrast, Figure 5.2 shows that the reflected signals cannot cover all area of the graph space (the area indicated by 'A'). Hence, their combination is a signal that has greater amplitude than the combined signal in Figure 5.2.

The example in the previous paragraph shows that the smaller number of rings decreases the ability of the beamsquint technique in cancelling the reflected signal. Therefore, this is the reason why the reflection coefficient of VSA-RLSA antennas that have small number of rings (less than 2) is high and why the normal beamsquint technique

fails to minimize the reflection coefficient of VSA-RLSA antennas. Next section will explain how the proposed extreme beamsquint technique can reduce the high reflection coefficient of VSA-RLSA antennas by increasing the number of rings.

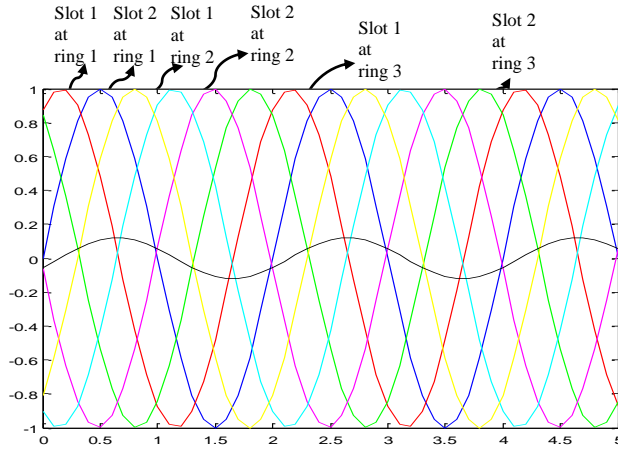


Figure 5.1 The reflected signal of a three ring RLSA antenna

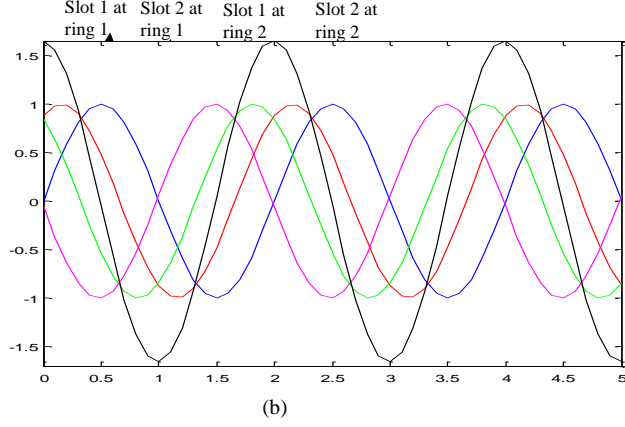


Figure 5.2 The reflected signal of a two ring RLSA antenna

### 5.1.2 How The Extreme Beamsquint Technique Minimize the Reflection Coefficient of VSA-RLSA Antennas

The ring tracks in radial directions ( $S_\rho$ ) can be expressed by Equation 5.1 below [5, 6]:

$$S_\rho = \frac{r\lambda_g}{1 - \xi \sin \theta_T \cos(\phi - \phi_T)} \quad (5.1)$$

$\theta_T$  is the beamsquint angle,  $\phi$  is the position of slots in azimuth,  $\phi_T$  is the azimuth angle of beamsquint and  $r$  is the ring number. Figure 5.3 illustrate the definition of all this parameters.

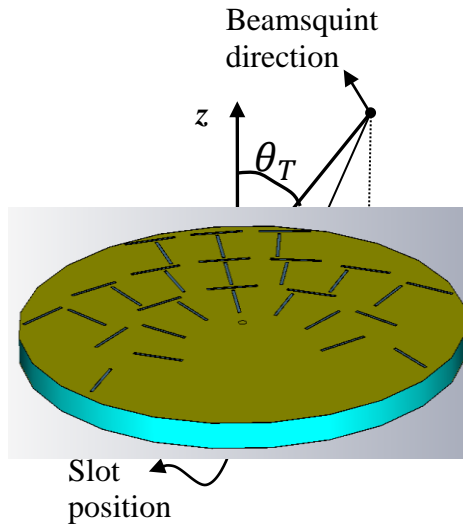


Figure 5.3 The illustration of some parameters of ring tracks

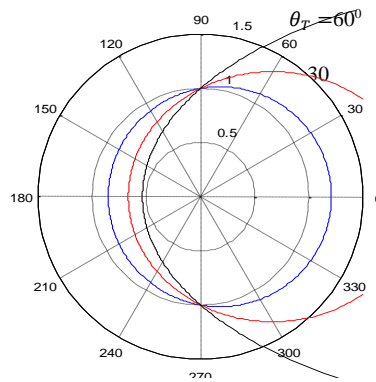


Figure 5.4 The plot of ring tracks for beamsquint of  $20^\circ$ ,  $30^\circ$ ,  $60^\circ$



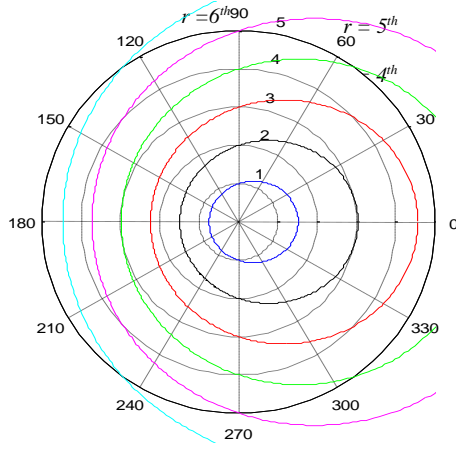


Figure 5.5 The plot of ring tracks for the beamsquint angle of  $20^\circ$

Based on Equation 5.1, by utilizing  $r = 1$ ,  $\phi_T = 0$  and  $\phi = 0$  to  $360^\circ$ , the rings for the beamsquint angle of  $10^\circ$ ,  $30^\circ$  and  $60^\circ$  are plotted as shown in Figure 5.4. Figure 5.4 illustrates that the implementation of the beamsquint technique obtains the ring tracks in a shape of ellipse like rather than in a shape of circular. Furthermore, the ring tracks at the left hand-side will shift closer to the antenna centre as the beamsquint values increase. In contrast, the ring tracks at the right hand-side will move farther from the antenna centre as the beamsquint increases.

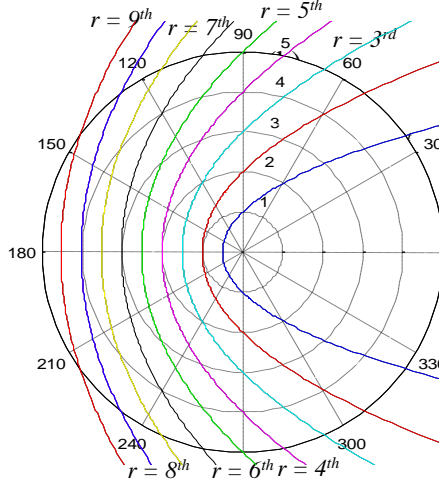


Figure 5.6 The plot of ring tracks for the beamsquint angle of  $80^\circ$

Still based on Equation 5.1, by utilizing  $\phi_T = 0$  and  $\phi = 0$  to  $360^\circ$ , ring tracks are plotted for various ring numbers both for beamsquint angles of  $20^\circ$  and  $80^\circ$  as shown by Figure 5.5 and 5.6, respectively. Based on the observation to these figures, at the left hand-side, the distance between the ring tracks for beamsquint angle of  $80^\circ$  is shorter than the distance between the ring tracks for beamsquint angle of  $20^\circ$ . Due to the shorter distance between the ring tracks, the design of the ring tracks using a beamsquint angle of  $80^\circ$  obtains more rings (9 rings) compared to the design of the ring tracks using a beamsquint angle of  $20^\circ$  (6 rings). Therefore, this research

concludes that the design of ring tracks using high beamsquint angles obtain more rings compared to the design of ring tracks using low beamsquint angles. This fact is very useful to increase the number of rings of VSA-RLSA antennas that is originally small (less than 2). The increase in the number of rings makes VSA-RLSA antennas have more ability in minimizing reflection coefficients.

The other effect of designs using high beamsquint angles is the effect of more concentrated slots. Figure 5.7 and Figure 5.8 show the slots of VSA-RLSA antennas designed using a beamsquint angle of  $80^\circ$  and  $20^\circ$ , respectively. This figure shows that the slots of the VSA-RLSA designed using a beamsquint angle of  $80^\circ$  is more concentrated at the left hand-side area compared to the slots of the VSA-RLSA designed using a beamsquint angle of  $20^\circ$ . Theoretically, the slots can be considered loads. Hence, the more concentrated slots mean the more concentrated loads. The more concentrated loads will effect to the distribution of the power supplied by the antenna feeder. When the slots equally spread the power also will equally spread in radial directions as illustrated by Figure 5.9. Since the number of slots is small in the antenna, the remaining power will be significant in the antenna perimeter and lead to a high reflection coefficient, as discussed in Section 2.3.1.

Conversely, when the slots are concentrated in certain area, most of the power also will be focused on the concentrated area, and only a small amount of the power will be sent to other areas, as illustrated by Figure 5.10. When most of the power is sent to the concentrated slots, the power will radiate more so that the remaining power at the antenna perimeter will be lower. The lower remaining power means a lower reflection coefficient.

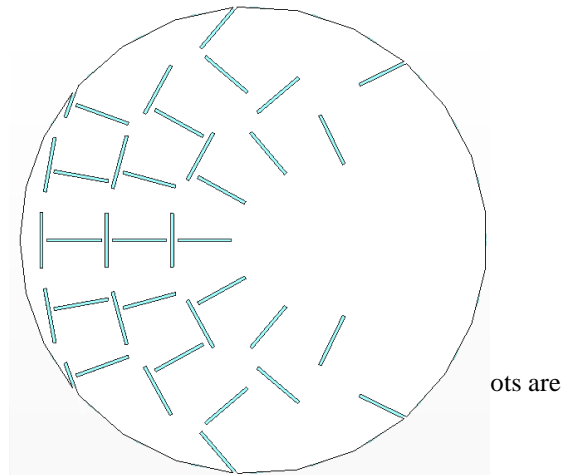


Figure 5.7 The RLSA antenna that has slots which are more concentrated in area A

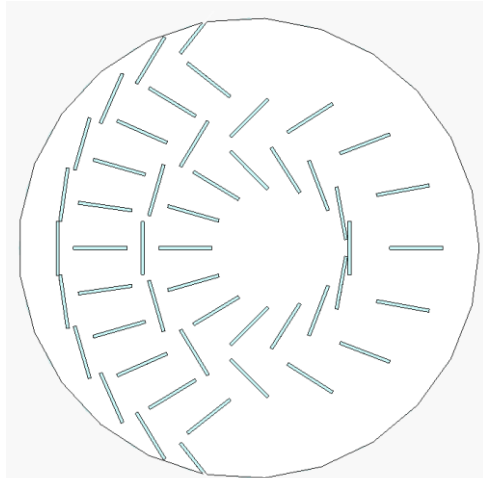


Figure 5.8 The power is almost spread to all direction

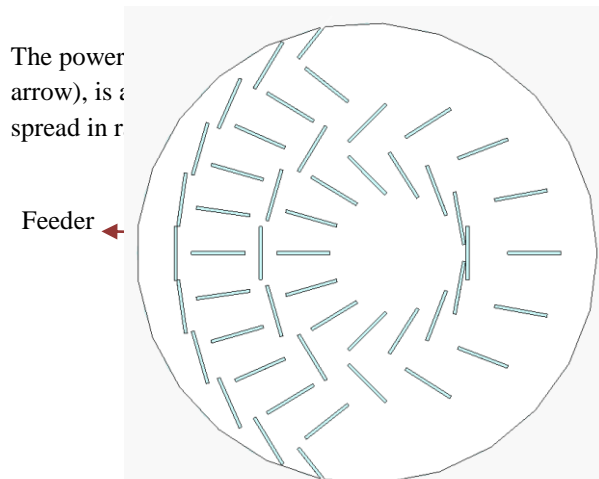


Figure 5.9 The power is equally spread to all directions

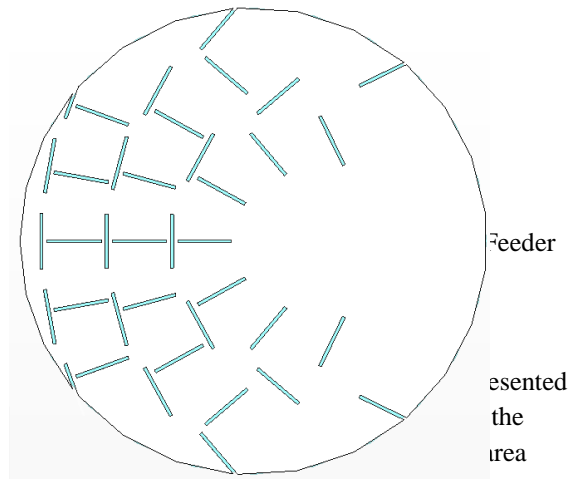


Figure 5.10 The power is mostly sent to the more concentrated slot areas.

The effect of the increase in the number of rings together with the effect of the more concentrated slots contribute to the reflection coefficient reduction as will be proven in the section 5.3.

## 5.2 The Structure and the Specification of Experimental Antennas

Figure 5.11 shows the structure of the VSA-RLSA antenna model that will be simulated and measured in Section 5.3. The structure consists of a radiating element (made of copper), a cavity (made of polypropylene), a background (made of copper) and a feeder. This research used CST-

MWS-2010 software to design and simulate the structure of the VSA-RLSA antenna model.

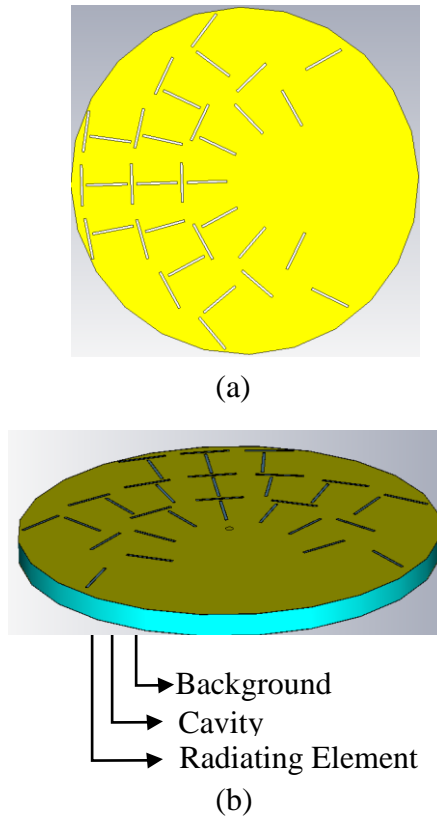


Figure 5.11 (a) The structure of VSA-RLSA antenna model  
(b) The slots configuration on the radiating element of VSA-RLSA antenna model

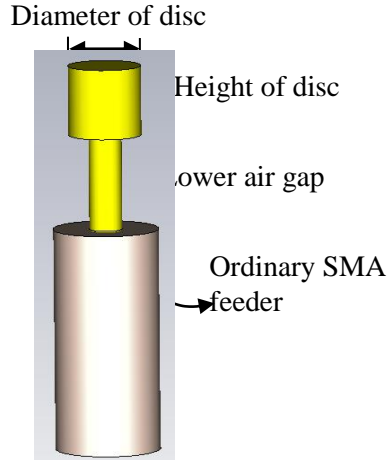


Figure 5.12 The feeder

To draw the antenna model automatically in CST-MWS-2010, a Visual Basic Application (VBA) based program was used and the program code was written in Section A.1 of Appendix A. The feeder shown by Figure 5.12 is an ordinary SMA feeder, which is modified by adding a head disc. The head disc has a function to convert the signal from a TEM coaxial mode into a TEM cavity mode (a radial mode), so that the signal fed by the feeder will propagate in a TEM mode and in radial direction within the antenna cavity. The detail specification of the VSA-RLSA antenna model and its feeder are listed in Table 5.1 and Table 5.2, respectively.



Table 5.1 The Specification Parameters of VSA-RLSA antenna model

Specification Parameters	Symbol	Value
Centre frequency	$f$	$5.8\text{ GHz}$
Wavelength inside the cavity	$\lambda_g$	$33.88\text{ mm}$
Slot length	$l$	$0.5\lambda_g$
Slot width	$w$	$1\text{ mm}$
Radius of antenna	$R$	$75\text{ mm}$
Number of slot pairs in first ring	$n$	$14$
Cavity thickness	$d_1$	$8\text{ mm}$
The thickness of radiating element and background	$d$	$0.1\text{ mm}$

Cavity permittivity	$\epsilon_{r1}$	2.47
Cavity material	-	<i>Polypropylene</i>
Radiating element and background material	-	<i>copper</i>

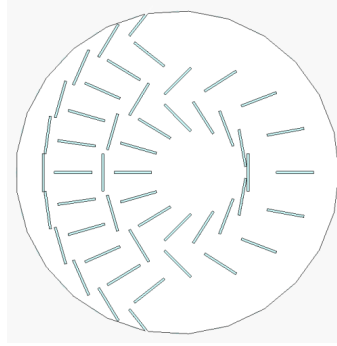
Table 5. 2 The Specification Parameters of Feeder

Specification Parameters	Symbol	Value
Disc height	$h$	3 mm
Disc radius	$r_a$	1.4 mm
Lower air gap	$b_1$	4 mm
Upper air gap	$b_2$	1 mm

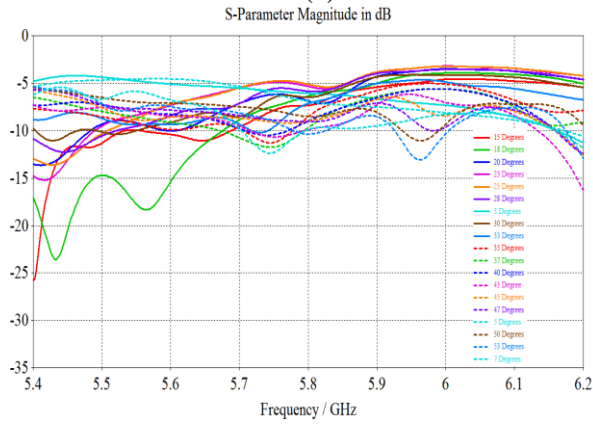
### 5.3 Results and Discussion

In order to observe the effect of the extreme beamsquint technique, this research simulated various VSA-RLSA antennas for various beamsquint values. The simulation used same antenna parameters as described in Section 5.2. The design of the VSA-RLSA antennas using low beamsquint values (ranging from  $3^{\circ}$  up to  $55^{\circ}$ ) obtains the VSA-RLSA antennas that have two rings. Figure 5.13(a) shows one of the antennas designed using a beamsquint value of  $20^{\circ}$ . In contrast, the design of the VSA-RLSA antennas using higher beamsquint values (ranging from  $58^{\circ}$  up to  $89^{\circ}$ ) obtains the VSA-RLSA antennas that have three rings. Figure 5.14(a) shows one of the antennas designed using a beamsquint value of  $87^{\circ}$ .

Figure 5.13(b) presents the reflection coefficient response of the VSA-RLSA antennas for various beamsquint ranging from  $3^{\circ}$  up to  $53^{\circ}$ . Figure 5.13(b) shows that the reflection coefficient responses around a centre frequency of 5.8 GHz averagely is above -10 dB. Figure 5.14(b) shows the reflection coefficient responses of the VSA-RLSA antennas for various beamsquint ranging from  $55^{\circ}$  up to  $89^{\circ}$ .

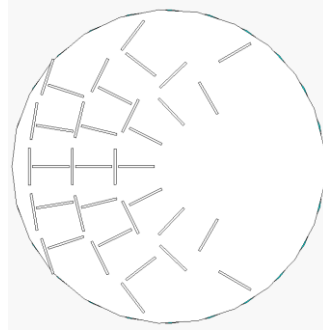


(a)

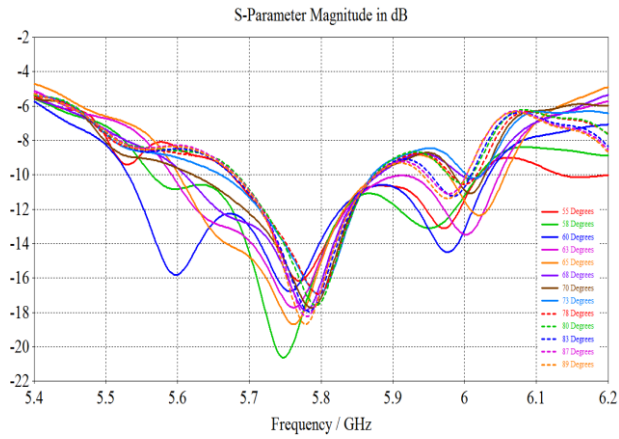


(b)

Figure 5.13 (a) The slots design for beamsquint of  $20^\circ$  (b) The reflection coefficient responses of VSA-RLSA antennas using low beamsquint values



(a)



(b)

Figure 5.14 (a) The slots design for beamsquint of  $87^\circ$  (b) The reflection coefficient responses of VSA-RLSA antennas using high beamsquint values.

In contrast to Figure 5.13(b), Figure 5.14(b) shows that the reflection coefficient around a centre frequency of 5.8 GHz averagely is -18 dB. Figure 5.14(b) also shows that the reflection coefficients form bandwidths of at least about

200 MHz. The better reflection coefficient response in Figure 5.14(b) compared to the reflection coefficient responses in Figure 5.13(b) is due to the effect of the utilization of high beamsquint values.

Figure 5.15 shows that the VSA-RLSA antennas designed using high beamsquint values (greater than  $60^\circ$ ) have higher efficiency (averagely above 90%) compared to the VSA-RLSA antennas designed using normal beamsquint values (smaller than  $60^\circ$ ). This result is the consequence of the better reflection coefficient that the high beamsquint VSA-RLSA antennas have, as discussed in previous paragraph.

Figure 5.16 shows that the gain of VSA-RLSA antennas designed using higher beamsquint values results lower gains. This is due to the emergence of grating lobes as the consequence of utilizing high beamsquint values [5, 6]. The grating lobe will influence the directivity of the VSA-RLSA antennas and thus lowering the gain.

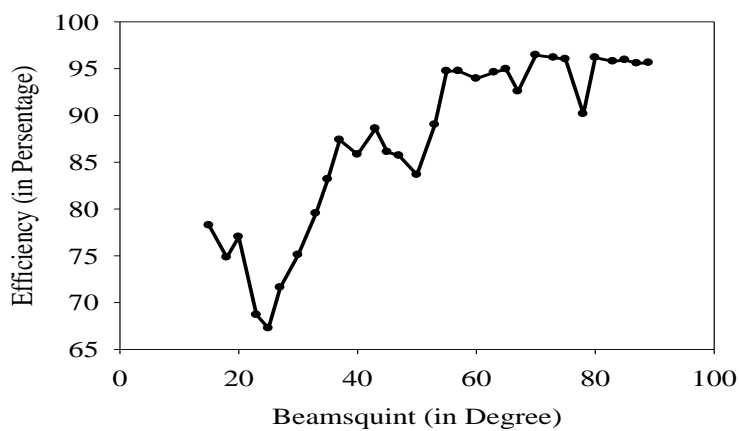


Figure 5.15 The Efficiency of the VSA-RLSA antennas for various beamsquint values.

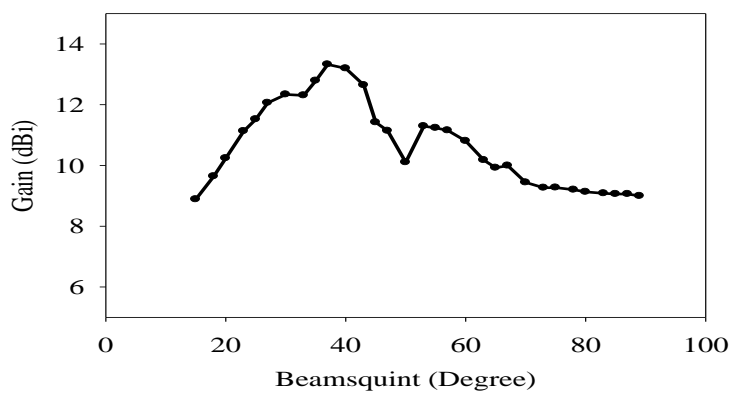


Figure 5.16 The Gain of the VSA-RLSA antennas for various beamsquint values

The beamsquint direction ( $\theta_T$ ) that can produce grating lobes is expressed by Equation (5.2) [5, 6].

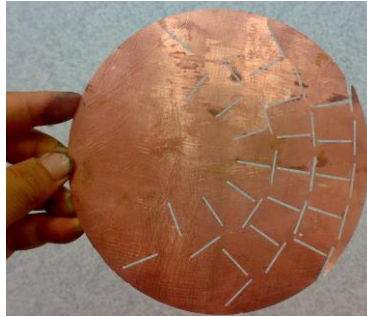
$$\theta_T = \sin^{-1} \left( \frac{\sqrt{\epsilon_r} - 1}{\cos(\phi - \phi_T)} \right) \quad (5.2)$$

For the simulation in this book, the permittivity of the cavity ( $\epsilon_r$ ) is set equal to 2.471. The minimum  $\theta_T$  ( $\theta_{Tmin}$ ) that can make the slots of VSA-RLSA antennas start to produce the grating lobes is calculated by setting the beamsquint in azimuth direction ( $\phi_T$ ) to be equal to  $0^\circ$  and the slot position in azimuth direction ( $\phi$ ) to be equal to  $0^\circ$ . Hence, by using Equation 5.2, we can get  $\theta_{Tmin} = 31.8^\circ$ . Still using Equation 5.2, other slots at respective  $\phi$  will start to produce the grating lobes as  $\theta_T$  increase greater than  $34.89^\circ$ . This means that the amount of the grating lobe increases proportionally with the increase of the designed beamsquint angle. Therefore, this is the reason why the gains in Figure 5.16 decrease as the beamsquint increase.

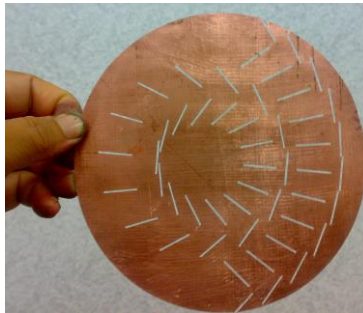
In order to verify the theoretical and simulation result, this research fabricated two prototypes of VSA-RLSA antennas, as shown by Figure 5.17(a) and 5.17(b). The first VSA-RLSA antenna utilizes the normal beamsquint technique (the beamsquint of  $20^\circ$ ) and the second VSA-RLSA antenna utilizes the extreme beamsquint technique



(the beamsquint of  $87^\circ$ ). The antennas parameters are same with the parameters tabulated in Table 5.1 and 5.2 in Section 5.2.



(a)



(b)

Figure 5.17 (a) The fabricated VSA-RLSA antenna for beamsquint  $87^\circ$  (b) The fabricated VSA-RLSA antenna for beamsquint  $20^\circ$



(a)



(b)

Figure 5.18 (a) The Cavity (b) The fabricated feeder

Figure 5.19 and 5.20 show the reflection coefficient response and the radiation pattern of the both VSA-RLSA antennas, respectively. Figure 5.19 shows that the first VSA-RLSA antenna which is using normal beamsquint has the

worse reflection coefficient compared to the second VSA-RLSA antenna which is using the extreme beamsquint technique, as appropriate with the explained theory in Section 5.2. Figure 5.20 shows that the directivity of the first VSA-RLSA antenna is higher than the directivity of the second VSA-RLSA antenna, as also appropriate with the explained theory in Section 5.2.

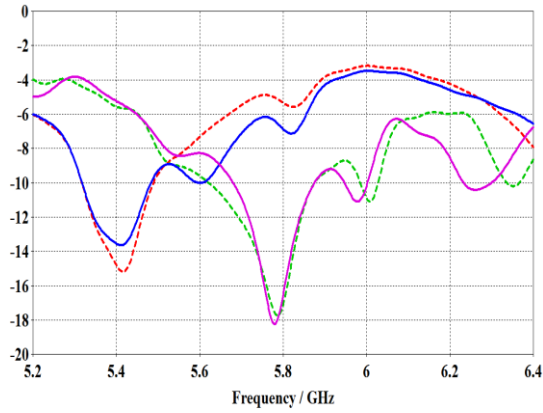


Figure 5.19 The measurement and the simulation result of VSA-RLSA antennas (the reflection coefficients)

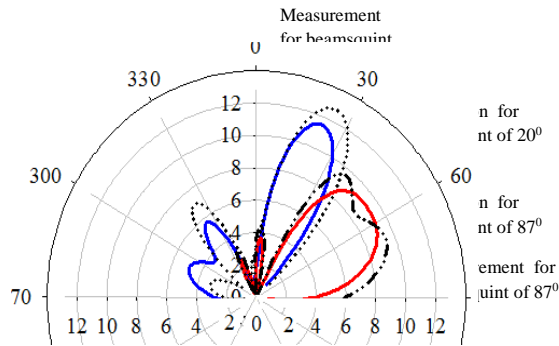


Figure 5.20 The measurement and the simulation result of VSA-RLSA antennas (the radiation patterns)

Figure 5.19 and 5.20 shows that the simulation result corresponds with the measurement result and the simulation result. A slight deviation of the measurement result from the simulation result is due to the imperfection in fabricating the antenna prototypes especially in drilling the hole for the antenna feeder at the exact position, aligning the radiating element, the cavity and the background, and in soldering the head disc for the SMA feeder in the correct position.

# Chapter 6

## Conclusions and Future Researches

### 6.1 Conclusions

A novel technique that aims to improve the reflection coefficient of VSA-RLSA antennas as well as to simplify the fabrication process of VSA-RLSA antennas is introduced and discussed in this book. This technique utilizes a FR4 board as an addition layer to the normal VSA-RLSA antenna. The fabrication process of the VSA-RLSA with FR4 board becomes simple since the slots are fabricated by cutting the copper part of FR4 board utilizing the simple photolithography etching process. In the other hand, the FR4 dielectric material can reduce the VSA-RLSA reflection coefficient significantly since the FR4 dielectric can change the phase of the signal reflected from the antenna slot. In order to observe the effect of the FR4 board, several antennas were simulated and parameterized.

Based on the discussion in Chapter 6, it is concluded that: Firstly, the thickness and permittivity of the FR4 board influences the ability of it to improve the reflection coefficient response and the antenna gain. For the antenna designed in this book, the most appropriate value of the permittivity and thickness are 4.3 and 1.6 mm, respectively. Secondly, the addition of the FR4 board can improve the reflection coefficient respond significantly from about -3 dB to -25 dB at frequency of 5.8 GHz. Thirdly, in this research, the addition of the FR4 board can improve the gain about 2.45 dB. Fourthly, the addition of the FR4 board obtains the antenna beamsquint that deviate the mainbeam from the boresight direction about  $-10^0$  up to  $10^0$ . In order to prove the concept of the novel technique, a VSA-RLSA with FR4 board and a VSA-RLSA without FR4 board were fabricated and measured. The measurement result and simulation result show that the VSA-RLSA with FR4 board has the better gain and the better reflection coefficient than the VSA-RLSA without FR4 board, thus prove the concept of the novel technique. This proposed novel technique would be a great step in simplifying the fabrication process and in realizing the mass production of VSA-RLSA antennas.

In addition to the FR4 technique, this book also discusses the implementation of the extreme beamsquint

technique to minimize the reflection coefficient of VSA-RLSA antennas theoretically. In order to prove the theory, this research designed the simulation models and prototype models of VSA-RLSA antennas. The analysis to the simulation and measurement results concludes that the implementation of the extreme beamsquint technique has successfully minimized the reflection coefficient from averagely above -10 dB to averagely -18 dB and formed the bandwidth about not less than 200 MHz. Furthermore, the implementation of the beamsquint technique improved the efficiency of VSA-RLSA antennas averagely 90 percent. The ability of this technique in minimizing the reflection coefficient response, forming the bandwidth and improving the efficiency of VSA-RLSA antennas would be a great step in realizing the development of RLSA technologies for small antenna applications.

## **6.2 Future Researches**

Based on the analysis on the theory of how the signal reflection generated in RLSA antenna. Other techniques are still possible to be developed. As stated in Section 2.3.1, VSA-RLSA antennas have high remaining power at the antenna perimeter, which will increase the reflection coefficient. This is due to its small number of slots. This problem can be overcome by increasing the number of slots.

The number of slots can increase by increasing the number of rings. The number of rings can increase by using high beamsquint values to design the antenna. This because that the high beamsquint values can add more ring on the antenna radiating element as discussed in Chapter 5. If we observe the slot arrangement of RLSA antenna designed using extreme beamsquint technique (discussed in Chapter 5), We can observed that a part of radiating element area is not covered by the slots. This area does not contribute to the antenna gain since there are no slots exist in this area. This area only used to keep the circular structure of the antenna radiating element. Hence, there is a possibility to cut away this area in order to make the antenna size to be smaller. Therefore, cutting this area in order to smaller the antenna size and analysis the effect of the cutting will be a quite interesting future research.



# References

- [1] M. Ando, *et al.*, "Radial Line Slot Antenna for 12 GHz Satellite TV Reception," *IEEE Transactions on Antennas and Propagation*, vol. AP-33, pp. 1347-1353, 1985.
- [2] P. W. Davis, "Experimental investigations into a linearly polarized radial slot antenna for DBS TV in Australia," *IEEE Transactions on Antennas and Propagation*, vol. 45, pp. 1123-1129, 1997.
- [3] M. F. Jamlos, *et al.*, "A beam steering radial line slot array (RLSA) antenna with reconfigurable operating frequency," *Journal of Electromagnetic Waves and Applications*, vol. 24, pp. 1079-1088, 2010.
- [4] M. F. Jamlos, *et al.*, "A reconfigurable radial line slot array (RLSA) antenna for beam shape and broadside

- application," *Journal of Electromagnetic Waves and Applications*, vol. 24, pp. 1171-1182, 2010.
- [5] M. F. Jamlos, *et al.*, "Adaptive beam steering of RLSA antenna with RFID technology," *Progress in Electromagnetics Research*, vol. 108, pp. 65-80, 2010.
  - [6] M.F. Jamlos, *et al.*, "A Novel Adaptive Wi-Fi System wiht RFID Technology," *Progress In Electromagnetics Research*, vol. 108, pp. 417-432, 2010.
  - [7] K. Sudo, *et al.*, "A millimeter-wave radial line slot antenna fed by a rectangular waveguide through a ring slot," *IEICE Transactions on Electronics*, vol. E84-C, pp. 1521-1527, 2001.
  - [8] J.-i. Takada, *et al.*, "Circularly polarized multibeam radial line slot antennas for mobile satellite communication," in *IEEE Antennas and Propagation Society, AP-S International Symposium (Digest)*, 1995, pp. 1430-1433.
  - [9] J. Hirokawa, *et al.*, "Matching slot pair for a circularly-polarised slotted waveguide array," *IEE Proceedings H: Microwaves, Antennas and Propagation*, vol. 137, pp. 367-371, 1990.

- [10] M. Takahashi, *et al.*, "Characteristics of small-aperture, single-layered, radial-line slot antennas," *IEE Proceedings H: Microwaves, Antennas and Propagation*, vol. 139, pp. 79-83, 1992.
- [11] K. S. Bialkowski and S. Zagriatski, "A dual band 2.4/5.2GHz antenna including a radial line slot array and a patch," in *IEEE Antennas and Propagation Society, AP-S International Symposium (Digest)*, 2004, pp. 3095-3098.
- [12] M. Ando, *et al.*, "Linearly polarized radial line slot antenna," *IEEE Transactions on Antennas and Propagation*, vol. 36, pp. 1675-1680, 1988.
- [13] P. W. Davis and M. E. Bialkowski, "Performance of a linearly polarized RLSA antenna for different beam squint angles," in *Asia-Pacific Microwave Conference Proceedings, APMC*, 1997, pp. 653-656.
- [14] M. E. Bialkowski and P. W. Davis, "Design and development of a Radial Line Slot Array antenna of arbitrary polarisation," in *Asia-Pacific Microwave Conference Proceedings, APMC*, 2000, p. 2.
- [15] M. R. U. Islam and T. A. Rahman, "Novel and simple design of multi layer Radial Line Slot Array

- (RLSA) antenna using FR-4 Substrate," in *2008 Asia-Pacific Symposium on Electromagnetic Compatibility and 19th International Zurich Symposium on Electromagnetic Compatibility, APEMC 2008*, 2008, pp. 843-846.
- [16] P. W. Davis, "A Linearly Polarised Radial Line Slot Array Antenna For Direct Broadcast Satellite Services," *University of Queensland Thesis Report*, 2000.
- [17] P. W. Davis and M. E. Bialkowski, "Performance of field matching and finite element methods on analysing coaxial-to-waveguide transitions," *Journal of Electrical and Electronics Engineering, Australia*, vol. 15, pp. 23-29, 1995.
- [18] P. W. Davis and M. E. Bialkowski, "Comparing beam squinting and reflection cancelling slot methods for return loss improvement in RLSA antennas," in *IEEE Antennas and Propagation Society, AP-S International Symposium (Digest)*, 1997, pp. 1938-1941.
- [19] P. W. Davis and M. E. Bialkowski, "Linearly polarized radial-line slot-array antennas with improved return-loss performance," *IEEE Antennas and Propagation Magazine*, vol. 41, pp. 52-61, 1999.

- [20] P. W. Davis and M. E. Bialkowski, "Beam synthesis in linearly polarized radial line slot array antennas," in *IEEE Antennas and Propagation Society, AP-S International Symposium (Digest)*, 2000, pp. 94-97.
- [21] M. I. Imran, "Pembangunan Antena Lubang Alur Untuk Aplikasi Capaian Wayarles Berjalur Lebar Tetap Pada Frekuensi 5725-5875 MHz," *Thesis, Universiti Teknologi Malaysia*, 2005.
- [22] M. I. Imran, *et al.*, "Beam squinted Radial Line Slot Array Antenna (RLSA) design for point-to-point WLAN application," in *2007 Asia-Pacific Conference on Applied Electromagnetics Proceedings, APACE2007*, 2007.
- [23] M. I. Imran and A. R. Tharek, "Radial line slot antenna development for outdoor point to point application at 5.8GHz band," in *2004 RF and Microwave Conference, RFM 2004 - Proceedings*, 2004, pp. 103-105.
- [24] M. I. Imran, *et al.*, "An optimization of beam squinted radial line slot array antenna design at 5.8 GHz," in *2008 IEEE International RF and Microwave Conference, RFM 2008*, Sabah, 2008, pp. 139-142.

- [25] K. C. Kelly, "Recent Annular Slot Array Experiments," *IRE National Convention Record*, vol. 5, pp. 144-151, 1957.
- [26] M. Ando, *et al.*, "Linearly-polarized radial line slot antenna," in *IEEE Antennas and Propagation Society, AP-S International Symposium (Digest)*, 1988, pp. 836-839.
- [27] M. Ando, *et al.*, "Radial line slot antenna for DBS reception," in *Conference Proceedings - European Microwave Conference*, 1988, pp. 306-311.
- [28] K. Endo, *et al.*, "Waveguide design of a radial line slot antenna," *Electronics and Communications in Japan, Part I: Communications (English translation of Denshi Tsushin Gakkai Ronbunshi)*, vol. 73, pp. 109-115, 1990.
- [29] J.-i. Takada, *et al.*, "A reflection cancelling slot set in a linearly polarized radial line slot antenna," *IEEE Transactions on Antennas and Propagation*, vol. 40, pp. 433-438, 1992.
- [30] M. Ando, *et al.*, "Single-layered radial line slot antenna for DBS reception," in *Conference Proceedings - European Microwave Conference*, 1990, pp. 1541-1546.

- [31] M. Ando, *et al.*, "A slot design for uniform aperture field distribution in single-layered radial line slot antennas," in *IEEE Antennas and Propagation Society, AP-S International Symposium (Digest)*, 1990, pp. 930-933.
- [32] M. Takahashi, *et al.*, "High efficiency flat array antennas for DBS reception," in *Conference Proceedings - European Microwave Conference*, 1991, pp. 629-634.
- [33] M. Takahashi, *et al.*, "Small aperture single-layered radial line slot antenna for DBS reception," in *IEE Conference Publication*, 1991, pp. 738-741.
- [34] M. Takahashi, *et al.*, "A slot design for uniform aperture field distribution in single-layered radial line slot antennas," *IEEE Transactions on Antennas and Propagation*, vol. 39, pp. 954-959, 1991.
- [35] J.-i. Takada, *et al.*, "Dual beam linearly-polarized radial line slot antenna," in *AP-S International Symposium (Digest) (IEEE Antennas and Propagation Society)*, 1993, pp. 1624-2627.
- [36] M. Takaahashi, *et al.*, "Dual circular polarized radial line slot antennas," in *AP-S International Symposium*

- (Digest) (*IEEE Antennas and Propagation Society*), 1993, pp. 1620-1623.
- [37] M. Takahashi, *et al.*, "Dual circularly polarized radial line slot antennas," *IEEE Transactions on Antennas and Propagation*, vol. 43, pp. 874-876, 1995.
  - [38] J.-i. Takada, *et al.*, "Azimuthal multibeam radial line slot antenna for mobile satellite communication," in *Annual International Conference on Universal Personal Communications - Record*, 1995, pp. 571-574.
  - [39] A. R. Tharek and I. K. Farah Ayu, "Theoretical investigations of linearly polarized radial line slot array (RLSA) antenna for wireless LAN indoor application at 5.5 GHz," in *Proceedings of the Mediterranean Electrotechnical Conference - MELECON*, 2002, pp. 364-367.
  - [40] M. R. Ul Islam, *et al.*, "Simple integrated system for wireless backhaul networks," in *Proceedings of the International Conference on Computer and Communication Engineering 2008, ICCCE08: Global Links for Human Development*, 2008, pp. 341-345.
  - [41] K. S. Bialkowski and S. Zagriatski, "Investigations into a dual band 2.4/5.2GHz antenna for WLAN



- applications," in *15th International Conference on Microwaves, Radar and Wireless Communications, MIKON - 2004*, 2004, pp. 660-663.
- [42] M. E. Bialkowski and P. W. Davis, "Predicting the radiation pattern of a radial line slot array antenna," *Asia-Pacific Microwave Conference Proceedings, APMC*, vol. 1, pp. 162-165, 1999.
- [43] M. E. Bialkowski and P. W. Davis, "Linearly polarized radial-line slot-array antenna with a broadened beam," *Microwave and Optical Technology Letters*, vol. 27, pp. 98-101, 2000.

# Appendix A

## The Program Code of VBA Software

### A.1. The Program Code to Draw RLSA with beamsquint technique

'=====

#### 'Preface

'=====

'This code program in used to draw RLSA antennas  
'automatically in CST-MWS-2010. Some of the formulas  
'used in this program were taken from PHd Thesis Report  
'written by Paul. W. Davis from University of Queensland,  
'Australia.

'This program was written by Teddy Purnamirza, from  
'Department of Electrical Engineering, Faculty Science and  
'Technology, Universitas Islam Sultan Syarif Kasim Riau,  
'Indonesia.

'This program is a free program and can be used or can be

'more developed by anyone provided acknowledging the  
 'programmer of the Program (Teddy Purnamirza). The  
 'programmer does not responsible to any misuse of this  
 'program and any damage caused by the utilization of this  
 'program.

' RLSA\_testing\_slot\_coupling  
 Sub Main ()  
 '=====  
 '@ use template: Antenna (Planar)  
 ' Template for Antenna in Free Space  
 ' (CSTxMWSxONLY)  
 ' =====

' Draw the bounding box  
 Plot.DrawBox True

' Set units to mm, ghz  
 With Units  
 .Geometry "mm"  
 .Frequency "ghz"  
 .Time "ns"  
 End With

' Set background material to vacuum

With Background

.Type "Normal"

.Epsilon "1.0"

.Mue "1.0"

.XminSpace "0.0"

.XmaxSpace "0.0"

.YminSpace "0.0"

.YmaxSpace "0.0"

.ZminSpace "0.0"

.ZmaxSpace "0.0"

End With

'Set boundary conditions to open

With Boundary

.Xmin "expanded open"

.Xmax "expanded open"

.Ymin "expanded open"

.Ymax "expanded open"

.Zmin "expanded open"

.Zmax "expanded open"

.Xsymmetry "none"

.Ysymmetry "none"

.Zsymmetry "none"

End With

' Optimize mesh settings for planar structures

With Mesh

.MergeThinPECLayerFixpoints "True"

.RatioLimit "20"

.AutomeshRefineAtPecLines "True", "6"

.FPBAAvoidNonRegUnite "True"

.ConsiderSpaceForLowerMeshLimit "False"

.MinimumStepNumber "5"

End With

' Change mesh adaption scheme to energy

' (planar structures tend to store high energy

' locally at edges rather than globally in volume)

MeshAdaption3D.SetAdaptionStrategy "Energy"

' Switch on FD-TET setting for accurate farfields

FDSolver.ExtrudeOpenBC "True"

'=====

'Declare all the general purpose variable

'=====

Dim er As Double 'permitivitas relatif cavity



```

'masukkan nilai parameter inputan
'=====

jari_kaviti=75: po=16: lebar_slot=1:tau=75:
fo=5.8: er=2.455: ur=1: teta=10^-5: z=1: n=0:
h=8: tebal_element_radiasi=0.1: jari_lubang_kaviti=1.4

'Hitung paramater-parameter yang berhubungan dengan
'parameter inputan
'=====

fd=fo+0.02257*fo 'hitung nilai frekuensi disain (GHz)
velocity=(2.9979)/Sqr(er*ur) 'Hitung kecepatan gelombang
                        'dalam cavity
lamda=velocity*10^2/fd 'Hitung panjang gelombang dalam
                        'cavity (mm)
inisial_panjang =0.5*lamda*fd/12.5

'Gambar cavity
'=====

WCS.ActivateWCS "local"

With Material 'setting material cavity
    .Reset

```

```

.Name "kaviti"
.FrqType "all"
.Type "Normal"
.Epsilon er
.Mue "1"
.Kappa "0"
.TanD "0.0"
.TanDFreq "0.0"
.TanDGiven "False"
.TanDModel "ConstTanD"
.KappaM "0"
.TanDM "0.0"
.TanDMFreq "0.0"
.TanDMGiven "False"
.TanDMModel "ConstTanD"
.DispModelEps "None"
.DispModelMue "None"
.DispersiveFittingSchemeEps "General 1st"
.DispersiveFittingSchemeMue "General 1st"
.UseGeneralDispersionEps "False"
.UseGeneralDispersionMue "False"
.Rho "0"
.ThermalType "Normal"
.ThermalConductivity "0"
.HeatCapacity "0"

```



```

.MetabolicRate "0"
.BloodFlow "0"
.Colour "0", "1", "1"
.Wireframe "False"
.Reflection "False"
.Allowoutline "True"
.Transparentoutline "False"
.Transparency "0"
.Create
End With

```

```

Component.New "antenna" 'setting komponen baru
'bernama antenna

```

```

With Cylinder 'gambar komponen kaviti
.Reset
.Name "kaviti"
.Component "antenna"
.Material "kaviti"
.OuterRadius jari_kaviti 'outer radius selinder adalah
                        'jari_terjauh
.InnerRadius "0"
.Axis "z"
.Zrange -h, "0"
.Xcenter "0"

```

```

.Ycenter "0"
.Segments "0"
.Create
End With

'Menggambar komponen radiating
'=====
Pick.PickFaceFromId "antenna:kaviti", "3" 'pick permukaan
                                     'cavity bagian depan

With Material 'setting material baru untuk komponen
    'radiating
    .Reset
    .Name "Copper"
    .FrqType "static"
    .Type "Normal"
    .Epsilon "1"
    .Mue "1.0"
    .Kappa "5.8e+007"
    .TanD "0.0"
    .TanDFreq "0.0"
    .TanDGiven "False"
    .TanDModel "ConstTanD"
    .KappaM "0"
    .TanDM "0.0"

```

```

.TanDMFreq "0.0"
.TanDMGiven "False"
.TanDMModel "ConstTanD"
.DispModelEps "None"
.DispModelMue "None"
.DispersiveFittingSchemeEps "General 1st"
.DispersiveFittingSchemeMue "General 1st"
.UseGeneralDispersionEps "False"
.UseGeneralDispersionMue "False"
.FrqType "all"
.Type "Lossy metal"
.Mue "1.0"
.Kappa "5.8e+007"
.Rho "0.0"
.ThermalType "Normal"
.ThermalConductivity "401.0"
.Colour "1", "1", "0"
.Wireframe "False"
.Transparency "0"
.Create
End With

```

```

With Extrude 'lakukan operasi extrude untuk membuat
    'komponen radiating
    .Reset

```

```

.Name "radiating"
.Component "antenna"
.Material "Copper"
.Mode "Picks"
.Height tebal_element_radiasi' tebal komponen radiating
.Twist "0.0"
.Taper "0.0"
.UsePicksForHeight "False"
.DeleteBaseFaceSolid "False"
.ClearPickedFace "True"
.Create
End With

```

```

'Menggambar ground
'=====
Pick.PickFaceFromId "antenna:kaviti", "1" 'pick permukaan
'belakang cavity

```

```

With Extrude 'lakukan operasi extrude untuk membuat
'komponen ground
.Reset
.Name "ground"
.Component "antenna"
.Material "Copper"

```

```

.Mode "Picks"
.Height tebal_element_radiasi 'tebal komponen ground
.Twist "0.0"
.Taper "0.0"
.UsePicksForHeight "False"
.DeleteBaseFaceSolid "False"
.ClearPickedFace "True"
.Create
End With

```

'Menggambar lubang pusat antena

'=====

With Cylinder

```

.Reset
.Name "lubang_feeder"
.Component "antenna"
.Material "Vacuum"
.OuterRadius jari_lubang_kaviti
.InnerRadius "0"
.Axis "z"
.Zrange -h-tebal_element_radiasi, "0"
.Xcenter "0"
.Ycenter "0"
.Segments "0"
.Create

```

End With

'Sisipkan lubang feeder ke kaviti

With Solid

.Version 9

.Insert "antenna:kaviti", "antenna:lubang\_feeder"

End With

With Solid

.Version 9

.Insert "antenna:ground", "antenna:lubang\_feeder"

End With

'Menghitung posisi slot dan Menggambar Slot

'=====

Dim kaunter As Double 'kaunter untuk increment keatas 1

'langkah

Dim kaunter1 As Double 'kaunter untuk increment keatas 1

'langkah

Dim sudut\_posisi\_slot1 As Double 'sudut (derajat) posisi

'slot1 (slot bagian dalam)

Dim kemiringan\_slot1 As Double 'kemiringan slot 1

'(derajat)

Dim total\_kemiringan\_slot1 As Double 'total kemiringan

'slot1 (derajat)

```
Dim posisi_slot1 As Double 'jarak slot 1 dari pusat
                                'koordinat (mm)
Dim posisi_slot1_x As Double 'jarak slot 1 dalam sumbu x
                                'dari pusat koordinat(mm)
Dim posisi_slot1_y As Double 'jarak slot 1 dalam sumbu y
                                'dari pusat koordinat(mm)
Dim sudut_posisi_slot2 As Double 'sudut (derajat) posisi
                                'slot2 (slot bagian luar)
Dim kemiringan_slot2 As Double ' kemiringan slot 2
                                '(derajat)
Dim total_kemiringan_slot2 As Double 'total kemiringan
                                'slot 2 (derajat)
Dim posisi_slot2 As Double 'jarak slot 2 dari pusat
                                'koordinat (mm)
Dim posisi_slot2_x As Double 'jarak slot 2 dalam sumbu x
                                'dari pusat koordinat(mm)
Dim posisi_slot2_y As Double 'jarak slot 2 dalam sumbu y
                                'dari pusat koordinat(mm)
Dim posisi_radiating_element As Double
Dim delta_sudut As Double
Dim busur_slot As Double
Dim sudut_posisi_unit_radiator As Double
Dim jarak_antar_slot_azimuth As Double
Dim posisi_unit_radiator As Double
```

```

For kaunter1=0 To n-1 'looping sebanyak jumlah ring, dari
    'ring ke 0 sampai ke n-1
    p=(kaunter1+z)*po/z 'hitung jumlah unit radiator
    'untuk setiap ring
    delta_sudut=0.01: busur_slot=0
    sudut_posisi_unit_radiator=0 'setting nilai inisial
    jarak_antar_slot_azimuth=2*pi*lamda*z/(po*Sqr(1-
    ((sinD(tau)^2)/er))) 'hitung jarak antar slot dalam
    'arah azimuth
    '(nilai ini sama untuk semua
    'slot di semua ring)

For kaunter=1 To p 'looping sebanyak jumlah unit
    'radiator, dari unit radiator ke
    '1 sampai ke p
    'Hitung posisi untuk unit radiator
    '=====
    While busur_slot < kaunter*
    jarak_antar_slot_azimuth 'lakukan operasi
        'integral untuk menentukan
        'sudut setiap unit radiator
    sudut_posisi_unit_radiator =
    sudut_posisi_unit_radiator+delta_sudut
    posisi_unit_radiator = (kaunter1+z)*lamda
    /(1-(1/Sqr(er)*SinD(tau)*CosD

```



```

(sudut_posisi_unit_radiator-teta)))
busur_slot = busur_slot +
posisi_unit_radiator*delta_sudut*(pi/180)
Wend

sudut_posisi_slot1=sudut_posisi_unit_radiator
kemiringan_slot1 = 45+0.5*((ATnD(cosD(tau)
/TanD(teta)))-
(sudut_posisi_slot1-teta))
'hitung kemiringan sudut
'slot1
total_kemiringan_slot1 = kemiringan_slot1 +
sudut_posisi_slot1 'hitung total
'kemiringan slot1
posisi_slot1 = (z+kaunter1-0.25)*lamda/(1-
(1/Sqr(er)*SinD(tau)
*CosD(sudut_posisi_slot1 teta)))'hitung posisi slot 1
'(mm)
posisi_slot1_x=posisi_slot1*
CosD(sudut_posisi_slot1)'hitung
'posisi slot1 pada sumbu x
posisi_slot1_y=posisi_slot1*
SinD(sudut_posisi_slot1) 'hitung posisi slot1 pada
'sumbu y

```

```
'hitung panjang slot1
'=====
panjang_slot=(inisial_panjang+6.415*10^-
3*posisi_slot1)*12.5/fd 'hitung panjang slot untuk
'posisi unit radiator yang
'bersesuaian
```

```
'gambar slot 1
'=====
WCS.ActivateWCS "local" 'aktifkan koordinat lokal
WCS.MoveWCS "local", posisi_slot1_x,
posisi_slot1_y, "0.0" 'pindahkan koordinat lokal ke
'posisi slot pada sumbu x dan
'sumbu y
WCS.RotateWCS "w", total_kemiringan_slot1 'putar
'koordinat lokal sebanyak total_kemiringan_slot
Component.New "ring"
With Brick 'buat gambar slot1
    .Reset
    .Name "slot1."
    .Component "ring"
    .Material "Vacuum"
    .Xrange -panjang_slot/2, panjang_slot/2
    .Yrange -lebar_slot/2, lebar_slot/2
```

```

.Zrange "0", tebal_element_radiasi
.Create
End With

Solid.Rename
"ring:slot1.", "slot."+CStr(kaunter1)+CStr(".") +CStr(
"1")+CStr(".") +CStr(kaunter) 'ubah nama slot agar
'namanya tidak overlap dengan nama slot selanjutnya
WCS.AlignWCSWithGlobalCoordinates 'kembalikan
'koordinat lokal ke koordinat global

'Hitung untuk slot 2 ('semua keterangan instruksi
sama dengan keterangan pada bagian hitung untuk
slot1
'=====

sudut_posisi_slot2 = sudut_posisi_unit_radiator
kemiringan_slot2=135+0.5*((ATnD(cosD(tau)
/TanD(teta)))-(sudut_posisi_slot2-teta))
total_kemiringan_slot2 = kemiringan_slot2 +
                        sudut_posisi_slot2

posisi_slot2 = (z+kaunter1+0.25)*lamda/(1-
                        (1/Sqr(er)*SinD(tau)*
                        CosD(sudut_posisi_slot2-teta)))
posisi_slot2_x=posisi_slot2*cosD

```

```
(sudut_posisi_slot2)
posisi_slot2_y=posisi_slot2*SinD
(sudut_posisi_slot2)
```

```
'hitung panjang slot2
'=====
panjang_slot=(inisial_panjang+6.415*10^-3*
posisi_slot2)*12.5/fd
```

```
'gambar slot 2
'=====
WCS.ActivateWCS "local"
WCS.MoveWCS "local", posisi_slot2_x,
posisi_slot2_y, "0.0"
WCS.RotateWCS "w", total_kemiringan_slot2
Component.New "ring"
With Brick
    .Reset
    .Name "slot2."
    .Component "ring"
    .Material "Vacuum"
    .Xrange -panjang_slot/2, panjang_slot/2
    .Yrange -lebar_slot/2, lebar_slot/2
    .Zrange "0", tebal_element_radiasi
    .Create
```

End With

Solid.Rename

"ring:slot2.", "slot."+CStr(kaunter1)+CStr(".") +CStr("2")+CStr(".") +CStr(kaunter)'ubah nama slot agar  
'namanya tidak overlap dengan nama slot selanjutnya

WCS.AlignWCSToGlobalCoordinates 'kembalikan  
'koordinat lokal ke koordinat global

Next

Next

'Menghitung dan menggambar slot tambahan

'=====

Dim posisi\_ujung\_slot2 As Double

Dim kaun1 As Double 'penghitung kaun naik 1 tingkat

Dim jari\_terdekat As Double 'jari-jari slot terdekat

Dim p\_c1 As Double 'jumlah element pada ring terdalam

Dim p1 As Double 'jumlah unit radiator untuk setiap ring

Dim sudut\_posisi\_slot\_terdekat As Double 'sudut posisi slot  
'yang memiliki jari-jari 'terbesar

Dim jari\_slot\_terdekat As Double 'jari-jari slot

Dim jari\_radiating\_element1 As Double 'jari-jari unit

```
'radiator pada ring terluar
Dim posisi_radiating_element1 As Double
Dim delta_sudut1 As Double
Dim busur_slot1 As Double
Dim jarak_antar_slot_azimuth1 As Double
Dim sudut_posisi_unit_radiator1 As Double
Dim posisi_unit_radiator1 As Double
Dim n1 As Double 'jumlah ring yang tidak penuh
```

```
'Menghitung jari-jari ring yang terdekat
'=====
p_c1=(0+z)*po/z 'Hitung jumlah unit radiator pada ring
'yang terdalam (n=0)
delta_sudut1=0.01: busur_slot1=0:
sudut_posisi_unit_radiator1=0 'setting nilai inisial
jarak_antar_slot_azimuth1=2*pi*lamda*z/(po*Sqr(1-
((sinD(tau)^2)/er)))'hitung jarak antar slot dalam arah
'azimuth
jari_terdekat=jari_kaviti 'setting nilai inisial untuk
'jari_terdekat
```

```
For kaun1=1 To p_c1 'looping dari 1 sampai sebanyak
'jumlah unit radiator
```

```
While busur_slot1 < kaun1*
```

```

jarak_antar_slot_azimuth1
    sudut_posisi_unit_radiator1=
    sudut_posisi_unit_radiator1+delta_sudut1
    posisi_unit_radiator1 = (0+z)*lamda/(1-
    (1/Sqr(er)*SinD(tau)*
    CosD(sudut_posisi_unit_radiator1-teta)))
    busur_slot1=busur_slot1+
    posisi_unit_radiator1*
    delta_sudut1*(pi/180)

```

Wend

```

    sudut_posisi_slot_terdekat =
    sudut_posisi_unit_radiator1
    jari_slot_terdekat = (z+0+0.25)*lamda/(1-
    (1/Sqr(er)*SinD(tau)*
    CosD(sudut_posisi_slot_terdekat-teta))) 'Hitung jari-
    'jari slot element terluar dan ring terdalam (slot2 dan
    'ring ke n=0)

```

```

While jari_terdekat > jari_slot_terdekat 'temukan
    'jari-jari slot terdekat
    jari_terdekat = jari_slot_terdekat

```

Wend

```

jari_terdekat = jari_terdekat

```

Next

```
n1=jari_kaviti\ (jari_terdekat/z) 'Hitung jumlah ring
'keseluruhan
```

```
'Menghitung posisi dan sudut slot 2
```

```
'=====
```

```
For kaunter1=n To n1-z+3
```

```
    p1=(kaunter1+z)*po/z 'hitung jumlah unit radiator
                                'untuk setiap ring
```

```
    delta_sudut=0.01: busur_slot=0:
```

```
    sudut_posisi_unit_radiator=0 'setting nilai inisial
```

```
    jarak_antar_slot_azimuth=2*pi*lamda*z/(po*Sqr(1-
'((sinD(tau)^2)/er)))'hitung jarak antar unit radiator
```

```
    '(nilai ini harus sama untuk setiap ring dan setiap unit
'radiator)
```

```
For kaunter=1 To p1
```

```
    While busur_slot <
```

```
        kaunter*jarak_antar_slot_azimuth 'lakukan
        'integral untuk dapat menentukan
```

```
        'sudut posisi unit radiator
```

```
        sudut_posisi_unit_radiator=
```

```
        sudut_posisi_unit_radiator+delta_sudut
```

```
        posisi_unit_radiator =
```

```
        (kaunter1+z)*lamda/(1-(1/Sqr(er))
```



```

*SinD(tau)*CosD
(sudut_posisi_unit_radiator-teta)))
busur_slot=busur_slot+
posisi_unit_radiator*delta_sudut*(pi/180)
Wend

```

```

sudut_posisi_slot2=sudut_posisi_unit_radiator
kemiringan_slot2 =
135+0.5*((ATnD(cosD(tau)/TanD(teta)))-
(sudut_posisi_slot2-teta))'hitung kemiringan sudut
'slot1

```

```

total_kemiringan_slot2 = kemiringan_slot2 +
sudut_posisi_slot2 'hitung total kemiringan slot1
posisi_slot2 = (z+kaunter1+0.25)*lamda/(1-
(1/Sqr(er)*SinD(tau)*CosD(sudut_posisi_slot2-
teta)))
posisi_slot2_x= posisi_slot2*
CosD(sudut_posisi_slot2)
posisi_slot2_y= posisi_slot2*
SinD(sudut_posisi_slot2)

```

```

'hitung posisi ujung slot2

```

```

'=====

```

```

panjang_slot=(inisial_panjang+6.415*10^-
3*posisi_slot2)*12.5/fd

```

posisi\_ujung\_slot2 = posisi\_slot2'+panjang\_slot/2  
 ' ini dirubah agar bisa menghasilkan penggambaran

'Hitung posisi untuk slot 1

'=====

sudut\_posisi\_slot1 = sudut\_posisi\_unit\_radiator

kemiringan\_slot1 =

$45 + 0.5 * ((A \tan D(\cos D(\tau) / \tan D(\text{teta}))) -$

$(\text{sudut\_posisi\_slot1} - \text{teta}))$

total\_kemiringan\_slot1 = kemiringan\_slot1 +

sudut\_posisi\_slot1

posisi\_slot1 =  $(z + \text{kaunter1} - 0.25) * \lambda / (1 -$

$(1 / \text{Sqr}(\epsilon) * \sin D(\tau) * \cos D(\text{sudut\_posisi\_slot1} - \text{teta})))$

posisi\_slot1\_x= posisi\_slot1\*

$\cos D(\text{sudut\_posisi\_slot1})$

posisi\_slot1\_y= posisi\_slot1\*

$\sin D(\text{sudut\_posisi\_slot1})$

'hitung panjang slot1

'=====

panjang\_slot=(inisial\_panjang+ $6.415 * 10^{-$

$3 * \text{posisi\_slot1}) * 12.5 / f_d$  'hitung panjang slot untuk

'posisi unit radiator yang bersesuaian

```
If posisi_ujung_slot2 < jari_kaviti Then
```

```
'gambar slot 2
```

```
'=====
```

```
WCS.ActivateWCS "local"
```

```
WCS.MoveWCS "local", posisi_slot2_x,
```

```
posisi_slot2_y, "0.0"
```

```
WCS.RotateWCS "w",
```

```
total_kemiringan_slot2
```

```
Component.New "ring"
```

```
With Brick
```

```
.Reset
```

```
.Name "slot2."
```

```
.Component "ring"
```

```
.Material "Vacuum"
```

```
.Xrange -panjang_slot/2,
```

```
panjang_slot/2
```

```
.Yrange -lebar_slot/2, lebar_slot/2
```

```
.Zrange "0", tebal_element_radiasi
```

```
.Create
```

```
End With
```

Solid.Rename

```
"ring:slot2.", "slot."+CStr(kaunter1)+CStr(".") +CStr(
"2")+CStr(".") +CStr(kaunter)'ubah
'nama slot agar namanya tidak overlap
'dengan nama slot selanjutnya
```

WCS.AlignWCSWithGlobalCoordinates

'gambar slot 1

'=====

WCS.ActivateWCS "local" 'aktifkan k

'koordinat lokal

WCS.MoveWCS "local", posisi\_slot1\_x,

'posisi\_slot1\_y, "0.0" 'pindahkan koordinat

'lokal ke posisi slot pada sumbu x dan sumbu

'y

WCS.RotateWCS "w",

total\_kemiringan\_slot1 'putar koordinat lokal

'sebanyak total\_kemiringan\_slot

Component.New "ring"

With Brick 'buat gambar slot1

.Reset

.Name "slot1."

.Component "ring"

```
.Material "Vacuum"
.Xrange -panjang_slot/2,
        panjang_slot/2
.Yrange -lebar_slot/2, lebar_slot/2
.Zrange "0", tebal_element_radiasi
.Create
```

End With

```
Solid.Rename"ring:slot1.", "slot."+
CStr(kaunter1)+CStr(".") +
CStr("1")+CStr(".") +CStr(kaunter)'ubah
'nama slot agar namanya tidak overlap
'dengan nama slot selanjutnya
WCS.AlignWCSWithGlobalCoordinates
'kembalikan koordinat lokal ke koordinat
'global
```

End If

Next

Next

```
'Menggambar feeder
'=====
```

Dim radius\_cincin As Double  
 Dim tinggi\_cincin As Double  
 Dim panjang\_core As Double  
 Dim radius\_core As Double  
 Dim radius\_dialektrik As Double  
 Dim panjang\_dialektrik As Double  
 Dim tinggi\_air\_gap\_atas As Double  
 Dim tinggi\_air\_gap\_bawah As Double  
 Dim tebal\_pelekat As Double  
 Dim radius\_loyang\_feeder As Double  
 Dim radius\_pelekat As Double

radius\_cincin = 1.4: tinggi\_cincin = 3: radius\_core=0.635:  
 radius\_dialektrik=2.025  
 panjang\_dialektrik=8:tinggi\_air\_gap\_atas=1:  
 tinggi\_air\_gap\_bawah=4.0  
 tebal\_pelekat=1.7:radius\_pelekat=5:  
 radius\_loyang\_feeder=10

'gambar inti feeder (core)

With Cylinder

.Reset  
 .Name "core"  
 .Component "feeder"  
 .Material "Copper"

```

.OuterRadius radius_core
.InnerRadius "0"
.Axis "z"
.Zrange-tinggi_air_gap_atas-tinggi_cincin-
    tinggi_air_gap_bawah-panjang_dialektrik-
    tebal_pelekat, -tinggi_air_gap_atas
.Xcenter "0"
.Ycenter "0"
.Segments "0"
.Create
End With

```

'Sisipkan inti feeder (core) ke lubang

With Solid

```

.Version 9
.Insert "antenna:lubang_feeder", "feeder:core"
End With

```

'gambar cincin

With Cylinder

```

.Reset
.Name "disk"
.Component "feeder"
.Material "Copper"
.OuterRadius radius_cincin

```

```

.InnerRadius "0"
.Axis "z"
.Zrange -tinggi_air_gap_atas-tinggi_cincin,-
        tinggi_air_gap_atas
.Xcenter "0"
.Ycenter "0"
.Segments "0"
.Create
End With

```

'Sisipkan cincin(disk) ke lubang

With Solid

```

.Version 9
.Insert "antenna:lubang_feeder", "feeder:disk"

```

End With

With Solid' gabungkan material cincin(disk)dan core

```

.Version 9
.Add "feeder:core", "feeder:disk"

```

End With

With Material ' defenisikan material untuk dialektrik yaitu

'teflon

```

.Reset
.Name "Teflon (PTFE) (lossy)"

```



.FrqType "all"  
.Type "Normal"  
.Epsilon "2.08"  
.Mue "1.0"  
.Kappa "0.0"  
.TanD "0.0004"  
.TanDFreq "0.0"  
.TanDGiven "True"  
.TanDModel "ConstTanD"  
.KappaM "0.0"  
.TanDM "0.0"  
.TanDMFreq "0.0"  
.TanDMGiven "False"  
.TanDMModel "ConstKappa"  
.DispModelEps "None"  
.DispModelMue "None"  
.DispersiveFittingSchemeEps "General 1st"  
.DispersiveFittingSchemeMue "General 1st"  
.UseGeneralDispersionEps "False"  
.UseGeneralDispersionMue "False"  
.Rho "0.0"  
.ThermalType "Normal"  
.ThermalConductivity "0.2"  
.SetActiveMaterial "all"  
.Colour "0.94", "0.82", "0.76"

```

        .Wireframe "False"
        .Transparency "0"
        .Create
End With

'gambar dialektrik
With Cylinder
    .Reset
    .Name "dialetrick"
    .Component "feeder"
    .Material "Teflon (PTFE) (lossy)"
    .OuterRadius radius_dialektrik
    .InnerRadius radius_core
    .Axis "z"
    .Zrange -tinggi_air_gap_atas-tinggi_cincin-
        tinggi_air_gap_bawah-
        panjang_dialektrik-tebal_pelekat,-
        tinggi_air_gap_atas-tinggi_cincin-
        tinggi_air_gap_bawah-tebal_element_radiasi
    .Xcenter "0"
    .Ycenter "0"
    .Segments "0"
    .Create
End With

```

'gambar loyang feeder

With Cylinder

.Reset

.Name "loyang"

.Component "feeder"

.Material "Copper"

.OuterRadius radius\_loyang\_feeder

.InnerRadius radius\_dialektrik

.Axis "z"

.Zrange -tinggi\_air\_gap\_atas-tinggi\_cincin-  
tinggi\_air\_gap\_bawah-  
panjang\_dialektrik,-tinggi\_air\_gap\_atas-  
tinggi\_cincin-tinggi\_air\_gap\_bawah-  
tebal\_element\_radiasi

.Xcenter "0"

.Ycenter "0"

.Segments "0"

.Create

End With

'gambar pelekat

With Cylinder

.Reset

.Name "pelekat"

.Component "feeder"

```

.Material "Copper"
.OuterRadius radius_pelekat
.InnerRadius radius_dialektrik
.Axis "z"
.Zrange -tinggi_air_gap_atas-tinggi_cincin-
        tinggi_air_gap_bawah-
        panjang_dialektrik-tebal_pelekat,-
        tinggi_air_gap_atas-tinggi_cincin-
        tinggi_air_gap_bawah-panjang_dialektrik
.Xcenter "0"
.Ycenter "0"
.Segments "0"
.Create
End With

```

```

'=====

```

```

Buat port untuk feeder

```

```

'=====

```

```

'Pick face feeder untuk mempersiapkan port

```

```

Pick.PickFaceFromId "feeder:dialektrik", "1"

```

```

'Letak kan port pada feeder

```

```

With Port

```

```

    .Reset

```

```

    .PortNumber "1"

```

```

.NumberOfModes "1"
.AdjustPolarization False
.PolarizationAngle "0.0"
.ReferencePlaneDistance "0"
.TextSize "50"
.Coordinates "Picks"
.Orientation "positive"
.PortOnBound "True"
.ClipPickedPortToBound "False"
.Xrange "-2.025", "2.025"
.Yrange "-2.025", "2.025"
.Zrange "-17.7", "-17.7"
.XrangeAdd "0.0", "0.0"
.YrangeAdd "0.0", "0.0"
.ZrangeAdd "0.0", "0.0"
.SingleEnded "False"
.Create
End With

```

```

'set frekuensi range
Solver.FrequencyRange "4.8", "6.8"

```

```

'set boundary condition dan simetri untuk xz=magnetik=0
With Boundary
    .Xmin "expanded open"

```

.Xmax "expanded open"  
.Ymin "expanded open"  
.Ymax "expanded open"  
.Zmin "expanded open"  
.Zmax "expanded open"  
.Xsymmetry "none"  
.Ysymmetry "magnetic"  
.Zsymmetry "none"  
.XminThermal "isothermal"  
.XmaxThermal "isothermal"  
.YminThermal "isothermal"  
.YmaxThermal "isothermal"  
.ZminThermal "isothermal"  
.ZmaxThermal "isothermal"  
.XsymmetryThermal "none"  
.YsymmetryThermal "isothermal"  
.ZsymmetryThermal "none"  
.ApplyInAllDirections "False"  
.XminTemperature ""  
.XminTemperatureType "None"  
.XmaxTemperature ""  
.XmaxTemperatureType "None"  
.YminTemperature ""  
.YminTemperatureType "None"  
.YmaxTemperature ""

```
.YmaxTemperatureType "None"  
.ZminTemperature ""  
.ZminTemperatureType "None"  
.ZmaxTemperature ""  
.ZmaxTemperatureType "None"  
End With
```

'Set monitor untuk farfield

```
With Monitor  
.Reset  
.Name "farfield (f=5.8)"  
.Domain "Frequency"  
.FieldType "Farfield"  
.Frequency "5.8"  
.Create  
End With
```

```
End Sub
```

## A.2. The Program Code to Draw RLSA with beamsquint technique

'=====

### 'Preface

'=====

"This code program in used to draw RLSA antennas  
'automatically in CST-MWS-2010. Some of the formulas  
'used in this program were taken from PHd Thesis Report  
'written by Paul. W. Davis from University of Queensland,  
'Australia.

"This program was written by Teddy Purnamirza, from  
'Department of Electrical Engineering, Faculty Science and  
'Technology, Universitas Islam Sultan Syarif Kasim Riau,  
'Indonesia.

"This program is a free program and can be used or can be  
'more developed by anyone provided acknowledging the  
'programmer of the Program (Teddy Purnamirza). The  
'programmer does not responsible to any misuse of this  
'program and any damage caused by the utilization of this  
'program.

Option Explicit

Sub Main



```
'=====
'Setting template antenna planar sebagai default template
'=====
'Template for Antenna in Free Space
'=====
```

```
'(CSTxMWSxONLY)
```

```
'draw the bounding box
```

```
Plot.DrawBox True
```

```
'set units to mm, ghz
```

```
With Units
```

```
    .Geometry "mm"
```

```
    .Frequency "ghz"
```

```
    .Time "ns"
```

```
End With
```

```
'set background material to vacuum
```

```
With Background
```

```
    .Type "Normal"
```

```
    .Epsilon "1.0"
```

```
.Mue "1.0"  
.XminSpace "0.0"  
.XmaxSpace "0.0"  
.YminSpace "0.0"  
.YmaxSpace "0.0"  
.ZminSpace "0.0"  
.ZmaxSpace "0.0"  
End With
```

'set boundary conditions to open

```
With Boundary  
.Xmin "expanded open"  
.Xmax "expanded open"  
.Ymin "expanded open"  
.Ymax "expanded open"  
.Zmin "expanded open"  
.Zmax "expanded open"  
.Xsymmetry "none"  
.Ysymmetry "none"  
.Zsymmetry "none"  
End With
```

'optimize mesh settings for planar structures

With Mesh

```
.MergeThinPECLayerFixpoints "True"  
.RatioLimit "20"  
.AutomeshRefineAtPecLines "True", "6"  
.FPBAAvoidNonRegUnite "True"  
.ConsiderSpaceForLowerMeshLimit "False"  
.MinimumStepNumber "5"
```

End With

```
'change mesh adaption scheme to energy  
'(planar structures tend to store high energy  
'locally at edges rather than globally in volume)
```

```
MeshAdaption3D.SetAdaptionStrategy "Energy"
```

```
'switch on FD-TET setting for accurate farfields
```

```
FDSolver.ExtrudeOpenBC "True"
```

```
'=====
```

```
'Deklarasikan seluruh variabel umum
```

```
'=====
```

```
Dim er As Double 'permitivitas relatif cavity
```

Dim ur As Double 'permeabilitas relatif cavity

Dim fo As Double 'frekuensi operasi (GHz)

Dim fd As Double 'frekuensi disain (GHz)

Dim z As Double 'Inner ring factor (faktor ring terdalam)

Dim n As Double 'jumlah ring (ring number)

Dim po As Double 'jumlah slot dalam ring pertama (n=0)

Dim p As Double 'Jumlah slot dalam suatu ring

Dim h As Double 'tinggi cavity

Dim velocity As Double 'kecepatan gelombang dalam cavity

Dim d As Double 'lebar slot (mm)

Dim lamda As Double 'panjang gelombang dalam cavity  
'(mm)

Dim panjang\_slot As Double 'panjang slot

Dim lebar\_slot As Double 'lebar slot

Dim tebal\_element\_radiasi As Double 'tebal permukaan  
'element radiasi

Dim jari\_kaviti As Double 'jari-jari kaviti atau jari-jari antenna

Dim jari\_lubang\_kaviti As Double 'jari-jari lubang untuk  
'tempat feeder

'=====

'masukkan nilai parameter inputan

'=====

fd=12: er=2.33: ur=1: po=16: z=2: n=1: jari\_kaviti=40

lebar\_slot=4: h=6: tebal\_element\_radiasi=0.1:

jari\_lubang\_kaviti=1.4

'=====

'Hitung paramater-parameter yang berhubungan dengan  
parameter inputan

'=====

velocity=(2.9979)/Sqr(er\*ur) 'Hitung kecepatan gelombang  
'dalam cavity

lamda=velocity\*10^2/fd 'Hitung panjang gelombang dalam  
'cavity (mm)

'=====

'Gambar cavity

'=====

WCS.ActivateWCS "local"

With Material 'setting material cavity

.Reset

.Name "kaviti"

.FrqType "all"

.Type "Normal"

.Epsilon er

.Mue "1"

.Kappa "0"

.TanD "0.0"

.TanDFreq "0.0"  
.TanDGiven "False"  
.TanDModel "ConstTanD"  
.KappaM "0"  
.TanDM "0.0"  
.TanDMFreq "0.0"  
.TanDMGiven "False"  
.TanDMModel "ConstTanD"  
.DispModelEps "None"  
.DispModelMue "None"  
.DispersiveFittingSchemeEps "General 1st"  
.DispersiveFittingSchemeMue "General 1st"  
.UseGeneralDispersionEps "False"  
.UseGeneralDispersionMue "False"  
.Rho "0"  
.ThermalType "Normal"  
.ThermalConductivity "0"  
.HeatCapacity "0"  
.MetabolicRate "0"  
.BloodFlow "0"  
.Colour "0", "1", "1"  
.Wireframe "False"  
.Reflection "False"  
.Allowoutline "True"  
.Transparentoutline "False"

End With

End With

'=====

Pick.PickFaceFromId "antenna:kaviti", "3"pick permukaan  
'cavity bagian depan

With Material 'setting material baru untuk komponen  
'radiating

.Reset  
.Name "Copper"  
.FrqType "static"  
.Type "Normal"  
.Epsilon "1"  
.Mue "1.0"  
.Kappa "5.8e+007"  
.TanD "0.0"  
.TanDFreq "0.0"  
.TanDGiven "False"  
.TanDModel "ConstTanD"  
.KappaM "0"  
.TanDM "0.0"  
.TanDMFreq "0.0"  
.TanDMGiven "False"  
.TanDMModel "ConstTanD"  
.DispModelEps "None"  
.DispModelMue "None"  
.DispersiveFittingSchemeEps "General 1st"



```

.DispersiveFittingSchemeMue "General 1st"
.UseGeneralDispersionEps "False"
.UseGeneralDispersionMue "False"
.FrqType "all"
.Type "Lossy metal"
.Mue "1.0"
.Kappa "5.8e+007"
.Rho "0.0"
.ThermalType "Normal"
.ThermalConductivity "401.0"
.Colour "1", "1", "0"
.Wireframe "False"
.Transparency "0"
.Create
End With

With Extrude 'lakukan operasi extrude untuk membuat
    'komponen radiating
    .Reset
    .Name "radiating"
    .Component "antenna"
    .Material "Copper"
    .Mode "Picks"
    .Height tebal_element_radiasi' tebal komponen radiating
    .Twist "0.0"

```

```

.Taper "0.0"
.UsePicksForHeight "False"
.DeleteBaseFaceSolid "False"
.ClearPickedFace "True"
.Create
End With

'=====
'Menggambar ground
'=====
Pick.PickFaceFromId "antenna:kaviti", "1" 'pick permukaan
                                'belakang cavity

With Extrude 'lakukan operasi extrude untuk membuat
                                'komponen ground
.Reset
.Name "ground"
.Component "antenna"
.Material "Copper"
.Mode "Picks"
.Height tebal_element_radiasi 'tebal komponen ground
.Twist "0.0"
.Taper "0.0"
.UsePicksForHeight "False"
.DeleteBaseFaceSolid "False"

```

```

        .ClearPickedFace "True"
    .Create
End With

'=====

'Menggambar lubang pusat antenna
'=====

With Cylinder
    .Reset
    .Name "lubang_feeder"
    .Component "antenna"
    .Material "Vacuum"
    .OuterRadius jari_lubang_kaviti
    .InnerRadius "0"
    .Axis "z"
    .Zrange -h-tebal_element_radiasi, "0"
    .Xcenter "0"
    .Ycenter "0"
    .Segments "0"
    .Create
End With

'Sisipkan lubang feeder ke kaviti
With Solid
    .Version 9
    .Insert "antenna:kaviti", "antenna:lubang_feeder"

```

End With

With Solid

.Version 9

.Insert "antenna:ground", "antenna:lubang\_feeder"

End With

'=====

'Menghitung posisi slot dan Menggambar Slot

'=====

Dim kaunter As Double 'kaunter untuk increment keatas 1  
'langkah

Dim kaunter1 As Double 'kaunter untuk increment keatas 1  
'langkah

Dim sudut\_posisi\_slot1 As Double 'sudut (derajat) posisi  
'slot1 (slot bagian dalam)

Dim kemiringan\_slot1 As Double ' kemiringan slot 1  
'(derajat)

Dim total\_kemiringan\_slot1 As Double 'total kemiringan  
'slot1 (derajat)

Dim posisi\_slot1 As Double 'jarak slot 1 dari pusat  
'koordinat (mm)

Dim posisi\_slot1\_x As Double 'jarak slot 1 dalam sumbu x  
'dari pusat koordinat(mm)

Dim posisi\_slot1\_y As Double 'jarak slot 1 dalam sumbu y

'dari pusat koordinat(mm)

Dim sudut\_posisi\_slot2 As Double 'sudut (derajat) posisi

'slot2 (slot bagian luar)

Dim kemiringan\_slot2 As Double 'kemiringan slot 2

'(derajat)

Dim total\_kemiringan\_slot2 As Double 'total kemiringan

'slot 2 (derajat)

Dim posisi\_slot2 As Double 'jarak slot 2 dari pusat

'koordinat (mm)

Dim posisi\_slot2\_x As Double 'jarak slot 2 dalam sumbu x

'dari pusat koordinat(mm)

Dim posisi\_slot2\_y As Double 'jarak slot 2 dalam sumbu y

'dari pusat koordinat(mm)

$n = (\text{jari\_kaviti} \backslash \text{lamda}) - (z - 1)$

For kaunter1=0 To n-1 'looping sebanyak jumlah ring, dari

'ring ke 0 sampai ke n-1

$p = p_o * (1 + \text{kaunter1} / z)$  'hitung jumlah unit radiator

'untuk setiap ring

For kaunter=1 To p 'looping sebanyak jumlah unit

'radiator, dari unit radiator ke 1 sampai ke p

'Hitung posisi untuk unit radiator

```

'-----
sudut_posisi_slot1 = kaunter*360/p
'Hitung sudut posisi untuk slot1
kemiringan_slot1 = 90-
sudut_posisi_slot1/2'hitung kemiringan
'sudut slot1
total_kemiringan_slot1 = kemiringan_slot1
+ sudut_posisi_slot1 'hitung total kemiringan
'slot1
posisi_slot1 = (z+kaunter1-0.25)*lamda
'hitung posisi slot 1 (mm)
posisi_slot1_x= posisi_slot1*
CosD(sudut_posisi_slot1) 'hitung posisi slot1
'pada sumbu x
posisi_slot1_y= posisi_slot1*
SinD(sudut_posisi_slot1) 'hitung posisi slot1
'pada sumbu y

'hitung panjang slot1
'-----
panjang_slot=(5.8678+6.415*10^-3*
posisi_slot1)*12.5/fd 'hitung panjang slot
'untuk posisi unit radiator yang bersesuaian

'gambar slot 1

```

'-----

WCS.ActivateWCS "local" 'aktifkan

'koordinat lokal

WCS.MoveWCS "local", posisi\_slot1\_x,

posisi\_slot1\_y, "0.0" 'pindahkan koordinat

'lokal ke posisi slot pada sumbu x dan sumbu

'y

WCS.RotateWCS "w",

total\_kemiringan\_slot1

'putar koordinal lokal sebanyak

'total\_kemiringan\_slot

Component.New "ring"

With Brick 'buat gambar slot1

.Reset

.Name "slot1."

.Component "ring"

.Material "Vacuum"

.Xrange -panjang\_slot/2, panjang\_slot/2

.Yrange -lebar\_slot/2, lebar\_slot/2

.Zrange "0", tebal\_element\_radiasi

.Create

End With

With Solid 'sisipkan slot pada elemen

```
'radiating
.Version 9
.Insert "antenna:radiating", "ring:slot1."
End With
```

```
Solid.Rename
"ring:slot1.", "slot1."+CStr(kaunter)'ubah
'nama slot agar namanya tidak overlap
'dengan nama slot selanjutnya
```

```
WCS.AlignWCSWithGlobalCoordinates
'kembalikan koordinat lokal ke koordinat
'global
```

```
'Hitung untuk slot 2 ('semua keterangan
'instruksi sama dengan keterangan pada
'bagian hitung untuk slot1
'-----
sudut_posisi_slot2 = kaunter*360/p 'Hitung
'sudut posisi untuk slot1
kemiringan_slot2 = 180-sudut_posisi_slot2
/2'hitung kemiringan sudut slot1
total_kemiringan_slot2 = kemiringan_slot2+
sudut_posisi_slot2 'hitung total kemiringan
'slot1
```



posisi\_slot2 = (z+kaunter1+0.25)\*lamda

'hitung posisi slot 1 (mm)

posisi\_slot2\_x= posisi\_slot2

\*CosD(sudut\_posisi\_slot2) 'hitung posisi

'slot1 pada sumbu x

posisi\_slot2\_y= posisi\_slot2

\*SinD(sudut\_posisi\_slot2) 'hitung posisi

'slot1 pada sumbu y

'hitung panjang slot 2

'-----

panjang\_slot=(5.8678+6.415\*10^-

3\*posisi\_slot2)\*12.5/fd 'hitung panjang slot

'untuk posisi unit radiator yang bersesuaian

'gambar slot 2

'-----

WCS.ActivateWCS "local"

WCS.MoveWCS "local", posisi\_slot2\_x,

posisi\_slot2\_y, "0.0"

WCS.RotateWCS "w",

total\_kemiringan\_slot2

```

Component.New "ring"
With Brick
.Reset
.Name "slot2."
.Component "ring"
.Material "Vacuum"
.Xrange -panjang_slot/2, panjang_slot/2
.Yrange -lebar_slot/2, lebar_slot/2
.Zrange "0", tebal_element_radiasi
.Create
End With

```

```

With Solid 'sisipkan slot pada elemen
'radiating
.Version 9
.Insert "antenna:radiating", "ring:slot2."
End With

```

```

Solid.Rename"ring:slot2.", "slot2." +
CStr(kaunter)'ubah nama slot agar namanya
'tidak overlap dengan nama slot selanjutnya

```

```

WCS.AlignWCSWithGlobalCoordinates
'kembalikan koordinat lokal ke koordinat
'global

```

Next

Component.Rename "ring", "ring"+ CStr(kaunter1)  
'ubah nama komponen agar nama komponen tidak  
'overlap dengan nama komponen selanjutnya

Next

'=====

'Menggambar feeder

'=====

Dim radius\_cincin As Double

Dim tinggi\_cincin As Double

Dim panjang\_core As Double

Dim radius\_core As Double

Dim radius\_dialektrik As Double

Dim panjang\_dialektrik As Double

Dim tinggi\_air\_gap\_atas As Double

Dim tinggi\_air\_gap\_bawah As Double

Dim tebal\_pelekat As Double

Dim radius\_loyang\_feeder As Double

Dim radius\_pelekat As Double

radius\_cincin = 1.4: tinggi\_cincin =3.6: radius\_core=0.635:

radius\_dialektrik=2.025

panjang\_dialektrik=6:tinggi\_air\_gap\_atas=0.8:  
tinggi\_air\_gap\_bawah=1.6  
tebal\_pelekat=1.7:radius\_pelekat=5:  
radius\_loyang\_feeder=30

'gambar inti feeder (core)

With Cylinder

```
.Reset  
.Name "core"  
.Component "feeder"  
.Material "Copper"  
.OuterRadius radius_core  
.InnerRadius "0"  
.Axis "z"  
.Zrange -tinggi_air_gap_atas-tinggi_cincin-  
tinggi_air_gap_bawah-panjang_dialektrik-  
tebal_pelekat, -tinggi_air_gap_atas  
.Xcenter "0"  
.Ycenter "0"  
.Segments "0"  
.Create
```

End With

'Sisipkan inti feeder (core) ke lubang

With Solid

```

.Version 9
.Insert "antenna:lubang_feeder", "feeder:core"
End With

```

```

'gambar cincin
With Cylinder
.Reset
.Name "disk"
.Component "feeder"
.Material "Copper"
.OuterRadius radius_cincin
.InnerRadius "0"
.Axis "z"
.Zrange -tinggi_air_gap_atas-tinggi_cincin,-
        tinggi_air_gap_atas
.Xcenter "0"
.Ycenter "0"
.Segments "0"
.Create
End With

```

```

'Sisipkan cincin(disk) ke lubang
With Solid

```

```

.Version 9
.Insert "antenna:lubang_feeder", "feeder:disk"

```

End With

With Solid' gabungkan material cincin(disk)dan core

.Version 9

.Add "feeder:core", "feeder:disk"

End With

With Material ' defenisikan material untuk diaklektrik yaitu

'teflon

.Reset

.Name "Teflon (PTFE) (lossy)"

.FrqType "all"

.Type "Normal"

.Epsilon "2.08"

.Mue "1.0"

.Kappa "0.0"

.TanD "0.0004"

.TanDFreq "0.0"

.TanDGiven "True"

.TanDModel "ConstTanD"

.KappaM "0.0"

.TanDM "0.0"

.TanDMFreq "0.0"

.TanDMGiven "False"

.TanDMModel "ConstKappa"

```

.DispModelEps "None"
.DispModelMue "None"
.DispersiveFittingSchemeEps "General 1st"
.DispersiveFittingSchemeMue "General 1st"
.UseGeneralDispersionEps "False"
.UseGeneralDispersionMue "False"
.Rho "0.0"
.ThermalType "Normal"
.ThermalConductivity "0.2"
.SetActiveMaterial "all"
.Colour "0.94", "0.82", "0.76"
.Wireframe "False"
.Transparency "0"
.Create

```

End With

'gambar dialektrik

With Cylinder

```

.Reset
.Name "dialetrict"
.Component "feeder"
.Material "Teflon (PTFE) (lossy)"
.OuterRadius radius_dialektrik
.InnerRadius radius_core
.Axis "z"

```

```

.Zrange -tinggi_air_gap_atas-tinggi_cincin-
tinggi_air_gap_bawah-panjang_dialektrik-
tebal_pelekat,-tinggi_air_gap_atas-tinggi_cincin-
tinggi_air_gap_bawah-tebal_element_radiasi
.Xcenter "0"
.Ycenter "0"
.Segments "0"
.Create
End With

```

'gambar loyang feeder

With Cylinder

```

.Reset
.Name "loyang"
.Component "feeder"
.Material "Copper"
.OuterRadius radius_loyang_feeder
.InnerRadius radius_dialektrik
.Axis "z"
.Zrange -tinggi_air_gap_atas-tinggi_cincin-
tinggi_air_gap_bawah-panjang_dialektrik,-
tinggi_air_gap_atas-tinggi_cincin-
tinggi_air_gap_bawah-tebal_element_radiasi
.Xcenter "0"
.Ycenter "0"

```



.Segments "0"

.Create

End With

'gambar pelekat

With Cylinder

.Reset

.Name "pelekat"

.Component "feeder"

.Material "Copper"

.OuterRadius radius\_pelekat

.InnerRadius radius\_dialektrik

.Axis "z"

.Zrange -tinggi\_air\_gap\_atas-tinggi\_cincin-

tinggi\_air\_gap\_bawah-panjang\_dialektrik-

tebal\_pelekat,-tinggi\_air\_gap\_atas-tinggi\_cincin-

tinggi\_air\_gap\_bawah-panjang\_dialektrik

.Xcenter "0"

.Ycenter "0"

.Segments "0"

.Create

End With

End Sub

### A.3. The VBA Program Code to cut the VBA-RLSA Antenna

```
'=====
```

#### 'Preface

```
'=====
```

'This code program in used to cut RLSA antennas into  
'sectors. automatically in CST-MWS-2010.

'Change the value of variable "sudut\_putar" (in degrees) to  
'determine the size of the sector that want to be obtained.

'This program was written by Teddy Purnamirza, from  
'Department of Electrical Engineering, Faculty Science and  
'Technology, Universitas Islam Sultan Syarif Kasim Riau,  
'Indonesia.

'This program is a free program and can be used or can be  
'more developed by anyone provided acknowledging the  
'programmer of the Program (Teddy Purnamirza). The  
'programmer does not responsible to any misuse of this  
'program and any damage caused by the utilization of this  
'program.

Sub Main ()

```
'=====
```

'Declare the variables

'=====

Dim sudut\_putar As Double 'Besar sudut yang

'digunakan untuk memutar penghapus antenna

'dalam arah berlawanan jarum jam

Dim sudut\_putar2 As Double 'Besar sudut yang

'digunakan untuk memutar penghapus antenna

'dalam arah berlawanan jarum jam

sudut\_putar=45

sudut\_putar2=-sudut\_putar

'=====

'Cut the antenna

'=====

'Create the eraser block

With Brick

.Reset

.Name "penghapus"

.Component "antenna"

.Material "Vacuum"

.Xrange "0", jari\_kaviti+5

.Yrange -jari\_kaviti, jari\_kaviti

.Zrange "-17.8", "0.1"

.Create  
End With

'Delete the antenna cavity  
With Solid

.Version 9  
.Insert "antenna:kaviti", "antenna:penghapus"  
.Version 1

End With

'delete the antenna radiating element  
With Solid

.Version 9  
.Insert "antenna:radiating", "antenna:penghapus"  
.Version 1

End With

'delete the ground antenna  
With Solid

.Version 9  
.Insert "antenna:ground", "antenna:penghapus"  
.Version 1

End With

'delete the feeder hole

With Solid

.Version 9

.Insert "antenna:lubang\_feeder",

"antenna:penghapus"

.Version 1

End With

'delete loyang

With Solid

.Version 9

.Insert "feeder:loyang", "antenna:penghapus"

.Version 1

End With

'delete pelekak

With Solid

.Version 9

.Insert "feeder:pelekat", "antenna:penghapus"

.Version 1

End With

'delete the antenna ring

With Solid

.Version 9

.Insert "ring:slot.0.2.4", "antenna:penghapus"

```

        .Version 1
End With

'=====
'Memutar blok penghapus untuk yang pertama
'=====

```

```

With Transform
    .Reset
    .Name "antenna:penghapus"
    .Origin "Free"
    .Center "0", "0", "0"
    .Angle "0", "0", sudut_putar
    .MultipleObjects "False"
    .GroupObjects "False"
    .Repetitions "1"
    .MultipleSelection "False"
    .RotateAdvanced
End With

```

```

'hilangkan kaviti
With Solid
    .Version 9
    .Insert "antenna:kaviti", "antenna:penghapus"
    .Version 1

```

End With

'hilangkan radiating

With Solid

.Version 9

.Insert "antenna:radiating", "antenna:penghapus"

.Version 1

End With

'hilangkan ground

With Solid

.Version 9

.Insert "antenna:ground", "antenna:penghapus"

.Version 1

End With

'hilangkan lubang feeder

With Solid

.Version 9

.Insert "antenna:lubang\_feeder",

"antenna:penghapus"

.Version 1

End With

'hilangkan loyang

With Solid

.Version 9

.Insert "feeder:loyang", "antenna:penghapus"

.Version 1

End With

'hilangkan pelekat

With Solid

.Version 9

.Insert "feeder:pelekat", "antenna:penghapus"

.Version 1

End With

'hilangkan ring

With Solid

.Version 9

.Insert "ring:slot.0.2.4", "antenna:penghapus"

.Version 1

End With

'Putar kembali penghapus ke posisi semula

'=====

With Transform

.Reset

.Name "antenna:penghapus"



```
.Origin "Free"
.Center "0", "0", "0"
.Angle "0", "0", -sudut_putar
.MultipleObjects "False"
.GroupObjects "False"
.Repetitions "1"
.MultipleSelection "False"
.RotateAdvanced
```

End With

```
'=====
'Memutar blok penghapus untuk yang kedua
'=====
```

With Transform

```
.Reset
.Name "antenna:penghapus"
.Origin "Free"
.Center "0", "0", "0"
.Angle "0", "0", sudut_putar2
.MultipleObjects "False"
.GroupObjects "False"
.Repetitions "1"
.MultipleSelection "False"
.RotateAdvanced
```

End With

'hilangkan kaviti

With Solid

.Version 9

.Insert "antenna:kaviti", "antenna:penghapus"

.Version 1

End With

'hilangkan radiating

With Solid

.Version 9

.Insert "antenna:radiating", "antenna:penghapus"

.Version 1

End With

'hilangkan ground

With Solid

.Version 9

.Insert "antenna:ground", "antenna:penghapus"

.Version 1

End With

'hilangkan lubang feeder

With Solid

.Version 9

.Insert "antenna:lubang\_feeder",  
"antenna:penghapus"  
.Version 1  
End With

'hilangkan loyang  
With Solid

.Version 9  
.Insert "feeder:loyang", "antenna:penghapus"  
.Version 1  
End With

'hilangkan pelekot  
With Solid

.Version 9  
.Insert "feeder:pelekat", "antenna:penghapus"  
.Version 1  
End With

'hilangkan ring  
With Solid

.Version 9  
.Insert "ring:slot.0.2.4", "antenna:penghapus"  
.Version 1  
End With

'Hapus blok penghapus  
Solid.Delete "antenna:penghapus"

'Hapus loyang  
Solid.Delete "feeder:loyang"

'hapus pelek  
Solid.Delete "feeder:pelek"

'Select permukaan dielektrik feeder untuk membuat  
'konduktor luar  
Pick.PickFaceFromId "feeder:dielektrik", "2"

'Buat konduktor luar menggunakan fasilitas extrude  
With Extrude

.Reset  
.Name "konduktor\_luar"  
.Component "feeder"  
.Material "Copper"  
.Mode "Picks"  
.Height "0.3"  
.Twist "0.0"  
.Taper "0.0"  
.UsePicksForHeight "False"

```
.DeleteBaseFaceSolid "False"  
.ClearPickedFace "True"  
.Create  
End With  
  
End Sub
```

#### **A.4. The VBA Program Code to Multiply the VBA-RLSA Antenna**

'This code program is used to multiply RLSA antennas  
'automatically in CST-MWS-2010.

'Change the value of variable "jarak\_antar\_feeder" (in mm)  
'to determine the distance between the antenna feeders.

'This program was written by Teddy Purnamirza, from  
'Department of Electrical Engineering, Faculty Science and  
'Technology, Universitas Islam Sultan Syarif Kasim Riau,  
'Indonesia.

'This program is a free program and can be used or can be  
'more developed by anyone provided acknowledging the  
'programmer of the Program (Teddy Purnamirza). The  
'programmer does not responsible to any misuse of this  
'program and any damage caused by the utilization of this  
'program.

Sub Main ()

Dim jarak\_antara\_feeder As Double

jarak\_antara\_feeder=20

WCS.MoveWCS "local", "jarak\_antara\_feeder/2", "0.0",  
"0.0"

'Putar antenna 90 derajat searah jarum jam dan buat hasil  
'kopinya

'=====

With Transform 'putar untuk komponen antena

```
.Reset  
.Name "antenna"  
.Origin "Free"  
.Center "0", "0", "0"  
.Angle "0", "0", "90"  
.MultipleObjects "True"  
.GroupObjects "False"  
.Repetitions "1"  
.MultipleSelection "True"  
.Component ""  
.Material ""  
.RotateAdvanced
```

End With

With Transform 'putar untuk komponen feeder

```
.Reset  
.Name "feeder"  
.Origin "Free"  
.Center "0", "0", "0"  
.Angle "0", "0", "90"  
.MultipleObjects "True"
```

```
.GroupObjects "False"  
.Repetitions "1"  
.MultipleSelection "True"  
.Component ""  
.Material ""  
.RotateAdvanced  
End With
```

With Transform 'putar untuk komponen ring

```
.Reset  
.Name "ring"  
.Origin "Free"  
.Center "0", "0", "0"  
.Angle "0", "0", "90"  
.MultipleObjects "True"  
.GroupObjects "False"  
.Repetitions "1"  
.MultipleSelection "False"  
.Component ""  
.Material ""  
.RotateAdvanced  
End With
```



'Putar antenna +hasil kopinya 180 derajat searah jarum jam  
'untuk menghasilkan 4 bagian antenna

'=====

With Transform 'putar untuk komponen antenna

```
.Reset  
.Name "antenna"  
.Origin "Free"  
.Center "0", "0", "0"  
.Angle "0", "0", "180"  
.MultipleObjects "True"  
.GroupObjects "False"  
.Repetitions "1"  
.MultipleSelection "True"  
.Component ""  
.Material ""  
.RotateAdvanced
```

End With

With Transform 'putar untuk komponen feeder

```
.Reset  
.Name "feeder"  
.Origin "Free"  
.Center "0", "0", "0"  
.Angle "0", "0", "180"  
.MultipleObjects "True"
```

```

.GroupObjects "False"
.Repetitions "1"
.MultipleSelection "True"
.Component ""
.Material ""
.RotateAdvanced
End With
With Transform 'putar untuk komponen ring
.Reset
.Name "ring"
.Origin "Free"
.Center "0", "0", "0"
.Angle "0", "0", "180"
.MultipleObjects "True"
.GroupObjects "False"
.Repetitions "1"
.MultipleSelection "False"
.Component ""
.Material ""
.RotateAdvanced
End With

End Sub

```

# Indeks

background	19, 28, 71, 75, 103, 106, 107, 118, 134, 172
beam-tilt technique	22
cavity	17, 18, 22, 26, 28, 30, 37, 40, 44, 45, 46, 47, 49, 50, 51, 54, 62, 65, 66, 68, 71, 72, 74, 75, 82, 83, 103, 105, 106, 114, 118, 136, 137, 138, 140, 142, 175, 176, 179, 181, 200
CP-RLSA	22
double layer RLSA	22
dual beam RLSA	23
dual circularly polarized RLSA	23
extreme beamsquint technique	18, 20, 55, 60, 92, 93, 95, 109, 115, 117, 121, 122

feeder	16, 25, 26, 28, 29, 30, 49, 51, 62, 65, 70, 71, 74, 76, 100, 104, 105, 116, 118, 137, 143, 144, 160, 161, 162, 163, 164, 165, 166, 167, 175, 182, 183, 190, 191, 192, 193, 195, 196, 201, 203, 204, 207, 208, 209, 210, 211, 213
FR4 technique	18, 19, 53, 54, 60, 61, 68, 81, 121
Linear Polarizations	32
LP-RLSA	21, 23, 48
multi beams RLSA	23
radial mode	30, 105
radiating element	17, 18, 25, 28, 32, 68, 71, 75, 92, 103, 104, 106, 118, 122, 200
reflected signal	16, 18, 48, 52, 94, 95, 96
reflection cancelling slot technique	22, 24, 27
reflection coefficient suppression	22
remaining power	16, 26, 48, 49, 50, 100, 122

RLSA	15, 16, 17, 18, 19, 20, 21, 22, 23, 24, 25, 26, 27, 28, 29, 30, 32, 33, 35, 37, 38, 47, 48, 50, 51, 53, 54, 55, 59, 61, 62, 63, 64, 68, 70, 71, 72, 74, 75, 76, 78, 83, 84, 85, 87, 88, 89, 90, 92, 93, 94, 95, 96, 100, 101, 103, 104, 105, 106, 109, 110, 111, 112, 113, 114, 115, 117, 118, 119, 121, 123, 124, 125, 126, 127, 130, 132, 133, 171, 198, 210
SA-RLSA	15, 16, 26, 27, 92
slot coupling technique	22
Slot Power Coupling	40
technique of matching spiral	23
technique of slot arrangements	21
technique of varying slots length	23
TEM cavity mode	30
TEM coaxial mode	30, 105
VSA-RLSA	16, 18, 19, 53, 59, 61, 70, 71, 74, 85, 88, 89, 92, 95, 100, 104, 109, 112, 114, 115, 117, 119, 121, 122